Evaluation of an Antiviral (Fusion Protein Inhibitor) and Ibuprofen on Neutrophil Extracellular Traps and Innate Lymphoid Cells in calves experimentally infected with Bovine Respiratory Syncytial Virus

By

VICTORIA NGONDU MUTUA

DISSERTATION

Submitted in partial satisfaction of the requirements for the degree of

DOCTOR OF PHILOSOPHY

in

Integrative Pathobiology

in the

OFFICE OF GRADUATE STUDIES

of the

UNIVERSITY OF CALIFORNIA, DAVIS

Approved:

Laurel J Gershwin, Chair

Nicole Baumgarth

Kevin Woolard

Committee in charge

2022

DEDICATION

I would like to dedicate my dissertation to my loving mother and precious twin nephews. Your love and endless encouragement throughout my life and career has been overwhelming.
I will forever cherish you, thank you.

And to my Big sister, you are missed but never forgotten.

ACKNOWLEDGEMENTS

Over the past five years I have received support and encouragement from a great number of individuals. Dr. Laurel J Gershwin has been a mentor, colleague, and .friend. Her guidance and encouragement have made this a very rewarding journey

I would like to thank my dissertation committee of Dr. Nicole Baumgarth and Dr. Kevin Woolard for their support, brilliant comments and suggestions.

Special thanks to Heather McEligot for providing valuable laboratory and experimental assistance. I would also like to thank Maksim Lebedev and the undergraduate / veterinary students for their assistance with the calf experiments.

I am thankful to my academic advisor Dr. Kevin Keel for the advice and encouragement.

In addition, I am grateful to Bridget McLaughlin for the training and numerous discussions on flow cytometry analysis.

Evaluation of an Antiviral (Fusion Protein Inhibitor) and Ibuprofen on Neutrophil Extracellular Traps and Innate Lymphoid Cells in calves experimentally infected with Bovine Respiratory Syncytial Virus

ABSTRACT

The function of neutrophils and innate lymphoid cells (ILCs) in viral infections has been established with most of the studies conducted in mice and humans but rarely in other species including cattle. The role of neutrophil extracellular traps (NETs) has also been evaluated in viral infections but due to excess tissue damage that maybe caused by NETs, further studies are needed to reveal a therapeutic target. ILCs have also been identified in viral conditions affecting mice and humans but currently very little is known about the isolation and identification of ILCs in bovine lung tissue. Here, we describe a method for sample collection, cell preparation and flow cytometric analysis of bovine lung samples to identify bovine ILCs.

This study aims to evaluate the effects of the treatments, FPI and ibuprofen a cyclooxygenase-2 inhibitor, on the innate immune response, focusing mainly on NETs and ILCs to test if their populations change with the different treatment protocols. We conducted a randomized placebo-controlled trial of ibuprofen, FPI, or as a dual therapy initiated at 3 or 5 days after experimental infection with BRSV in 36 five to six-week-old Holstein calves (Bos Taurus).

Lung tissue samples were collected and stained with antibodies conjugated with fluorescence dyes to visualize and quantify the NETs in situ. There were significantly fewer NETs in the lung tissue from calves that were given ibuprofen and both ibuprofen and fusion protein inhibitor from day 3 post infection compared to the placebo (no treatment) group.

The last chapter of this dissertation depicts the experiments carried out in an attempt to identify ILCs from the lung samples. This is the preliminary analysis of ILCs, and further studies will be performed to characterize the cells and assess their function.

TABLE OF CONTENTS

LIST OF TABLES

LIST OF FIGURES

CHAPTER 1

1. LITERATURE REVIEW

1.1 BOVINE RESPIRATORY SYNCYTIAL VIRUS

1.1.a. Introduction

Bovine respiratory syncytial virus (BRSV) is a pathogen of cattle that causes respiratory disease by itself and as a part of the bovine respiratory disease complex (BRDC) and is thus an extremely important bovine pathogen[1, 2]. BRSV is closely related to a human respiratory syncytial virus (HRSV), one of the most important causes of infectious bronchiolitis in children less than two years of age, the elderly and immune compromised, with high rates of morbidity and mortalities[3–5]. The pathogenesis of disease in both, the bovine and human hosts, is closely related to the host response to virus infection[6–8]. Much has been learned about BRSV since its original discovery, but there are still unanswered questions regarding the variable pathogenesis, mechanisms of immune protection and modes of transmission within the cattle population.

Vaccines against BRSV have been approved and are in use, however, they have been linked to enhanced disease pathophysiology[9, 10]. Effective treatment and preventative options for HRSV infection are lacking after the failure of a formalin-inactivated virus vaccine trial in the 1960s[3, 11]. Management of HRSV infection is a significant unmet medical need, with the majority of treatment strategies being supportive. Hence, much research is needed to develop safe and effective control and treatment options. Information obtained about these closely related but distinct viruses and the host response is important for both species.

Since BRSV infection in calves is similar to HRSV disease in children, BRSV is one of the best models to study the effects of various treatments and control options for HRSV [3, 7, 12].

In return, findings from studying HRSV in vivo in humans, in small animal models, or in vitro have allowed a better understanding of some virological and pathogenic characteristics of its counterpart in bovines. The two viruses are genetically and antigenically closely related but highly host specific.

1.1.b. The Virus

Respiratory Syncytial Virus (RSV) in an enveloped, non-segmented, negative-stranded RNA virus, belonging to the genus Pneumovirus, within the family Paramyxoviridae[13–15]. The virion is made up of a lipid bilayer envelope with three virally encoded transmembrane surface glycoproteins including, large glycoprotein (G), fusion protein (F) and the small hydrophobic protein (SH)[16–19]. The envelope encloses a helical nucleocapsid consisting of the nucleoprotein (N), phosphoprotein (P) polymerase protein (L) and a genomic RNA of around 15000 nucleotides. A matrix (M) protein forms a layer on the inner face of the envelope and the virus encodes a transcriptional anti-termination factor M2-1. The viral genome also encodes an RNA regulatory protein M2-2 and two non-structural proteins, NS1 and NS2. The viral particle contains cellular proteins including actin, caveolin-1 and MHC class I molecules [20, 21] Thus, the viral mRNA is translated into 11 viral proteins. The morphology of the RSV virion appears to be either pleomorphic, with a roughly round shape and a diameter between 150 and 35 nm, or filamentous with a length that can reach 5 μm and a diameter between 60 and 100 nm. The infectious particle contains a single functional copy of the genome [11, 18, 19, 22].

The two non- structural (NS) proteins, NS1 and NS2 make the virus different from other Pneumoviruses and from the other Paramyxoviridae[23, 24]. The NS1 protein co-precipitates with

the M protein and together with NS2 are important in regulating IFNα/β and have a strong inhibitory effect on viral RNA transcription and replication[23, 24].

The SH protein is the smallest of the three viral membrane proteins and is not essential for virus replication in vitro [25–27]. There is evidence that the SH protein may play a role in virus mediated cell fusion by interacting with the F protein[27].

The G protein is the largest RSV protein with approximately 260 amino acids (AA). It is a type II glycoprotein and was identified as the major attachment protein, since antibodies specific to the G protein blocked the binding of virus to cells, making it a major target of protective neutralizing antibodies against BRSV[28, 29]. It is synthesized in two forms, a membrane-anchored form and a secreted form, the latter arises from translational initiation at a second AUG in the ORF. Around 80% of G proteins are produced in the secreted form 24 h after infection [30]. The G protein aids in the attachment of the virion at the cell surface, by interaction of its heparin-binding domains with glycosaminoglycans on cell membranes [28, 31]. The G protein may also interact with L-selectin (CD62L), and surfactant proteins[26].

The RSV fusion (F) protein is synthesized as a 547 AA precursor that is cleaved into F1 and F2 subunits[26, 32, 33]. The F protein facilitates fusion of virus to the cell and delivering the nucleocapsid to the cytoplasm[34, 35]. The virus then causes infected host-cells to fuse with other host cells forming characteristic syncytia that lead to virus spread. The F protein is synthesized as an inactive precursor, F0, which has to be proteolytically cleaved at two furin consensus sequences to yield a fusion-active, disulphide-linked heterodimer, composed of the F2 and F1 subunits. A 27 AA peptide released from the F protein after proteolytic cleavage into F1 and F2 has a homology with tachykinins. This virokinin may have a role in pathogenesis by acting as a smooth muscle

constrictor [30]. The F protein is highly conserved between different BRSV isolates and induces neutralizing antibodies that confer resistance to BRSV infection [35].

The RSV nucleocapsid consists of the nucleoprotein (N), the phosphoprotein (P) and the polymerase (L) and has a length of 391 AA [26]. The P protein has 241 AA and appears to act as a chaperone for soluble N and is implicated as a regulation factor for viral transcription and replication [36]. The polymerase L of BRSV has a size of 2162 AA and is an RNA-dependent RNA polymerase [11, 36]. In combination with P, L and possibly M2-2, the N protein is a major element of the nucleocapsid and protects the viral genome RNA from degradation by RNAse [36]. The M protein is 256 AA in length and has little sequence relatedness with other paramyxovirus M proteins[13, 36]. This protein is located on the inner surface of the viral envelope and plays an important role in the formation of virus-like particles. The M2-1 protein is an anti-termination factor that promotes transcriptional chain elongation and increases the frequency of readthrough at gene junctions. The M2-2 protein mediates a regulatory switch from transcription to RNA replication [23, 37, 38].

Following fusion of the viral envelope and the cell membrane, the ribonucleoprotein (RNP) complex is released into the cytoplasm and transcription of the viral RNA by the polymerase begins [39–41]. Transcription involves a sequential start-stop mechanism that produces sub-genomic RNA. RNA replication occurs when the polymerase switches to a readthrough mode. This results in the synthesis of a positive-sense replicative intermediate, which acts as a template for replicating the negative strand genomic RNA[23]. Both genomic and antigenomic RNA are packaged. The nucleocapsids are assembled in the cytoplasm and then migrate with the M protein toward the cellular membrane, which contain the viral glycoproteins. Budding of the virus from the host cell membrane can occur directly at the surface of the cellular membrane or into

cytoplasmic vesicles [18, 38, 42]. In polarized airway epithelial cells, budding of HRSV occurs at the apical surface and this is also true for BRSV infection of polarized bovine airway epithelial cells [24].

1.1.c. Pathogenesis of BRSV

BRSV virus replicates in the superficial layer of the respiratory ciliated epithelium type II pneumocytes, resulting in activation of NF-κB, which leads to the induction of proinflammatory chemokines and cytokines, such as RANTES (CCL5), MIP-1α (CCL3), MCP-1 (CCL2), eotaxin (CCL11), interleukin (IL)-8 (CXCL8), TNF-α, IL-6, and IL-1 [23, 30, 43]. These compounds contribute to inflammation by recruiting neutrophils, macrophages and lymphocytes to the airways. The virus attaches to respiratory epithelial cells via glycosaminoglycans and the interaction of the F protein with TLR4 leads to activation of NF-κB via the Myd88-dependent pathway. Double-stranded (ds)RNA, a by-product of virus replication, binds to TLR3 leading to activation of the transcription factors NF-κB, IRF-3 and AP-1, which act cooperatively to fully activate the IFNβ promoter [44]. The NS proteins decrease STAT2 expression and inhibit IFN signaling. Activation of NF-κB via TLR4 and TLR3 leads to the induction of pro-inflammatory cytokines and chemokines with recruitment of polymorphonuclear neutrophils (PMN), macrophages (MQ) and NK cells to the sites of infection[12, 30]. The virokinin released following cleavage of the BRSV F protein may contribute to eosinophil recruitment or to bronchoconstriction, as it induces smooth muscle contraction [45–48].

BRSV infection is associated with a reduction in mitogen-induced lymphocyte proliferation in both, calves and lambs. Studies have shown that the basis for the inefficient immune response triggered by the virus may be a result of induction of a Th2-biased response with

decreased production of IFNγ and the induction of IgE antibodies[48]. Interleukin-4 (IL-4) production by lymphocytes is shown to indicate a Th2 immune response with studies demonstrating presence of BRSV-specific IgE in the serum of calves experimentally infected with BRSV, which also showed a correlation between severity of clinical signs and the presence of BRSV-specific IgE in serum and lymph [8, 49–51].

BRSV and HRSV are closely related but display a highly restricted host range[52]. Although HRSV does not replicate very efficiently in the bovine nasopharynx, it replicates moderately well in bovine lungs in vivo and induces some pneumonic lesions, resulting in a mild respiratory disease in calves upon experimental infection [53].

1.1.d. Clinical signs of BRSV

The incubation period for BRSV is between 2 and 5 days with the infection being either asymptomatic, limited to the upper airways or involving both the upper (URT) and lower respiratory tracts (LRT)[45, 54, 55]. Generally, BRSV infection presents with pyrexia, anorexia, depression, cough, increased respiratory rate, and in severe cases dyspnea with open mouth breathing and wheezes. URT disease is characterized by a cough with sero-mucoid nasal and ocular discharge [56]. On auscultation of the lung, abnormal breathing sounds caused by bronchopneumonia or bronchiolitis might be detected [57]. Severe clinical signs are commonly observed in calves but might also be observed in adult cattle [45, 58]. In naïve herds clinical signs are usually observed in cattle of all ages when BRSV is introduced. However, it is observed only in calves when the virus circulates regularly in the herd. Maternally-derived antibodies provide partial protection against clinical signs after natural and experimental BRSV infection [48, 59, 60].

1.1.e. Pathology of BRSV infection

Pathological evaluation of lungs of infected animals shows large areas of consolidation, occasionally with emphysematous bulla in those most severely affected [19,52–54]. Histologically, broncho-interstitial pneumonia may be observed. Immuno-peroxidase staining for BRSV antigen shows the presence of virus in bronchial epithelial cells and sometimes in type 2 alveolar cells. In experimental models viral shedding begins around day 3 or 4, and diminishes by day 10 [3, 46, 55]. The host response to the virus accounts for the majority of the lung pathology with the virus modulating the host immune response causing ranging implications that impact on the response to vaccination, to secondary bacterial invaders and to inhaled environmental antigens [46]. Lung pathology shows the cranio-ventral parts of the lung to be consolidated and a mucopurulent discharge may be seen from the bronchus and small bronchi. The caudo-dorsal parts of the lungs are often distended because of interlobular, lobular and sub-pleural emphysematic lesions [8, 64–66]. Tracheobronchial and mediastinal lymph nodes may be enlarged, edematous and sometimes hemorrhagic. If bacterial co-infections occur, the lung parenchyma is seen to be more swollen and consolidated with fibrin or suppurative bronchopneumonia. Microscopic lesions are characterized by an exudative and proliferative bronchiolitis with accompanying alveolar collapse and a peribronchiolar infiltration by mononuclear cells. Giant cells or syncytia may be present, either free in the bronchi lumen, in the bronchiolar epithelium or in the alveolar walls and lumina [9, 45, 67]. The lumen of bronchi, bronchioles and the alveoli are obstructed by cellular debris, consisting mostly of neutrophils, desquamated epithelial cells, macrophages and sometimes eosinophils, and may be aggravated by bronchiolar repair and re-organization. Eosinophils and lymphocytes (CD4+, CD8+ and WC1+γ/δ T cells) are also observed in the lamina propria [9, 62,

68, 69]. Neutrophils become activated in this pro-inflammatory micro-environment and contribute to RSV clearance thus limiting viral spread [70–72]

Stimulated neutrophils are able to form Neutrophil extracellular traps (NETs), extracellular networks of DNA covered with antimicrobial proteins, as part of the first line of defense against pathogens, with the fusion protein of RSV shown to induce the formation of NETs in vitro [19, 73, 74]. The viral-induced NETosis appears to be induced through a TLR-4 dependent mechanism [19]. NETs can capture and neutralize the RSV virions, which prevents viral binding to target epithelial cells. As such, the formation of NETs by neutrophils may be an important mechanism of the local anti-BRSV response limiting viral spread. NET-rich plugs with or without BRSV antigen were observed in calves occluding the small airways during severe BRSV infection [74–76]. This suggests that NETs can negatively contribute to airway obstruction and immunopathology in BRSV disease. Alveolar changes are marked by an interstitial pneumonia and atelectasis in the consolidated areas and there may be severe emphysema and edema with a rupture of alveolar walls in the caudo-dorsal area of the lung [71, 77]. Alveolar epithelization with a pneumocyte hyperplasia contributes to the enlargement of the alveolar septa with the cell infiltration[71].

1.1.f. Epidemiology

The impact of BRSV on the economy of the cattle industry is considerable. Studies estimate that more than 60% of epizootic respiratory disease in dairy herds is caused by BRSV and the disease can exert a strong negative impact on the dairy and beef industries with mortality varying from 2% to as high as 20% in some outbreaks [23, 78, 79].

Although cattle are the natural host of BRSV, it is possible that other species such as ovine, caprine, bison, or camelids may play an epidemiological role in certain circumstances [26]. The distribution of BRSV is worldwide and the virus has been isolated from cattle in Europe, America and Asia [80, 81]. The virus causes regular winter outbreaks of respiratory disease in cattle. A seroprevalence of 30– 70% have been detected in cattle, and the virus might be responsible for more than 60% of the epizootic respiratory diseases observed in dairy herds and up to 70% in beef herds [3, 23]. BRSV antibodies have been detected in 35% of calves between 5 and 11 months of age in dairy herds in a Swedish study [82]. The frequency of infections in adult bovine is difficult to assess because of the high BRSV seroprevalence in this category of animals.

BRSV infection has a high rate of morbidity, reaching 60 to 80% and mortality rates reached up to 20% in some outbreaks [3, 78]. BRSV is transmitted by direct contact between infected animals or by aerosol and might also be spread by humans carrying the virus [66, 83].

1.1.g. Prevention, control and vaccination

In contrast to HRSV, several vaccines against BRSV are available. However, the development of a second generation of BRSV vaccines with greater efficacy in inducing maternal antibodies and more durable protection would be facilitated by a greater understanding of BRSV pathogenesis. Since the peak incidence of severe BRSV disease is in calves between 2 and 6 months of age [84, 85], an effective BRSV vaccine must be capable of stimulating an effective immune response within the first months of life. The presence of maternally-derived, RSV-neutralizing, serum antibodies poses a major obstacle to successful vaccination at this time [86]. There is evidence also that vaccination can exacerbate RSV disease [23, 87, 88]. A formalin-inactivated (FI)-HRSV vaccine not only failed to protect human infants against HRSV infection

but increased the severity of respiratory disease in those that became infected [11, 50]. Vaccine-augmented respiratory disease after RSV infection has been experimentally-reproduced in calves[89, 90]. Direct and significant correlation was made between disease severity and the production of BRSV specific IgE after vaccination [50]. In addition, vaccine exacerbated disease was shown with a β- propiolactone-inactivated virus [91]. It has been suggested that in this latter example immunopathogenic immune responses may have been mediated by the deposition of immune complexes and complement activation in the lungs. Alternatively, a strong Th-2 biased immune response may have been induced, which resulted in exaggerated recruitment of other inflammatory cells into the lung [48, 50, 64, 92]. Although it is possible to generate live, attenuated viruses by passage in cell culture, it has been difficult to produce a genetically stable HRSV with an appropriate balance between attenuation and immunogenicity. Deletion of non-essential genes, or incorporation of immune-stimulatory components, represent attractive options for producing a live-attenuated virus vaccine with minimal negative effects [28, 86, 93].

Altering the positions of the BRSV F and G proteins from positions 7 and 8 to positions 3 and 4 in the genome resulted in increased expression of the F and G proteins in vitro and attenuation of the virus after infection of young calves. Furthermore, vaccination with this attenuated virus induced protection against subsequent challenge with virulent BRSV [94].

It is well documented that much of the clinical and pathological observations in BRSV infection result from the host response to the virus. There are unique aspects of this virus that facilitate development of pro-inflammatory responses that fail to induce protection and long-lived immunity. When examined, most observations made with HRSV have proven to be shared with BRSV. Thus, it is likely that continued efforts to develop new treatment and control strategies would have reciprocal benefits for both species. The goal of this dissertation is to evaluate the

effect of a combination therapy consisting of an antiviral (fusion protein inhibitor) and an immune modulator, ibuprofen, on the management of BRSV and its effects on the immune system.

1.2. NEUTROPHIL EXTRACELLULAR TRAPS

1.2.a. Introduction

Neutrophils are one of the main effectors and abundant cells in the innate immune system discovered more than 100 years ago [95]. They are produced in the bone marrow and released into blood vessels, from where they can be rapidly recruited to the infection site. Neutrophils' main function is to bind, engulf, and kill invading microbes through phagocytosis [96]. However, it has been discovered that stimulated neutrophils can also produce extracellular structures called neutrophil extracellular traps (NETs) through a process termed NETosis, that further assist in the capture and destruction of microorganisms [97–99]. NETs are large, extracellular, web-like structures composed of proteins assembled on a scaffold of decondensed chromatin [100]. Studies have shown that NETs trap, neutralize and kill bacteria, fungi, viruses and parasites. If left unchecked, NETs have been shown to contribute to the pathogenesis of immune-related diseases and exacerbation of certain conditions[101–103].

1.2.b. Formation of NETs

The formation of NETs is a highly organized process and can be divided into 3 phases.

Phase 1 – this is the initial phase which involves neutrophil stimulation and is governed by the degradation of the cytoskeleton as well as membrane rearrangements. Neutrophils arrest their actin dynamics and depolarize, leading to cell rounding and the formation of micro-vesicles on the

surface. There is induction of chromatin decondensation and the nuclear membrane starts to be modified and weakened [104–106].

Phase 2 - this phase begins when the chromatin is getting decondensed and involves disassembly of the nuclear envelope and the chromatin decondensing into the cytoplasm of intact cells, mixing with cytoplasmic and granule components. It also marks the point of no return, where the NETs formation and release cannot be inhibited. There is swelling of the expanding chromatin as well as destabilization and softening of the cell membrane. In this phase there is also histone citrullination and phosphorylation of alarmins [107–109].

Phase 3 – this phase involves the rounding of the cell and entropic swelling of the chromatin, which increases the pressure within the cell, leading to the rupture of the cell membrane and release of DNA and cellular components forming NETs into the extracellular space. The whole NETosis process takes approximately 3-8 hours [109–111].

1.2.c. Proteins associated with NET formation

NET formation involves a number of proteins that have been identified upon stimulation of neutrophils using various stimulants and antigens. The main proteins that play a key role in NETosis are chromatin and histones. Chromatin is a mass of genetic material, located in the nucleus, composed of DNA and histones, that condense to form chromosomes during eukaryotic cell division [112, 113]. Peptidyl arginine deiminase, type IV (PAD4) [106, 111] is another important protein in NETosis responsible for converting arginine residues to citrulline in a variety of protein substrates. PAD4 is expressed in granulocytes and is essential for the formation of NETs by mediating histone citrullination [106, 114]. Citrullination of histones is thought to promote NET formation by inducing chromatin decondensation, and facilitates the expulsion of chromosomal

DNA that is coated with antimicrobial molecules [109, 115, 116]. The key antimicrobial effector proteins of NETs are histones (H2A, H2B, H3, and H4) [117, 118] and granule proteases, including neutrophil elastase (NE) [119, 120], cathepsin G (CatG), proteinase 3 (PR3), as well as myeloperoxidase (MPO) and lactotransferrin [121, 122]. The proteases remain enzymatically active, even when the NET is exposed to endogenous protease inhibitors. Other proteins identified within NETs include azurocidin, lysozyme C, and α-defensins [123, 124]. NETs also contain cytoplasmic and cytoskeleton proteins such as S100 calcium-binding proteins, actin, myosin, and cytokeratin [125]. Some proteomic studies have identified about 24 proteins within PMA-induced NETs and 80 proteins within NETs induced by nonmucoid and mucoid strains of *Pseudomonas aeruginosa* [126, 127]. We can speculate that the composition of the NET can be influenced by the stimulating pathogen or compound, however, the differences in NETs composition and their impact on NETs function is a gap in knowledge that needs to be fully investigated.

1.2.d. Mechanism of NETs formation

The release of NETs is a slow process and requires reactive oxygen species (ROS) production. The pathways that promote NETosis upstream of ROS involve ROS-inducing receptors (BOX 1) and kinases, such as MEK (MAPK/ERK kinase), extracellular-signal-regulated kinase (ERK), IL-1 receptor-associated kinase (IRAK), PKC, phosphoinositide 3-kinase (PI3K) and AKT [73, 108, 128, 129]. These kinases induce nicotinamide adenine dinucleotide phosphate (NADPH) oxidase enzyme complex, which produces large amounts of superoxide during neutrophil oxidative burst. On activation by PMA, neutrophils up-regulate glycolysis, which induces signaling by extracellular signal-regulated kinase (ERK), leading to the phosphorylation of p47phox[120], one of the three cytoplasmic regulatory subunits of the NADPH oxidase. On

phosphorylation, p47phox is recruited to the granule and plasma membranes, where it interacts with other subunits to assemble the NADPH oxidase complex and generate superoxide. ROS generated by NADPH oxidase stimulates MPO to trigger the activation and translocation of NE from azurophilic granules to the nucleus, where NE proteolytically processes histones to disrupt chromatin packaging [106, 112]. The exact mechanism by which NE is released into the cytosol to initiate NETosis is not very clear and is proposed to occur without granule rupture but may involve cooperation between granule proteins. MPO then binds chromatin and synergizes with NE in decondensing chromatin. NE binds to F-actin filaments in the cytoplasm and degrades them in order to enter the nucleus, where it inactivates histones such as H4 and H2B, leading to chromatin relaxation and DNA decondensation [112, 117]. Some stimuli inducing NET formation, such as immune complexes, ionomycin and nicotine, have been proposed to trigger NETosis independently of NADPH oxidase, relying instead on mitochondrial ROS [130, 131]. ROS has also been shown to induce autophagy, which in turn is required to sustain the ROS burst and might also help accelerate NETosis [132].

PAD4 lies downstream of ROS and calcium signaling during NETosis and contributes to chromatin relaxation and histone citrullination. PAD4 is activated by a cytosolic spike in calcium and the degree and specificity of citrullination seems to vary depending on the stimulus owing to the activation of different PKC isoforms that activate or suppress PAD4 [106, 109, 111]. Histone citrullination occurs independently of NE activity, but histone citrullination might not be sufficient to drive chromatin decondensation.

1.2.e. Neutrophil's decision to cast NETs

Neutrophil have a microbe size-sensing mechanism that allows them to decide whether or not to launch a NET in response to extracellular pathogens [133]. Neutrophils seem to preferentially deploy NETs against large microorganisms, while small microorganisms are taken up into phagosomes that fuse with azurophilic granules, sequestering NE away from the nucleus and blocking chromatin decondensation [134, 135]. The absence of phagosomes in neutrophils that engage large microorganisms allows NE to translocate to the nucleus via the slower azurosome pathway and to drive NETosis [133]. Furthermore, NE release into the cytosol promotes actin cytoskeleton degradation, blocking phagocytosis and committing the cell to NETosis. Phagosome formation, hence, serves as a checkpoint to prevent NETosis[136].

The influence of particle size on NETosis also applies to sterile stimuli. Larger urate crystals have been shown to trigger NETosis more potently than urate microaggregates that are small enough to be ingested [137]. The selective induction of NETosis limits unnecessary tissue damage during infection by pathogens that are small enough to be killed intracellularly. However, NETosis induced by small bacteria and viruses has also been widely reported [133]. A number of studies have shown an increase in both, phagocytosis and NET formation, upon bacterial invasion or disruption of the bacterial capsule. This may indicate that NETosis is reserved for small virulent microorganisms that interfere with phagosomal killing. Large aggregates of *Mycobacterium bovis* Bacillus Calmette–Guérin drive NETosis in a microorganism size-dependent manner [133, 138, 139], while *S. aureus*, has been shown to stimulate NETosis in mouse models of sepsis by forming large abscesses and aggregates [140, 141].

Large microbes induce the extracellular deployment of ROS and strong interleukin (IL)-1β [133] secretion with resultant neutrophil clustering. In contrast, small phagocytosed microbes

trigger the intracellular deployment of ROS, suppressing cytokine release and neutrophil clustering, and thereby preventing neutrophil accumulation, excessive NETosis and tissue damage during microbial clearance[136]. Viruses that have been shown to induce NETs include influenza A, HIV-1, myxoma, encephalomyocarditis virus and respiratory syncytial virus (RSV)[76, 142, 143]. These viruses are detected by recognition of viral particles by pattern recognition receptors PRR on the neutrophil (TLR2, TLR4,TLR7 and TLR8) or via secondary signals produced upon infection of other host cells[144, 145].

1.2.f. Neutrophil Extracellular Traps in Disease

NETosis leads to the release of enzymatic proteins. Due to the nonspecific effects of these proteins, NETs may lead to uncontrolled inflammatory responses causing tissue pathology. There is direct cell damage, recruitment of other pro-inflammatory cells and proteins, and formation of immune complexes that induce autoantibody production, leading to tissue damage [146, 147]. NETs can capture metastatic tumors, aggravating cancerous condition [148] and in diabetic cases they lead to a delay in wound healing [149, 150]. Neutrophil can also form interactions with platelets mediated by P-selectin [151]. This leads to induction of platelet-derived high mobility group protein B1 (HMGB1) [152], which stimulates NETs [151, 153] causing occlusion in the vasculature by promoting thrombosis and obstruction causing organ damage. Although NETs promote inflammation, a study done by Christine et al shows that an accumulation of NETs aggregates can reduce inflammation in a mouse model of gout through the degeneration of cytokines and chemokines [137].

NETs can have positive effects on controlling bacterial infections. They possess antimicrobial properties with components including, histones, cathepsin G, NE, MPO, lactoferrin,

antimicrobial peptide-LL37, pentraxin 3, gelatinase, proteinase 3 and peptidoglycan-binding proteins that are bactericidal [154–156]. In viral infections, including influenza, HIV and RSV there can be excessive neutrophil recruitment [3, 143].

Although NETs may protect the host against microbes, excessive NETosis can be detrimental to the host. Large amounts of circulating NETs demonstrated in septic patients have been associated with poor outcome and multiple organ failure [118, 157, 158]. This could be due to increased NETosis, apoptosis, necrosis or decreased clearance of extruded products, with studies suggesting that cell free DNA exacerbate inflammation by inducing TNF-α mRNA [134, 159]. Histones also function as damage-associated molecular patterns and can induce organ damage by promoting proinflammatory cytokine release, causing endothelial dysfunction by inducing cytotoxicity and increasing ROS production[158, 160, 161].

Control of NET formation is quickly becoming a target for therapeutic intervention in the management of various diseases[162]. The different compounds known to inhibit or clear NETs, often have other, unwanted effects on the immune system. This makes identifying one particular compound as being particularly effective difficult. The management of NETs may require a combination therapy approach that incorporates conventional treatments, such fluid therapy, antibiotics, antivirals with NET-targeted drugs. To optimize treatment efficacy and outcome in patients, it is important to conduct additional studies that evaluate the mode of action of potential compounds, and their effects on the overall immune system. This will ensure that they lack detrimental effects. The goal of the work described in this dissertation is to evaluate the effects of a combination therapy consisting of an antiviral against BRSV with ibuprofen, an immune modulator. Expected results are that the antiviral reduces virus replication, thus indirectly inhibiting NETosis. In addition, ibuprofen, a non-steroidal anti-inflammatory drug, would interfere

with the COX-2 pathway, thereby impairing the production proinflammatory cytokines and thus interfering with neutrophil recruitment and NETosis.

1.3. INNATE LYMPHOID CELLS (ILCs)

1.3.a. Introduction

Innate lymphoid cells (ILCs) are comprised of populations of innate immune cells that have lymphoid morphology but lack rearranged antigen receptors. ILCs are tissue-resident cells that adapt to an organ, establishing close interactions with other hematopoietic and non-hematopoietic cells [163]. The latter include neurons, epithelial cells, stromal cells, and other parenchymal cells, such as adipocytes and hepatocytes[164]. ILCs are the innate counterparts of T lymphocytes and have been classified as non-myeloid, non-T, non-B, lymphocytic cells defined as lineage marker-negative (Lin−) $CD45^{+}CD90^{+}$ $CD127^{+}$ cells[165]. ILCs have been identified and extensively studied in mouse and human lungs and other organs, but little is known about their population in bovines and other vertebrates[166–168].

ILCs and T cells play key roles in instituting an immune response to infections, where ILC1s and Th1 cells react to intracellular pathogens, such as viruses, ILC2s and Th2 cells respond to large extracellular parasites and allergens, while ILC3s and Th17 cells target extracellular microbes, such as bacteria and fungi [169, 170]. ILCs mainly respond to signals or inducer cytokines expressed by tissue-resident cells.

1.3.b. Development of ILCs

Pluripotent hematopoietic stem cells in the bone marrow give rise to myeloid and lymphoid lineage cells, common myeloid precursor (CMP) and common lymphoid precursor (CLP), respectively[171]. ILCs have been shown to develop initially in the fetal liver (FL) and later in the adult bone marrow from CLPs, which in mice are defined as Lin^{-} $Thy\text{-}1^{-}$ $Sca1^{lo}$ c-kit^{lo} $Flt3^{+}$ IL-$7R\alpha^{+}$ cells[172–174]. Early commitment into the ILC lineage requires Tcf-1, the inhibitor of DNA binding 2 (Id2), the nuclear factor IL-3 regulated protein and thymocyte selection-associated high mobility group box protein (TOX). CLP lose the potential to generate B and T cells, becoming the common ILC progenitor (CILP), $Id2^{+}$ IL-$7R\alpha^{+}$ $\alpha_4\beta_7^{+}$ $CD25^{-}$ $PLZF^{+/-}$ (promyelocytic leukemia zinc finger), which then differentiate into ILCs. This progenitor population is known as helper innate lymphoid cell precursor (CHILP)[169, 172, 174].

1.3.c. Types of ILCs

ILCs have been broadly divided into cytotoxic (interleukin-7 receptor α^{-}, IL-$7R\alpha^{-}$) and non-cytotoxic (or helper-like, IL-$7R\alpha^{+}$) ILCs[175, 176]. ILCSs were previously sub-grouped into three classes (ILC1,ILC2 and ILC3) but have been reclassified into five subsets including: Natural killer (NK) cells, ILC1s, ILC2s, ILC3s, and lymphoid-tissue inducer (LTi) cells based on their development and function[177, 178].

a.Natural killer cells - Natural killer (NK) cells are the earliest-discovered member of the ILC family and the only cytotoxic ILCs. NK cells express the lineage-specifying T-box transcription factor Eomesodermin (Eomes), and mediate their effects through perforin-dependent

cytotoxicity and production of IFN-γ[179]. They protect the host from intracellular pathogens and tumors and are regulated by cytokines, such as IL-15, IFN-I, IL-27, IL-12, and transforming growth factor (TGF-β), but also glucocorticoids. IL-15 is essential for the development and activation of NK cells and is often trans-presented via the IL-15Rα-chain expressed by dendritic cells (DCs) [180–182]. Glucocorticoids prevent IFN-γ production by NK cells in conjunction with the inhibitory receptor PD-1 and thus control susceptibility of certain infections and sepsis[183].

b.*ILC1* - The term ILC1 includes several populations of innate lymphocytes developmentally dependent on the transcription factor T-bet and the cytokine IL-15 [184–186]. ILC1s have been shown to mediate protection against acute viral infections, such as Murine Cytomegalovirus infection by secreting IFN-γ and TNF[187, 188]. They can also negatively impact some conditions by leading to the development of chronic or excessive inflammation during certain condition such as colitis, multiple sclerosis, and sepsis. ILC1-derived IFN-γ regulates macrophage polarization towards an M1 phenotype, which has the potential to promote a proinflammatory environment, obesity and insulin resistance [180, 189]. ILC1s have been described in many tissues including the liver, intestinal lamina propria, epithelium, adipose tissue and in the uterus [190–192]. These ILC1 populations found in different tissues sometimes have slightly different phenotype or developmental requirements. It is still unclear whether this reflects tissue adaption within one lineage, or several lineages of innate lymphocytes[193]. ILC1s have been shown to express a similar array of killer receptors as NK cells, such as NKp46, NKG2D, and NK1.1, although development and regulation of NK cells and ILC1s are distinct[194, 195].

c.*ILC2* - ILC2s are mainly regulated by soluble factors, including cytokines, neuronal factors, inflammatory mediators, and hormones. ILC2 development depends on the transcription factors GATA-3 and RORα. ILC2s are activated in the presence of IL-2, IL-7, IL-4, TNF-like

ligand 1 A (TL1A), TGF-β, stem cell factor (SCF) [196–198]. The alarmins IL-25 IL-33, and thymic stromal lymphopoietin (TSLP) are also major activators of ILC2s [163, 199]. IL-25, secreted by tuft cells, is released following helminth infections and triggers activation and generation of inflammatory ILC2s that were described in the mesenteric lymph nodes and lungs following worm infection. IL-33 is expressed in PDGFRα^{+} stromal cell and pre-adipocytes in different tissues, including adipose tissue, lung and intestine [199, 200]. ILC2 activation is further regulated by other mediators such as prostaglandin (PG) D2[201] and leukotriene D4 via chemoattractant receptor expressed on Th2 cells (CRTH2)[202] and Cysteinyl leukotriene receptor 1 (CysLTR1) [203]. On the other hand, PGE2 and lipoxin A4 (LX4) inhibit ILC2 activation via EP4 and ALX receptors, respectively [201]. Other inhibitors of ILC2 function include cytokines that promote type 1 immune responses, such as type I and II interferons, as well as glucocorticoids. ILC2s present in human peripheral blood lack ST2, expressed by mouse ILC2s but selectively express CRTH2 and high levels of CD161 [202, 204]. ILC2s mediate their function by secreting IL-5, IL-9, and IL-13 as well as amphiregulin (AREG) and under some conditions, IL-4 [125, 205]. These cytokines generally promote type 2 inflammation by acting on diverse cell types. This milieu of cytokines promotes migration of ILC2s from their tissue of origin to the blood, and subsequent dissemination to other tissues, where they promote systemic type 2 inflammation. Excessive type 2 immune responses can become detrimental and form the underlying mechanism in the pathogenesis of atopic diseases, including allergic asthma, atopic dermatitis, and allergic rhinitis. Multiple studies support a role for ILC2s in wound healing and tissue remodeling after infection or tissue damage in the skin, lung, and intestine [206–209].

d.*ILC3* - Similar to other ILCs, ILC3 activation is mainly regulated by cytokines, in the case of ILC3s, IL-23 and IL-1β [175, 180]. ILC3 activation is regulated to a large extent by

humoral factors released by myeloid cells and parenchymal cells in the tissue. ILC3s comprise cells that rely on RORγt transcription factor for development. They secrete IL-22 and are separated into two main subsets by expression of CCR6 ($CCR6^-$ ILC3s and $CCR6^+$ILC3s) [210, 211]. IL-22 helps maintain barrier integrity and also mediates effects on other epithelial cells, such as paneth cells, intestinal stem cells, and enterocytes via engagement of IL-22Rα1 and IL-10Rβ2 chains [212, 213]. This triggers a signaling cascade, resulting in phosphorylation of STAT3 with the activation of intracellular signaling that results in secretion of antimicrobial peptides, such as Reg3β, Reg3γ, S108a, and S109a from Paneth cells [214, 215]. IL-22 production has also been shown to protect intestinal stem cells from damage caused by chemotherapy and irradiation. ILC3s modulate myeloid cell activation via secretion of GM-CSF and in this way indirectly regulate adaptive immune responses. Additionally, ILC3-derived GM-CSF was shown to attract neutrophils to sites of infection [216, 217].

e..LTi - LTi cells are essential for the formation of secondary lymphoid tissues and Peyer's patches during embryonic development through the action of lymphotoxin. These cells express c-Kit and CCR6 and depend on RORγt transcription factor [176, 218, 219]. $CXCR5^+$ LTi cells cluster and form lymph node anlagen together with mesenchymal stromal cells. Factors promoting lymph node organogenesis include IL-7, SCF, TSLP, TNF-related activation-induced cytokine (TRANCE), and tumor necrosis factor superfamily member 14 (TNFSF14 or LIGHT), leading to the expression of LTα1β2 on ILC3s, which binds LTβ receptors on mesenchymal cells [206, 220, 221]. This interaction results in further secretion of chemokines CXCL13, CCL19, and CCL21, attracting adaptive lymphocytes to the lymph node, facilitating the formation of lymphoid organs [222, 223]. $CCR6^+$ ILC3s interact with myeloid cells via LTα1β2-LTβ receptor to stimulate secretion of IL-23, which leads to an increase in IL-22 secretion [220].

1.3.d. Effect of ILCs on adaptive immune responses

The transition of the innate to the adaptive immune response takes place in the secondary lymphoid organs, where antigen-presenting cells present peptides via major histocompatibility complex (MHC) molecules to patrolling naïve T cells, which scan numerous cells searching for their specific antigen. ILCs present peptides on MHC II molecules and are therefore able to directly interact with CD4 T cells via MHC II-peptide-TCR complexes. Expression of co-stimulatory molecules on ILCs, such as ICOSL, GITRL and PD-1L also provides a second signal for T cell activation[176, 178]. IL-2 and GM-CSF secreted by ILC3s, are important for Treg cell-mediated tolerance induction. $CCR6^+$ ILC3s in the intestine present peptides on MHC II without providing co-stimulation, causing clonal deletion of the antigen-specific T cells, also known as intestinal selection of T cells. $CCR6^+$ ILC3s have also been implicated in the recruitment and maturation of B cells into lymph nodes[165]. The role of ILCs in the onset and/or maintenance of inflammation, their preferential homing to mucosal tissues, and the expression of several checkpoint receptors on their surface should encourage researchers to explore the potential of ILC manipulation for innovative therapies.

1.3.e. ILCs plasticity

ILCs are negatively regulated by the cytokine milieu or lineage-specifying transcription factors of other ILC subsets[194]. For example, IL-25 and TSLP have been reported to repress ILC3 activation and IL-22 production in colitis and may therefore exacerbate intestinal inflammation. Cytokines promoting type 1 immune responses, IFN-γ or IL-27, were found to inhibit ILC2s and additionally limit allergic inflammation. Studies have also shown that ILCs are

able to adopt alternative cell fates after lineage commitment [224, 225]. This plasticity is driven by the down-modulation of the lineage-specifying transcription factors and was first observed in CCR6^{-} ILC3s These cells lost expression of RORγt and upregulated T-bet, which led to the transformation of ILC3s to a cell type that phenotypically mirrored ILC1s, with the expression of NKp46, NK1.1, NKG2D, IL12Rβ2, and IFN-γ. These ex-RORγt^{+} ILC3s have receptors for IL-12 and IL-23, thus are capable of driving chronic inflammation and immunopathology during chronic conditions [193, 226]. Differentiation towards an ILC1-like phenotype was also described for ILC2s and NK cells. NK cells were converted into ILC1-like cells by down-modulation of Eomes by TGF-β, a cytokine acting on ILC1. These ILC1-like NK cells are distinct from both, NK cells and ILC1s. They appear functionally impaired, as they failed to control tumor growth as well as reduce cytomegalovirus replication [227]. Plasticity of ILC2s towards ILC1 was observed in patients with chronic obstructive pulmonary disease (COPD) and was promoted by the cytokines IL-1, IL-12 and IL-18 and induced by T-bet [228]. ILC2 conversion to IL-17-producing ILC3s was also reported as promoted by Notch signals that lead to upregulation of RORγt and IL-17A in ILC2s, enabling them to produce IL-13 and IL-17A, thus promoting allergic airway inflammation [229]. ILC2s have also been shown to switch their cytokine profile to IL-10 production, a process promoted by various cytokines, including IL-2. The degree of plasticity defines a mechanism of tissue adaption or immune regulation.

1.3.f. ILCs in RSV infection

Studies on the role of ILCs in response to RSV infection have focused on ILC2s. This is because the immune response to RSV infection skews towards a type 2 response, instead of the typical type 1 response observed for most other viral infections [230, 231]. Some studies strongly

suggested that IL-33 drives this type 2 response and is associated with severe RSV-induced bronchiolitis, and possibly induction of childhood asthma [232, 233]. Elevated levels of IL-4, IL-13, IL1-β, and IL-33 following RSV infection was correlated with elevated frequencies of ILC2s and increased disease severity [234]. ILC2 may provide an early source of IL-4/IL-13 in RSV infection, which could promote Th2 polarization, although more studies are required to explore this possibility.

Over the last 10 years research on ILCs has focused on their functional diversity. They have been detected in almost every tissue, where they form a first line of defense against infections. Most studies on ILCs have been conducted on mice and humans, which have identified various species-specific differences especially in surface molecule expression. More work is required to characterize these cells in other species, so as to fully understand their immunoregulatory pathways and their functions. The goal of work described in this dissertation is to identify and isolate ILCs in the bovine, and to define how they respond to BRSV infection.

REFERENCES

1. Gershwin LJ, Van Eenennaam AL, Anderson ML, et al (2015) Single pathogen challenge with agents of the bovine respiratory disease complex. PLoS One 10:. https://doi.org/10.1371/journal.pone.0142479
2. Ellis JA (2009) Update on viral pathogenesis in BRD. Anim. Health Res. Rev. 10:149–153
3. Borchers AT, Chang C, Gershwin ME, Gershwin LJ (2013) Respiratory syncytial virus - A comprehensive review. Clin. Rev. Allergy Immunol. 45:331–379
4. Cortjens B, de Jong R, Bonsing JG, et al (2019) Human respiratory syncytial virus infection in the pre-clinical calf model. Comp Immunol Microbiol Infect Dis 65:213–218. https://doi.org/10.1016/j.cimid.2019.04.006
5. Nwankwo MU, Okuonghae HO, Currier G, Schuit KE (1994) Respiratory syncytial virus infections in malnourished children. Ann Trop Paediatr. https://doi.org/10.1080/02724936.1994.11747704
6. Russell CD, Unger SA, Walton M, Schwarze J (2017) The human immune response to respiratory syncytial virus infection. Clin. Microbiol. Rev.
7. Guzman E, Taylor G (2015) Immunology of bovine respiratory syncytial virus in calves. Mol. Immunol. 66:48–56
8. Gershwin LJ, Berghaus LJ, Arnold K, et al (2005) Immune mechanisms of pathogenetic synergy in concurrent bovine pulmonary infection with Haemophilus somnus and bovine respiratory syncytial virus. Vet Immunol Immunopathol 107:119–130. https://doi.org/10.1016/j.vetimm.2005.04.004
9. Schreiber P, Matheise JP, Dessy F, et al (2000) High mortality rate associated with Bovine

Respiratory Syncytial Vires (BRSV) infection in Belgian White Blue calves previously vaccinated with an inactivated BRSV vaccine. J Vet Med Ser B 47:535–550. https://doi.org/10.1046/j.1439-0450.2000.00380.x

10. Taylor G, Thom M, Capone S, et al (2015) Efficacy of a virus-vectored vaccine against human and bovine respiratory syncytial virus infections. Sci Transl Med. https://doi.org/10.1126/scitranslmed.aac5757
11. Collins PL, Fearns R, Graham BS (2013) Respiratory syncytial virus: Virology, reverse genetics, and pathogenesis of disease. Curr Top Microbiol Immunol. https://doi.org/10.1007/978-3-642-38919-1-1
12. Cortjens B, De Boer OJ, Antonis AFG, et al (2015) Neutrophil Extracellular Trap Formation In Severe Respiratory Syncytial Virus Lung Infection. Am J Respir Crit Care Med 191:no pagination
13. Ghildyal R, Mills J, Murray M, et al (2002) Respiratory syncytial virus matrix protein associates with nucleocapsids in infected cells. J Gen Virol. https://doi.org/10.1099/0022-1317-83-4-753
14. Killikelly AM, Kanekiyo M, Graham BS (2016) Pre-fusion F is absent on the surface of formalin-inactivated respiratory syncytial virus. Sci Rep. https://doi.org/10.1038/srep34108
15. Chen W, Wang Q, Ke Y, et al (2018) Review Article Neutrophil Function in an Inflammatory Milieu of Rheumatoid Arthritis. https://doi.org/10.1155/2018/8549329
16. Bénet T, Sylla M, Messaoudi M, et al (2015) Etiology and factors associated with pneumonia in children under 5 years of age in Mali: A prospective case-control study. PLoS One. https://doi.org/10.1371/journal.pone.0145447

17. Bataki EL, Evans GS, Everard ML (2005) Respiratory syncytial virus and neutrophil activation. Clin Exp Immunol 140:470–477. https://doi.org/10.1111/j.1365-2249.2005.02780.x

18. Shaikh FY, Utley TJ, Craven RE, et al (2012) Respiratory syncytial virus assembles into structured filamentous virion particles independently of host cytoskeleton and related proteins. PLoS One. https://doi.org/10.1371/journal.pone.0040826

19. Funchal GA, Jaeger N, Czepielewski RS, et al (2015) Respiratory syncytial virus fusion protein promotes TLR-4-dependent neutrophil extracellular trap formation by human neutrophils. PLoS One 10:1–14. https://doi.org/10.1371/journal.pone.0124082

20. Brown G, Aitkein J, Rixon HWML, Sugrue RJ (2002) Caveolin-1 is incorporated into mature respiratory syncytial virus particles during virus assembly on the surface of virus-infected cells. J Gen Virol 83:611–621. https://doi.org/10.1099/0022-1317-83-3-611

21. Ludwig A, Nguyen TH, Leong D, et al (2017) Caveolae provide a specialized membrane environment for respiratory syncytial virus assembly. J Cell Sci 130:1037–1050. https://doi.org/10.1242/JCS.198853

22. Kong XH, Shou HC, Liu CY, Jiang ZF (2001) Molecular epidemiology of respiratory syncytial virus. Chin Med J (Engl). https://doi.org/10.1002/rmv.v11:2

23. Collins PL, Melero JA (2011) Progress in understanding and controlling respiratory syncytial virus: Still crazy after all these years. Virus Res.

24. Van Drunen Littel-Van Den Hurk S, Watkiss ER (2012) Pathogenesis of respiratory syncytial virus. Curr. Opin. Virol. 2:300–305

25. Goodwin E, Gilman MSA, Wrapp D, et al (2018) Infants Infected with Respiratory Syncytial Virus Generate Potent Neutralizing Antibodies that Lack Somatic

Hypermutation. Immunity. https://doi.org/10.1016/j.immuni.2018.01.005

26. Valarcher J-F, Schelcher F, Bourhy H (2000) Evolution of Bovine Respiratory Syncytial Virus. J Virol 74:10714–10728. https://doi.org/10.1128/jvi.74.22.10714-10728.2000

27. Fuentes S, Tran KC, Luthra P, et al (2007) Function of the Respiratory Syncytial Virus Small Hydrophobic Protein. J Virol. https://doi.org/10.1128/jvi.02717-06

28. Techaarpornkul S, Barretto N, Peeples ME (2001) Functional Analysis of Recombinant Respiratory Syncytial Virus Deletion Mutants Lacking the Small Hydrophobic and/or Attachment Glycoprotein Gene. J Virol. https://doi.org/10.1128/jvi.75.15.6825-6834.2001

29. Deplance M, Lemaire M, Mirandette C, et al (2007) In vivo evidence for quasispecies distributions in the bovine respiratory syncytial virus genome. J Gen Virol 88:1260–1265. https://doi.org/10.1099/vir.0.82668-0

30. Valarcher JF, Taylor G (2007) Bovine respiratory syncytial virus infection. Vet. Res. 38:153–180

31. Cortjens B, Yasuda E, Yu X, et al (2017) Broadly Reactive Anti-Respiratory Syncytial Virus G Antibodies from Exposed Individuals Effectively Inhibit Infection of Primary Airway Epithelial Cells. J Virol. https://doi.org/10.1128/jvi.02357-16

32. Durbin JE, Johnson TR, Durbin RK, et al (2002) The Role of IFN in Respiratory Syncytial Virus Pathogenesis. J Immunol. https://doi.org/10.4049/jimmunol.168.6.2944

33. Smith BJ, Lawrence MC, Colman PM (2002) Modelling the structure of the fusion protein from human respiratory syncytial virus. Protein Eng. https://doi.org/10.1093/protein/15.5.365

34. McNamara PS, Smyth RL (2002) The pathogenesis of respiratory syncytial virus disease in childhood. Br. Med. Bull.

35. McLellan JS, Ray WC, Peeples ME (2013) Structure and Function of Respiratory Syncytial Virus Surface Glycoproteins. Curr Top Microbiol Immunol. https://doi.org/10.1007/978-3-642-38919-1-4

36. Collins PL, Hill MG, Camargo E, et al (1995) Production of infectious human respiratory syncytial virus from cloned cDNA confirms an essential role for the transcription elongation factor from the 5′ proximal open reading frame of the M2 mRNA in gene expression and provides a capability for vaccine . Proc Natl Acad Sci U S A. https://doi.org/10.1073/pnas.92.25.11563

37. Oshansky CM, Zhang W, Moore E, Tripp RA (2009) The host response and molecular pathogenesis associated with respiratory syncytial virus infection. Future Microbiol.

38. Bermingham A, Collins PL (1999) The M2-2 protein of human respiratory syncytial virus is a regulatory factor involved in the balance between RNA replication and transcription. Proc Natl Acad Sci U S A. https://doi.org/10.1073/pnas.96.20.11259

39. Tayyari F, Marchant D, Moraes TJ, et al (2011) Identification of nucleolin as a cellular receptor for human respiratory syncytial virus. Nat Med. https://doi.org/10.1038/nm.2444

40. Attur M, Krasnokutsky S, Statnikov A, et al (2015) Low-grade inflammation in symptomatic knee osteoarthritis: Prognostic value of inflammatory plasma lipids and peripheral blood leukocyte biomarkers. Arthritis Rheumatol. https://doi.org/10.1002/art.39279

41. Graham BS (2011) Biological challenges and technological opportunities for respiratory syncytial virus vaccine development. Immunol Rev. https://doi.org/10.1111/j.1600-065X.2010.00972.x

42. Shin HB, Choi MS, Yi CM, et al (2015) Inhibition of respiratory syncytial virus

replication and virus-induced p38 kinase activity by berberine. Int Immunopharmacol. https://doi.org/10.1016/j.intimp.2015.04.045

43. Tan L, Lemey P, Houspie L, et al (2012) Genetic Variability among Complete Human Respiratory Syncytial Virus Subgroup A Genomes: Bridging Molecular Evolutionary Dynamics and Epidemiology. PLoS One. https://doi.org/10.1371/journal.pone.0051439

44. Vandini S, Biagi C, Lanari M (2017) Respiratory syncytial virus: The influence of serotype and genotype variability on clinical course of infection. Int. J. Mol. Sci.

45. Sacco RE, McGill JL, Pillatzki AE, et al (2014) Respiratory Syncytial Virus Infection in Cattle. Vet Pathol 51:427–436. https://doi.org/10.1177/0300985813501341

46. Walsh P, Behrens N, Chaigneau FRC, et al (2016) A Randomized Placebo Controlled Trial of Ibuprofen for Respiratory Syncytial Virus Infection in a Bovine Model. PLoS One 11:e0152913. https://doi.org/10.1371/journal.pone.0152913

47. Kim TH, Lee HK (2014) Innate immune recognition of respiratory syncytial virus infection. BMB Rep.

48. Lambert L, Sagfors AM, Openshaw PJM, Culley FJ (2014) Immunity to RSV in early-life. Front. Immunol.

49. Gershwin LJ (1996) Bovine respiratory syncytial virus infection: Immunopathogenic mechanisms. Anim. Heal. Res. Rev. 8:207–213

50. Kalina W V., Woolums AR, Berghaus RD, Gershwin LJ (2004) Formalin-inactivated bovine RSV vaccine enhances a Th2 mediated immune response in infected cattle. Vaccine 22:1465–1474. https://doi.org/10.1016/j.vaccine.2003.10.024

51. Gershwin LJ, Gunther RA, Anderson ML, et al (2000) Bovine respiratory syncytial virus-specific IgE is associated with interleukin-2 and -4, and interferon-γ expression in

pulmonary lymph of experimentally infected calves. Am J Vet Res 61:291–298. https://doi.org/10.2460/ajvr.2000.61.291

52. Van der Poel WHM, Brand A, Kramps JA, Van Oirschot JT (1994) Respiratory syncytial virus infections in human beings and in cattle. J. Infect. 29:215–228

53. Baker JC, Ellis JA, Clark EG (1997) Bovine respiratory syncytial virus. Vet Clin North Am Food Anim Pract 13:425–454. https://doi.org/10.1016/S0749-0720(15)30307-8

54. Klem TB, Kjæstad HP, Kummen E, et al (2016) Bovine respiratory syncytial virus outbreak reduced bulls' weight gain and feed conversion for eight months in a Norwegian beef herd. Acta Vet Scand 58:. https://doi.org/10.1186/s13028-016-0190-y

55. Gershwin LJ, Schelegle ES, Gunther RA, et al (1998) A bovine model of vaccine enhanced respiratory syncytial virus pathophysiology. Vaccine 16:1225–1236. https://doi.org/10.1016/S0264-410X(98)80123-0

56. Thornton H V., Blair PS, Lovering AM, et al (2015) Clinical presentation and microbiological diagnosis in paediatric respiratory tract infection: A systematic review. Br J Gen Pract. https://doi.org/10.3399/bjgp15X683497

57. Panciera RJ, Confer AW (2010) Pathogenesis and pathology of bovine pneumonia. Vet. Clin. North Am. - Food Anim. Pract. 26:191–214

58. Law BJ, Carbonell-Estrany X, Simoes EAF (2002) An update on respiratory syncytial virus epidemiology: A developed country perspective. Respir Med. https://doi.org/10.1053/rmed.2002.1294

59. Mazur NI, Martinón-Torres F, Baraldi E, et al (2015) Lower respiratory tract infection caused by respiratory syncytial virus: Current management and new therapeutics. Lancet Respir. Med.

60. Kim HW, Canchola JG, Brandt CD, et al (1969) Respiratory syncytial virus disease in infants despite prior administration of antigenic inactivated vaccine. Am J Epidemiol 89:422–434. https://doi.org/10.1093/oxfordjournals.aje.a120955

61. Ciszewski DK, Baker JC, Slocombe RF, et al (1991) Experimental reproduction of respiratory tract disease with bovine respiratory syncytial virus. Vet Microbiol 28:39–60. https://doi.org/10.1016/0378-1135(91)90098-Z

62. Peebles RS, Graham BS (2005) Pathogenesis of respiratory syncytial virus infection in the murine model. In: Proceedings of the American Thoracic Society

63. Griffiths C, Drews SJ, Marchant DJ (2017) Respiratory syncytial virus: Infection, detection, and new options for prevention and treatment. Am Soc Microbiol. https://doi.org/10.1128/CMR.00010-16

64. Antonis AFG, Schrijver RS, Daus F, et al (2003) Vaccine-Induced Immunopathology during Bovine Respiratory Syncytial Virus Infection: Exploring the Parameters of Pathogenesis. J Virol 77:12067–12073. https://doi.org/10.1128/jvi.77.22.12067-12073.2003

65. González PA, Bueno SM, Carreño LJ, et al (2012) Respiratory syncytial virus infection and immunity. Rev. Med. Virol.

66. Hall CB, Simoes EAF, Anderson LJ, et al (2013) Clinical and Epidemiologic Features of Respiratory Syncytial Virus. Curr Top Microbiol Immunol. https://doi.org/10.1007/978-3-642-38919-1_2

67. Altincicek B, Stötzel S, Wygrecka M, et al (2008) Host-Derived Extracellular Nucleic Acids Enhance Innate Immune Responses, Induce Coagulation, and Prolong Survival upon Infection in Insects. J Immunol 181:2705–2712.

https://doi.org/10.4049/jimmunol.181.4.2705

68. Kalina W V., Anderson ML, Gershwin LJ (2006) Alternaria aerosol during a bovine respiratory syncytial virus infection alters the severity of subsequent re-infection and enhances IgE production. Comp Immunol Microbiol Infect Dis 29:138–156. https://doi.org/10.1016/j.cimid.2006.03.002

69. Baker DG, Gershwin LJ, Giri SN, Li C (1993) Cellular and chemical mediators of type 1 hypersensitivity in calves infected with Ostertagia ostertagi: Histamine, prostaglandin D2 prostaglandin E2 and leukotriene C4. Int J Parasitol 23:333–339. https://doi.org/10.1016/0020-7519(93)90008-M

70. Olivier A, Gallup J, De MacEdo MMMA, et al (2009) Human respiratory syncytial virus A2 strain replicates and induces innate immune responses by respiratory epithelia of neonatal lambs. Int J Exp Pathol. https://doi.org/10.1111/j.1365-2613.2009.00643.x

71. Johnson JE, Gonzales RA, Olson SJ, et al (2007) The histopathology of fatal untreated human respiratory syncytial virus infection. Mod Pathol. https://doi.org/10.1038/modpathol.3800725

72. Cortjens B, Lutter R, Boon L, et al (2016) Pneumovirus-induced lung disease in mice is independent of neutrophil-driven inflammation. PLoS One. https://doi.org/10.1371/journal.pone.0168779

73. Muraro SP, De Souza GF, Gallo SW, et al (2018) Respiratory Syncytial Virus induces the classical ROS-dependent NETosis through PAD-4 and necroptosis pathways activation. Sci Rep 8:1–12. https://doi.org/10.1038/s41598-018-32576-y

74. de Boer OJ, de Jong R, Antonis AFFGF, et al (2016) Neutrophil extracellular traps cause airway obstruction during respiratory syncytial virus disease. J Pathol 238:401–411.

https://doi.org/10.1002/path.4660

75. Cortjens B, De Boer OJ, De Jong R, et al (2016) Neutrophil extracellular traps cause airway obstruction during respiratory syncytial virus disease. J Pathol. https://doi.org/10.1002/path.4660

76. B. C, O.J. DB, A.F.G. A, et al (2015) Neutrophil extracellular trap formation in severe respiratory syncytial virus lung infection. Am. J. Respir. Crit. Care Med.

77. Saffarzadeh M, Juenemann C, Queisser MA, et al (2012) Neutrophil extracellular traps directly induce epithelial and endothelial cell death: A predominant role of histones. PLoS One 7:. https://doi.org/10.1371/journal.pone.0032366

78. Paes BA, Mitchell I, Banerji A, et al (2011) A decade of respiratory syncytial virus epidemiology and prophylaxis: Translating evidence into everyday clinical practice. Can. Respir. J.

79. Bont L, Checchia PA, Fauroux B, et al (2016) Defining the Epidemiology and Burden of Severe Respiratory Syncytial Virus Infection Among Infants and Children in Western Countries. Infect. Dis. Ther.

80. Holman RC, Curns AT, Cheek JE, et al (2004) Respiratory syncytial virus hospitalizations among American Indian and Alaska Native infants and the general United States infant population. Pediatrics. https://doi.org/10.1542/peds.2004-0049

81. Obando-Pacheco P, Justicia-Grande AJ, Rivero-Calle I, et al (2018) Respiratory syncytial virus seasonality: A global overview. J. Infect. Dis.

82. Jansen AGSC, Sanders EAM, Van der Ende A, et al (2008) Invasive pneumococcal and meningococcal disease: Association with influenza virus and respiratory syncytial virus activity? Epidemiol Infect. https://doi.org/10.1017/S0950268807000271

83. Yusuf S, Piedimonte G, Auais A, et al (2007) The relationship of meteorological conditions to the epidemic activity of respiratory syncytial virus. Epidemiol. Infect.

84. Urban-Chmiel R, Wernicki A, Puchalski A, et al (2015) Detection of bovine respiratory syncytial virus infections in young dairy and beef cattle in Poland. Vet Q 35:33–36. https://doi.org/10.1080/01652176.2014.984366

85. Pecchini R, Berezin EN, Felício MCC, et al (2008) Incidence and clinical characteristics of the infection by the Respiratory Syncytial Virus in children admitted in Santa Casa de São Paulo Hospital. Brazilian J Infect Dis. https://doi.org/10.1590/S1413-86702008000600006

86. Schickli JH, Dubovsky F, Tang RS (2009) Challenges in developing a pediatric RSV vaccine. Hum. Vaccin.

87. Blanco JCG, Boukhvalova MS, Shirey KA, et al (2010) New insights for development of a safe and protective RSV vaccine. Hum. Vaccin.

88. Openshaw PJM, Chiu C, Culley FJ, Johansson C (2017) Protective and harmful immunity to RSV infection. Annu. Rev. Immunol.

89. Olson MR, Varga SM (2007) CD8 T Cells Inhibit Respiratory Syncytial Virus (RSV) Vaccine-Enhanced Disease. J Immunol. https://doi.org/10.4049/jimmunol.179.8.5415

90. Lindell DM, Morris SB, White MP, et al (2011) A Novel Inactivated Intranasal Respiratory Syncytial Virus Vaccine Promotes Viral Clearance without Th2 Associated Vaccine-Enhanced Disease. PLoS One 6:e21823. https://doi.org/10.1371/journal.pone.0021823

91. Donner L, Turek L, Svoboda J (1974) Absence of RSV production in enucleated RSV-transformed virogenic mammalian cells fused with chick embryo fibroblasts. Int J Cancer.

https://doi.org/10.1002/ijc.2910140513

92. Knudson CJ, Varga SM (2015) The Relationship Between Respiratory Syncytial Virus and Asthma. Vet Pathol. https://doi.org/10.1177/0300985814520639

93. Schmidt U, Beyer J, Polster U, et al (2002) Mucosal Immunization with Live Recombinant Bovine Respiratory Syncytial Virus (BRSV) and Recombinant BRSV Lacking the Envelope Glycoprotein G Protects against Challenge with Wild-Type BRSV. J Virol 76:12355–12359. https://doi.org/10.1128/jvi.76.23.12355-12359.2002

94. Tripp RA, Power UF, Openshaw PJM, Kauvar LM (2017) Respiratory Syncytial Virus: Targeting the G Protein Provides a New Approach for an Old Problem. J Virol. https://doi.org/10.1128/jvi.01302-17

95. Amulic B, Cazalet C, Hayes GL, et al (2012) Neutrophil Function: From Mechanisms to Disease. Annu Rev Immunol 30:459–489. https://doi.org/10.1146/annurev-immunol-020711-074942

96. McCarthy AJ, Lindsay JA (2013) Staphylococcus aureus innate immune evasion is lineage-specific: A bioinfomatics study. Infect Genet Evol. https://doi.org/10.1016/j.meegid.2013.06.012

97. Brinkmann V, Zychlinsky A (2007) Beneficial suicide: Why neutrophils die to make NETs. Nat Rev Microbiol 5:577–582. https://doi.org/10.1038/nrmicro1710

98. Fuchs TA, Abed U, Goosmann C, et al (2007) Novel cell death program leads to neutrophil extracellular traps. J Cell Biol 176:231–241. https://doi.org/10.1083/jcb.200606027

99. Brinkmann V, Reichard U, Goosmann C, et al (2004) Neutrophil Extracellular Traps Kill Bacteria. Science (80-) 303:1532–1535. https://doi.org/10.1126/science.1092385

100. Rodríguez-Espinosa O, Rojas-Espinosa O, Moreno-Altamirano MMB, et al (2015) Metabolic requirements for neutrophil extracellular traps formation. Immunology 145:213–224. https://doi.org/10.1111/imm.12437

101. Kolaczkowska E, Jenne CN, Surewaard BGJ, et al (2015) Molecular mechanisms of NET formation and degradation revealed by intravital imaging in the liver vasculature. Nat Commun 6:6673. https://doi.org/10.1038/ncomms7673

102. Parkes G, Clare S, Goulding D, et al (2006) Neutrophil activation and neutrophil extracellular trap formation in inflammatory bowel disease. Gastroenterology

103. Kaplan MJ, Radic M (2012) Neutrophil Extracellular Traps: Double-Edged Swords of Innate Immunity. J Immunol 189:2689–2695. https://doi.org/10.4049/jimmunol.1201719

104. Lee KH, Kronbichler A, Park DDY, et al (2017) Neutrophil extracellular traps (NETs) in autoimmune diseases: A comprehensive review. Autoimmun. Rev.

105. Manda-Handzlik A, Fiok K, Cieloch A, et al (2020) Convolutional Neural Networks–Based Image Analysis for the Detection and Quantification of Neutrophil Extracellular Traps. Cells 9:508. https://doi.org/10.3390/cells9020508

106. Sørensen OE, Borregaard N (2016) Neutrophil extracellular traps - The dark side of neutrophils. J. Clin. Invest. 126:1612–1620

107. Khandpur R, Carmona-Rivera C, Vivekanandan-Giri A, et al (2013) NETs are a source of citrullinated autoantigens and stimulate inflammatory responses in rheumatoid arthritis. Sci Transl Med 5:178ra40. https://doi.org/10.1126/scitranslmed.3005580

108. Abdallah DSA, Lin C, Ball CJ, et al (2012) Toxoplasma gondii triggers release of human and mouse neutrophil extracellular traps. Infect Immun 80:768–777. https://doi.org/10.1128/IAI.05730-11

109. Wang Y, Li M, Stadler S, et al (2009) Histone hypercitrullination mediates chromatin decondensation and neutrophil extracellular trap formation. J Cell Biol 184:205–213. https://doi.org/10.1083/jcb.200806072

110. Delgado-Rizo V, Martínez-Guzmán MA, Iñiguez-Gutierrez L, et al (2017) Neutrophil extracellular traps and its implications in inflammation: An overview. Front. Immunol. 8:81

111. Martinod K, Demers M, Fuchs TA, et al (2013) Neutrophil histone modification by peptidylarginine deiminase 4 is critical for deep vein thrombosis in mice. Proc Natl Acad Sci U S A 110:8674–8679. https://doi.org/10.1073/pnas.1301059110

112. Parker H, Winterbourn CC (2013) Reactive oxidants and myeloperoxidase and their involvement in neutrophil extracellular traps. Front Immunol 3:424. https://doi.org/10.3389/fimmu.2012.00424

113. Chen R, Kang R, Fan XG, Tang D (2014) Release and activity of histone in diseases. Cell Death Dis.

114. Lewis HD, Liddle J, Coote JE, et al (2015) Inhibition of PAD4 activity is sufficient to disrupt mouse and human NET formation. Nat Chem Biol 11:189–191. https://doi.org/10.1038/nchembio.1735

115. Nakashima K, Arai S, Suzuki A, et al (2013) PAD4 regulates proliferation of multipotent haematopoietic cells by controlling c-myc expression. Nat Commun. https://doi.org/10.1038/ncomms2862

116. Opasawatchai A, Amornsupawat P, Jiravejchakul N, et al (2019) Neutrophil activation and early features of net formation are associated with dengue virus infection in human. Front Immunol 10:. https://doi.org/10.3389/fimmu.2018.03007

117. Hoeksema M, Tripathi S, White M, et al (2015) Arginine-rich histones have strong antiviral activity for influenza A viruses. Innate Immun 21:736–745. https://doi.org/10.1177/1753425915593794

118. Li RHL, Johnson LR, Kohen C, Tablin F (2018) A novel approach to identifying and quantifying neutrophil extracellular trap formation in septic dogs using immunofluorescence microscopy. BMC Vet Res 14:1–7. https://doi.org/10.1186/s12917-018-1523-z

119. Reeves EP, Lu H, Jacobs HL, et al (2002) Killing activity of neutrophils is mediated through activation of proteases by K+ flux. Nature 416:291–297. https://doi.org/10.1038/416291a

120. Patel S, Kumar S, Jyoti A, et al (2010) Nitric oxide donors release extracellular traps from human neutrophils by augmenting free radical generation. Nitric Oxide - Biol Chem 22:226–234. https://doi.org/10.1016/j.niox.2010.01.001

121. Souza PSS, Barbosa LV, Diniz LFA, et al (2018) Neutrophil extracellular traps possess anti-human respiratory syncytial virus activity: Possible interaction with the viral F protein. Virus Res 251:68–77. https://doi.org/10.1016/j.virusres.2018.04.001

122. Kühnle A, Lütteke T, Bornhöfft K, Galuska S (2019) Polysialic Acid Modulates the Binding of External Lactoferrin in Neutrophil Extracellular Traps. Biology (Basel) 8:20. https://doi.org/10.3390/biology8020020

123. Moraes TJ, Zurawska JH, Downey GP (2006) Neutrophil granule contents in the pathogenesis of lung injury. Curr. Opin. Hematol. 13:21–27

124. Papayannopoulos V, Metzler KD, Hakkim A, Zychlinsky A (2010) Neutrophil elastase and myeloperoxidase regulate the formation of neutrophil extracellular traps. J Cell Biol

191:677–691. https://doi.org/10.1083/jcb.201006052

125. Castellana B, Lerma E, Serrano E, et al (2011) Down-regulation of proliferation and cell adhesion and up-regulation of cell migration associated genes in lobular breast carcinomas. Lab Investig

126. Gray RD, McCullagh BN, McCray PB (2015) NETs and CF lung disease: Current status and future prospects. Antibiotics 4:62–75

127. Farley K, Stolley JM, Zhao P, et al (2012) A SerpinB1 Regulatory Mechanism Is Essential for Restricting Neutrophil Extracellular Trap Generation. J Immunol 189:4574–4581. https://doi.org/10.4049/jimmunol.1201167

128. Huang H, Tohme S, Al-Khafaji AB, et al (2015) Damage-associated molecular pattern-activated neutrophil extracellular trap exacerbates sterile inflammatory liver injury. Hepatology 62:600–614. https://doi.org/10.1002/hep.27841

129. Dinallo V, Marafini I, Fusco D Di, et al (2019) Neutrophil extracellulartraps sustain inflammatory signals in ulcerative colitis. J Crohn's Colitis. https://doi.org/10.1093/ecco-jcc/jjy215

130. Kenny EF, Herzig A, Krüger R, et al (2017) Diverse stimuli engage different neutrophil extracellular trap pathways. Elife 6:. https://doi.org/10.7554/eLife.24437

131. Tang D, Kang R, Zeh HJ, Lotze MT (2011) High-mobility group box 1, oxidative stress, and disease. Antioxidants Redox Signal.

132. Bravo-Barrera J, Kourilovitch M, Galarza-Maldonado C (2017) Neutrophil Extracellular Traps, Antiphospholipid Antibodies and Treatment. Antibodies 6:4. https://doi.org/10.3390/antib6010004

133. Branzk N, Lubojemska A, Hardison SE, et al (2014) Neutrophils sense microbe size and

selectively release neutrophil extracellular traps in response to large pathogens. Nat Immunol 15:1017–1025. https://doi.org/10.1038/ni.2987

134. Keshari RS, Jyoti A, Dubey M, et al (2012) Cytokines Induced Neutrophil Extracellular Traps Formation: Implication for the Inflammatory Disease Condition. PLoS One 7:. https://doi.org/10.1371/journal.pone.0048111

135. Díaz-Godínez C, Carrero JC (2019) The state of art of neutrophil extracellular traps in protozoan and helminthic infections. Biosci. Rep. 39

136. Manfredi AA, Ramirez GA, Rovere-Querini P, Maugeri N (2018) The neutrophil's choice: Phagocytose vs make neutrophil extracellular traps. Front. Immunol. 9:1

137. Schauer C, Janko C, Munoz LE, et al (2014) Aggregated neutrophil extracellular traps limit inflammation by degrading cytokines and chemokines. Nat Med 20:511–517. https://doi.org/10.1038/nm.3547

138. Ramos-Kichik V, Mondragón-Flores R, Mondragón-Castelán M, et al (2009) Neutrophil extracellular traps are induced by Mycobacterium tuberculosis. Tuberculosis 89:29–37. https://doi.org/10.1016/j.tube.2008.09.009

139. Dang G, Cui Y, Wang L, et al (2018) Extracellular Sphingomyelinase Rv0888 of Mycobacterium tuberculosis Contributes to Pathological Lung Injury of Mycobacterium smegmatis in Mice via Inducing Formation of Neutrophil Extracellular Traps. Front Immunol 9:677. https://doi.org/10.3389/fimmu.2018.00677

140. Spaan AN, Surewaard BGJ, Nijland R, van Strijp JAG (2013) Neutrophils Versus Staphylococcus aureus : A Biological Tug of War . Annu Rev Microbiol 67:629–650. https://doi.org/10.1146/annurev-micro-092412-155746

141. Jin T, Bokarewa M, Foster T, et al (2004) Staphylococcus aureus Resists Human

Defensins by Production of Staphylokinase, a Novel Bacterial Evasion Mechanism . J Immunol 172:1169–1176. https://doi.org/10.4049/jimmunol.172.2.1169

142. Narayana Moorthy A, Narasaraju T, Rai P, et al (2013) In vivo and in vitro studies on the roles of neutrophil extracellular traps during secondary pneumococcal pneumonia after primary pulmonary influenza infection. Front Immunol 4:56. https://doi.org/10.3389/fimmu.2013.00056

143. Saitoh T, Komano J, Saitoh Y, et al (2012) Neutrophil extracellular traps mediate a host defense response to human immunodeficiency virus-1. Cell Host Microbe 12:109–116. https://doi.org/10.1016/j.chom.2012.05.015

144. Murawski MR, Bowen GN, Cerny AM, et al (2009) Respiratory Syncytial Virus Activates Innate Immunity through Toll-Like Receptor 2. J Virol. https://doi.org/10.1128/jvi.00671-08

145. Kurt-Jones EA, Popova L, Kwinn L, et al (2000) Pattern recognition receptors TLR4 and CD14 mediate response to respiratory syncytial virus. Nat Immunol. https://doi.org/10.1038/80833

146. Petretto A, Bruschi M, Pratesi F, et al (2019) Neutrophil extracellular traps (NET) induced by different stimuli: A comparative proteomic analysis. PLoS One 14:e0218946. https://doi.org/10.1371/journal.pone.0218946

147. Bruschi M, Bonanni A, Petretto A, et al (2020) Neutrophil Extracellular Traps Profiles in Patients with Incident Systemic Lupus Erythematosus and Lupus Nephritis. J Rheumatol 47:377–386. https://doi.org/10.3899/jrheum.181232

148. Park J, Wysocki RW, Amoozgar Z, et al (2016) Cancer cells induce metastasis-supporting neutrophil extracellular DNA traps. Sci Transl Med 8:.

https://doi.org/10.1126/scitranslmed.aag1711

149. Liu D, Yang P, Gao M, et al (2019) NLRP3 activation induced by neutrophil extracellular traps sustains inflammatory response in the diabetic wound. Clin Sci 133:565–582. https://doi.org/10.1042/CS20180600

150. Hirota T, Levy JH, Iba T (2020) The influence of hyperglycemia on neutrophil extracellular trap formation and endothelial glycocalyx damage in a mouse model of type 2 diabetes. Microcirculation. https://doi.org/10.1111/micc.12617

151. Clark SR, Ma AC, Tavener SA, et al (2007) Platelet TLR4 activates neutrophil extracellular traps to ensnare bacteria in septic blood. Nat Med 13:463–469. https://doi.org/10.1038/nm1565

152. Vogel S, Bodenstein R, Chen Q, et al (2015) Platelet-derived HMGB1 is a critical mediator of thrombosis. J Clin Invest 125:4638–4654. https://doi.org/10.1172/JCI81660

153. Etulain J, Martinod K, Wong SL, et al (2015) P-selectin promotes neutrophil extracellular trap formation in mice. Blood 126:242–246. https://doi.org/10.1182/blood-2015-01-624023

154. Brinkmann V, Zychlinsky A (2012) Neutrophil extracellular traps: Is immunity the second function of chromatin? J. Cell Biol. 198:773–783

155. Neumann A, Berends ETM, Nerlich A, et al (2014) The antimicrobial peptide LL-37 facilitates the formation of neutrophil extracellular traps. Biochem J 464:3–11. https://doi.org/10.1042/BJ20140778

156. Burgener SS, Schroder K (2019) Neutrophil Extracellular Traps in Host Defense. https://doi.org/10.1101/cshperspect.a037028

157. Li RHL, Tablin F (2018) A comparative review of neutrophil extracellular traps in sepsis.

Front. Vet. Sci. 5:291

158. Ekaney ML, Otto GP, Sossdorf M, et al (2014) Impact of plasma histones in human sepsis and their contribution to cellular injury and inflammation. Crit Care 18:543. https://doi.org/10.1186/s13054-014-0543-8

159. Akgul C, Moulding DA, Edwards SW (2001) Molecular control of neutrophil apoptosis. FEBS Lett. 487:318–322

160. Xu J, Zhang X, Pelayo R, et al (2009) Extracellular histones are major mediators of death in sepsis. Nat Med 15:1318–1321. https://doi.org/10.1038/nm.2053

161. Abrams ST, Zhang N, Manson J, et al (2013) Circulating histones are mediators of trauma-associated lung injury. Am J Respir Crit Care Med 187:160–169. https://doi.org/10.1164/rccm.201206-1037OC

162. Mutua V, Gershwin LJ (2020) A Review of Neutrophil Extracellular Traps (NETs) in Disease: Potential Anti-NETs Therapeutics. Clin. Rev. Allergy Immunol. 1

163. Pasha MA, Patel G, Hopp R, Yang Q (2019) Role of innate lymphoid cells in allergic diseases. Allergy Asthma Proc 40:138–145. https://doi.org/10.2500/aap.2019.40.4217

164. Goldberg R, Prescott N, Lord GM, et al (2015) The unusual suspects - Innate lymphoid cells as novel therapeutic targets in IBD. Nat. Rev. Gastroenterol. Hepatol.

165. De Obaldia ME, Bhandoola A (2015) Transcriptional regulation of innate and adaptive lymphocyte lineages. Annu Rev Immunol. https://doi.org/10.1146/annurev-immunol-032414-112032

166. Monticelli LA, Sonnenberg GF, Abt MC, et al (2011) Innate lymphoid cells promote lung-tissue homeostasis after infection with influenza virus. Nat Immunol. https://doi.org/10.1038/ni.2131

167. Monticelli LA, Sonnenberg GF, Abt MC, et al (2016) Human innate lymphoid cells. Nat Immunol 40:1–12. https://doi.org/10.1016/j.immuni.2017.01.008

168. Sonnenberg GF, Artis D (2015) Innate lymphoid cells in the initiation, regulation and resolution of inflammation. Nat. Med.

169. Klose CSN, Flach M, Möhle L, et al (2014) Differentiation of type 1 ILCs from a common progenitor to all helper-like innate lymphoid cell lineages. Cell. https://doi.org/10.1016/j.cell.2014.03.030

170. Hepworth MR, Monticelli LA, Fung TC, et al (2013) Innate lymphoid cells regulate CD4 + T-cell responses to intestinal commensal bacteria. Nature. https://doi.org/10.1038/nature12240

171. Robinette ML, Fuchs A, Cortez VS, et al (2015) Transcriptional programs define molecular characteristics of innate lymphoid cell classes and subsets. Nat Immunol. https://doi.org/10.1038/ni.3094

172. Constantinides MG, McDonald BD, Verhoef PA, Bendelac A (2014) A committed precursor to innate lymphoid cells. Nature. https://doi.org/10.1038/nature13047

173. Gronke K, Kofoed-Nielsen M, Diefenbach A (2016) Innate lymphoid cells, precursors and plasticity. Immunol Lett. https://doi.org/10.1016/j.imlet.2016.07.004

174. Ishizuka IE, Chea S, Gudjonson H, et al (2016) Single-cell analysis defines the divergence between the innate lymphoid cell lineage and lymphoid tissue-inducer cell lineage. Nat Immunol. https://doi.org/10.1038/ni.3344

175. Diefenbach A, Colonna M, Koyasu S (2014) Development, differentiation, and diversity of innate lymphoid cells. Immunity

176. Bar-Ephraïm YE, Mebius RE (2016) Innate lymphoid cells in secondary lymphoid organs.

Immunol Rev. https://doi.org/10.1111/imr.12407

177. Spits H, Artis D, Colonna M, et al (2013) Innate lymphoid cells-a proposal for uniform nomenclature. Nat Rev Immunol. https://doi.org/10.1038/nri3365

178. Vivier E, Artis D, Colonna M, et al (2018) Innate Lymphoid Cells: 10 Years On. Cell

179. Kruse PH, Matta J, Ugolini S, Vivier E (2014) Natural cytotoxicity receptors and their ligands. Immunol. Cell Biol.

180. Mortha A, Burrows K (2018) Cytokine networks between innate lymphoid cells and myeloid cells. Front. Immunol.

181. Cortez VS, Cervantes-Barragan L, Robinette ML, et al (2016) Transforming Growth Factor-β Signaling Guides the Differentiation of Innate Lymphoid Cells in Salivary Glands. Immunity. https://doi.org/10.1016/j.immuni.2016.03.007

182. Banchereau J, Steinman RM (1998) Dendritic cells and the control of immunity. Nature

183. Bellucci R, Martin A, Bommarito D, et al (2015) Interferon-γ-induced activation of JAK1 and JAK2 suppresses tumor cell susceptibility to NK cells through upregulation of PD-L1 expression. Oncoimmunology. https://doi.org/10.1080/2162402X.2015.1008824

184. Cortez VS, Colonna M (2016) Diversity and function of group 1 innate lymphoid cells. Immunol. Lett.

185. Hazenberg MD, Spits H (2014) Human innate lymphoid cells. Blood

186. Hazenberg MD, Spits H (2014) Human innate lymphoid cells. Blood. https://doi.org/10.1182/blood-2013-11-427781.There

187. Wang X, Tian Z, Peng H (2020) Tissue-resident memory-like ILCs: innate counterparts of TRM cells. Protein Cell

188. Mace EM, Orange JS (2019) Emerging insights into human health and NK cell biology

from the study of NK cell deficiencies. Immunol. Rev.

189. Ma Q (2020) Polarization of Immune Cells in the Pathologic Response to Inhaled Particulates. Front. Immunol.

190. D. M, K. M, V. G-F, et al (2018) Innate lymphoid cells in the maternal and fetal compartments. Front Immunol. https://doi.org/10.3389/fimmu.2018.02396

191. Mamareli P, Kruse F, Lu C wen, et al (2020) Targeting cellular fatty acid synthesis limits T helper and innate lymphoid cell function during intestinal inflammation and infection. Mucosal Immunol. https://doi.org/10.1038/s41385-020-0285-7

192. Boulenouar S, Michelet X, Duquette D, et al (2017) Adipose Type One Innate Lymphoid Cells Regulate Macrophage Homeostasis through Targeted Cytotoxicity. Immunity. https://doi.org/10.1016/j.immuni.2017.01.008

193. Lim AI, Verrier T, Vosshenrich CA, Di Santo JP (2017) Developmental options and functional plasticity of innate lymphoid cells. Curr. Opin. Immunol.

194. Crome SQ, Nguyen LT, Lopez-Verges S, et al (2017) A distinct innate lymphoid cell population regulates tumor-associated T cells. Nat Med. https://doi.org/10.1038/nm.4278

195. Moskalenko M, Pan M, Fu Y, et al (2015) Requirement for innate immunity and CD90 NK1.1 lymphocytes to treat established melanoma with chemo-immunotherapy. Cancer Immunol Res. https://doi.org/10.1158/2326-6066.CIR-14-0120

196. Brady CM, Brosens JJ, Moffett A, et al (2015) Uterine Innate Lymphoid Cells Composition, Development, and Function of Composition, Development, and Function of Uterine Innate Lymphoid Cells. J Immunol

197. Mckenzie ANJ, Mckenzie NJ (2014) TRANSATLANTIC AIRWAY CONFERENCE Type-2 Innate Lymphoid Cells in Asthma and Allergy. Ann Am Thorac Soc

198. Forkel M, Berglin L, Kekäläinen E, et al (2017) Composition and functionality of the intrahepatic innate lymphoid cell-compartment in human nonfibrotic and fibrotic livers. Eur J Immunol. https://doi.org/10.1002/eji.201646890

199. Kim BS, Siracusa MC, Saenz SA, et al (2013) TSLP elicits IL-33-independent innate lymphoid cell responses to promote skin inflammation. Sci Transl Med. https://doi.org/10.1126/scitranslmed.3005374

200. Hams E, Locksley RM, Mckenzie ANJ, Fallon PG (2013) IL-25 elicits innate lymphoid type 2 and type II natural killer T cells that regulate obesity in mice 1 Europe PMC Funders Group. J Immunol

201. Barnig C, Cernadas M, Dutile S, et al (2013) Lipoxin A4 regulates natural killer cell and type 2 innate lymphoid cell activation in asthma. Sci Transl Med. https://doi.org/10.1126/scitranslmed.3004812

202. Mjösberg JM, Trifari S, Crellin NK, et al (2011) Human IL-25-and IL-33-responsive type 2 innate lymphoid cells are defined by expression of CRTH2 and CD161. Nat Immunol. https://doi.org/10.1038/ni.2104

203. Doherty TA, Khorram N, Lund S, et al (2013) Lung type 2 innate lymphoid cells express cysteinyl leukotriene receptor 1, which regulates TH2 cytokine production. J Allergy Clin Immunol. https://doi.org/10.1016/j.jaci.2013.03.048

204. Monticelli LA, Sonnenberg GF, Abt MC, et al (2012) Innate lymphoid cells promote lung tissue homeostasis following acute influenza virus infection. Nat Immunol

205. Monticelli LA, Osborne LC, Noti M, et al (2015) IL-33 promotes an innate immune pathway of intestinal tissue protection dependent on amphiregulin-EGFR interactions. Proc Natl Acad Sci U S A. https://doi.org/10.1073/pnas.1509070112

206. Katsikis PD, Schoenberger SP, Mourao-sa D, Roy S (2013) Crossroads Between Innate and Adaptive Immunity IV. Adv Exp Med Biol

207. Tait Wojno ED, Artis D (2012) Innate lymphoid cells: Balancing immunity, inflammation, and tissue repair in the intestine. Cell Host Microbe

208. Hung LY, Sen D, Oniskey TK, et al (2019) Macrophages promote epithelial proliferation following infectious and non-infectious lung injury through a Trefoil factor 2-dependent mechanism. Mucosal Immunol. https://doi.org/10.1038/s41385-018-0096-2

209. Omar SZ, Blom B, Hazenberg MD (2020) Innate lymphoid cells in treatment-induced gastrointestinal pathogenesis. Curr Opin Support Palliat Care. https://doi.org/10.1097/SPC.0000000000000499

210. Allan DSJ, Kirkham CL, Aguilar OA, et al (2015) An in vitro model of innate lymphoid cell function and differentiation. Mucosal Immunol. https://doi.org/10.1038/mi.2014.71

211. Leijten EFA, van Kempen TS, Boes M, et al (2015) Brief report: enrichment of activated group 3 innate lymphoid cells in psoriatic arthritis synovial fluid. Arthritis Rheumatol (Hoboken, NJ). https://doi.org/10.1002/art.39261

212. Yang FC, Chiu PY, Chen Y, et al (2019) TREM-1-dependent M1 macrophage polarization restores intestinal epithelium damaged by DSS-induced colitis by activating IL-22-producing innate lymphoid cells. J Biomed Sci. https://doi.org/10.1186/s12929-019-0539-4

213. Geremia A, Arancibia-Cárcamo C V., Fleming MPP, et al (2011) IL-23-responsive innate lymphoid cells are increased in inflammatory bowel disease. J Exp Med. https://doi.org/10.1084/jem.20101712

214. F. C, G. G, A. R, et al (2014) Gut derived IL-23r+CD3+/CD3-CD4-CD8-CD56+RORc-T-

bet+ NKp44+ innate lymphoid cells are expanded in the peripheral blood, synovial fluid and bone marrow of ankylosing spondylitis patients. Clin. Exp. Rheumatol.

215. C.A. L, A. M, M.H. O, et al (2014) IL-22 is an intestinal stem cell growth factor, and IL-22 administration in vivo reduces morbidity and mortality in murine GvHD. Blood

216. Castro-Dopico T, Fleming A, Dennison TW, et al (2020) GM-CSF Calibrates Macrophage Defense and Wound Healing Programs during Intestinal Infection and Inflammation. Cell Rep. https://doi.org/10.1016/j.celrep.2020.107857

217. Mortha A, Chudnovskiy A, Hashimoto D, et al (2014) Microbiota-dependent crosstalk between macrophages and ILC3 promotes intestinal homeostasis. Science (80-). https://doi.org/10.1126/science.1249288

218. Baerenwaldt A, von Burg N, Kreuzaler M, et al (2016) Flt3 Ligand Regulates the Development of Innate Lymphoid Cells in Fetal and Adult Mice. J Immunol. https://doi.org/10.4049/jimmunol.1501380

219. Bando JK, Liang HE, Locksley RM (2015) Identification and distribution of developing innate lymphoid cells in the fetal mouse intestine. Nat Immunol. https://doi.org/10.1038/ni.3057

220. Vondenhoff MF, Greuter M, Goverse G, et al (2009) LTβR Signaling Induces Cytokine Expression and Up-Regulates Lymphangiogenic Factors in Lymph Node Anlagen. J Immunol. https://doi.org/10.4049/jimmunol.0801165

221. Spits H, Di Santo JP (2011) The expanding family of innate lymphoid cells: Regulators and effectors of immunity and tissue remodeling. Nat. Immunol.

222. Bénézech C, White A, Mader E, et al (2010) Ontogeny of Stromal Organizer Cells during Lymph Node Development. J Immunol. https://doi.org/10.4049/jimmunol.0903113

223. Van De Pavert SA, Olivier BJ, Goverse G, et al (2009) Chemokine cxcl13 is essential for lymph node initiation and is induced by retinoic acid and neuronal stimulation. Nat Immunol. https://doi.org/10.1038/ni.1789

224. Gury-BenAri M, Thaiss CA, Serafini N, et al (2016) The Spectrum and Regulatory Landscape of Intestinal Innate Lymphoid Cells Are Shaped by the Microbiome. Cell. https://doi.org/10.1016/j.cell.2016.07.043

225. Colonna M (2018) Innate Lymphoid Cells: Diversity, Plasticity, and Unique Functions in Immunity. Immunity

226. Bal SM, Golebski K, Spits H (2020) Plasticity of innate lymphoid cell subsets. Nat. Rev. Immunol.

227. Nussbaum K, Burkhard SH, Ohs I, et al (2017) Tissue microenvironment dictates the fate and tumorsuppressive function of type 3 ILCs. J Exp Med. https://doi.org/10.1084/jem.20162031

228. Silver JS, Kearley J, Copenhaver AM, et al (2016) Inflammatory triggers associated with exacerbations of COPD orchestrate plasticity of group 2 innate lymphoid cells in the lungs. Nat Immunol. https://doi.org/10.1038/ni.3443

229. Mjösberg J, Bernink J, Peters C, Spits H (2012) Transcriptional control of innate lymphoid cells. Eur. J. Immunol.

230. Stier MT, Bloodworth MH, Toki S, et al (2016) Respiratory syncytial virus infection activates IL-13–producing group 2 innate lymphoid cells through thymic stromal lymphopoietin. J Allergy Clin Immunol. https://doi.org/10.1016/j.jaci.2016.01.050

231. Stier MT, Goleniewska K, Cephus JY, et al (2017) STAT1 Represses Cytokine-Producing Group 2 and Group 3 Innate Lymphoid Cells during Viral Infection. J Immunol.

https://doi.org/10.4049/jimmunol.1601984

232. Mjösberg J, Spits H (2016) Human innate lymphoid cells. J Allergy Clin Immunol. https://doi.org/10.1016/j.jaci.2016.09.009

233. Licona-Limón P, Kim LK, Palm NW, Flavell RA (2013) TH2, allergy and group 2 innate lymphoid cells. Nat. Immunol.

234. Saravia J, You D, DeVincenzo J, et al (2014) Group 2 innate lymphoid cells and IL-33 in infant respiratory syncytial virus infection. J Immunol

CHAPTER 2

2. Animal Experimental Design and Treatment

2.1 Abstract

A number of antiviral drugs for RSV are under development. Unfortunately, bovine studies suggest that most of these drugs will need to be given very early in the course of illness[1]. The Gershwin lab has previously evaluated the effect of a fusion protein inhibitor (FPI), GS-1 manufactured by Gilead), which blocks the fusion of the virus, thus affecting its replication. They demonstrated that the benefit is reduced substantially when the FPI is started on Day 3 following viral challenge, after the first clinical symptoms of viral infection[2]. A human study of an almost identical compound (GS-5806) showed decreased viral shedding in adult volunteers when the treatment was started within 12 hours of infection[3, 4]. Non-steroidal anti-inflammatory drugs (NSAIDs) have been used to manage clinical symptoms in children infected with RSV [5, 6]. Studies using NSAIDs (Ibuprofen) in calves as a potential therapy for RSV indicate that together with reducing the clinical and pathological score, they lead to an increase of RSV shedding[6].

These studies evaluated the effects of the FPI and ibuprofen starting12-24 hours post infection. RSV infection is characterized by onset of clinical signs normally visualized from day 3 post infection [7–9] necessitating the need for further studies to evaluate the effectiveness of these therapies when administered post onset of clinical signs thus mimicking the field settings. We tested the effects of combining a FPI with an NSAID initiated at different time points post infection starting on day 3. The results show the benefits of FPI treatment alone and with an NSAID at clinically relevant time points as published [10] and indicate a reduced clinical and

pathological score in the treatment group, when treatment was started at day 3 post infection compared to the placebo.

This study aims to evaluate the effects of the treatments, FPI and ibuprofen a COX-2 inhibitor, on the innate immune response, focusing mainly on neutrophil extracellular traps (NETs) and innate lymphoid cells (ILCs). We used a bovine RSV infection model with pre-ruminant 5-6 week-old bottle-fed outbred Holstein dairy calves, a calf model used in previous studies[6, 11]. We assessed the effects of the FPI and ibuprofen as a monotherapy or a combination therapy on the formation of NETs and ILCs with treatment started at different time points. In addition to guiding therapy for management of RSV in the livestock industry, our results will be applicable to treatment of RSV in children.

2.2. Introductions

Bovine Respiratory Syncytial Virus affects the animal industry directly through calf mortality and indirectly through loss of productivity and increased animal care costs. In the US, there is a $1 billion direct annual cost with substantial indirect costs [6, 12]. Bovine and human RSV are characterized by a strong T helper cell type 2 (Th2) response, which is less effective for virus clearance and host survival than the more characteristic T helper cell type 1 (Th1) response stimulated by most other intracellular pathogens and viruses [11, 13, 14]. RSV infection predisposes to the development of an allergic profile with production of IgE with asthma a likely sequela [15, 16]. Since cattle do not develop asthma, they tend to have respiratory challenges and are generally not in good condition leading to early slaughter for financial reasons. During RSV infection the respiratory epithelial cells up-regulate the cyclooxygenase (COX-2) enzyme system responsible for synthesis of prostaglandin E2 (PGE2) from arachidonic acid precursors. PGE2 is

the most abundant of the prostaglandins that exerts its effects by binding to prostaglandin E receptors (EPR) [6, 17]. PGE2 has various effects including dampening Th1 cell differentiation, increasing development of regulatory T cells, inhibiting T cell proliferation and also decreasing IL-2 production[18]. This leads to lowering of IFN-γ production and providing an environment that favors a Th2 response, making successful killing of RSV infected cells less likely. The Th2 response is associated with activation of COX-2, leading to elevations of PGE2 and other eicosanoids[17, 19]. PGE2 exerts its effects on IL-4 or lipopolysaccharide stimulated B cells via EPR2 and EPR4 and stimulates class switching to IgE [20]. PGE2 further drives the Th1/Th2 skew in favor of Th2 thereby also indirectly increasing IgE.

Histologically, RSV bronchiolitis is characterized by predominantly neutrophilic infiltrates in the bronchioles and alveoli of affected bovines[21, 22]. There is associated obstruction of the airways with neutrophils, NETs, cellular debris and mucous[23–25]. As the disease progresses, obliterative changes develop and a picture of patchy bronchoalveolar pneumonitis and bronchiolitis emerges, resulting in a clinical picture of progressive respiratory distress[26, 27].

COX inhibitors may prevent the progression of bronchiolitis and the development of asthma. Randomized trials have been done to evaluate the effect of ibuprofen a COX-2 inhibitor on fever in infants, which unexpectedly found decreased subsequent wheezing in those randomized to ibuprofen [6]. Another study demonstrated decreased asthma in women randomized to 100 mg of aspirin (a COX-1 & 2 inhibitor) compared to placebo([28, 29]). A randomized study using ibuprofen in bovine RSV calves demonstrated a lower clinical score in calves administered ibuprofen after challenging them with BRSV compared to placebo although they also showed increased RSV replication. Ibuprofen statistically significantly increased viral shedding as measured by quantitative RT-PCR. In this study, ibuprofen improved clinical scores and weight

gain at the price of increased RSV replication[6]. A treatment strategy which combines an antiviral to prevent RSV replication with an NSAID to modulate the immune response might thus be more beneficial.

2.3. Research Methods and Analysis

2.3.a Study outline

The project used 36, five to six-week-old calves obtained from a dairy and transported to the University of California, Davis, where they were housed in an enclosed barn. An approved IACUC protocol was followed. Prior to shipment, calves were tested for BRSV infection by qRT-PCR on nasal swabs and BRSV antibody titers by indirect immunofluorescence on blood samples. Only calves with low maternal BRSV antibody titers and negative for BRSV virus were used. Candidate unvaccinated bull calves were examined for clinical signs of illness. Upon arrival they were re-examined, and nasal swabs again obtained to retest for RSV. The calves were administered a broad-spectrum antibiotic, Ceftiofur (Zoetis Services LLC, Parsippany, NJ) once daily for three days to prevent stress induced bacterial pneumonia and given a week to acclimatize to the new area before we started the study. The calves were weighed prior to randomization and divided into three cohorts of 12 calves each. For each cohort, the 12 animals were randomized into 6 groups of calves (n=2 per treatment group per cohort, Table 2.1).

Calves were randomized to receive either ibuprofen, FPI, both FPI and ibuprofen, or placebo. Placebo was used to ensure blinding of the investigators performing the study and to control for any effect of the carrier solutions on parameters measured. The animals were randomized to one of six treatment arms, which differed in start times of the treatments. We randomized using minimization based first on animal weight and then maternal anti-RSV titers.

These three cohort studies were performed separately between October 2017 and November 2018. For each cohort, the day of inoculation with virus was staggered by one day thereby dividing each cohort into two groups (A and B). Each drug treatment arm contained a group A and a group B calf. Infection days (study day 0) were one calendar day apart to ensure a maximum of six animals would need to be necropsied on study day 10. This was necessary because of workload and necropsy laboratory space considerations

2.3.b. Viral infection

The calves were infected using nebulized bovine RSV on Day 0 over a period of 15-20 min. Calves were infected using the method described elsewhere [6, 30]. Briefly, this method uses a face mask fitted tightly with a nebulizer attached to a DeVilbiss electric home nebulizer air compressor (DeVilbiss Healthcare Inc., Somerset, PA, USA).The virus isolate (CA-1) was grown in the lab on bovine turbinate cells using identical technique for all infections. It is important to note that the virus titers varied slightly between inoculants. Virus titers were determined by using a plaque assay on an aliquot of the virus administered to the calves. Virus inoculum for each replicate is shown in table 2.2.

2.3.c. Clinical score and end points

Calves were examined every morning and the clinical signs were recorded. We measured rectal temperatures twice daily and assessed each animal's wellbeing as published [10]. Euthanasia (either when indicated or as planned on day 10 after infection) was performed by a veterinarian and consisted of an overdose of sodium pentobarbital administered through the jugular vein. Two of the 36 calves required early euthanasia.

2.3.d. Necropsy sampling and Lung histology

We collected blood, swabs for bacterial culture, lymph nodes, broncho alveolar fluid, and lung tissue for histopathological and cellular analysis.

Histopathology was performed in collaboration with a board-certified veterinary pathologist. The right lung was examined grossly, and selected areas taken for histologic examination. Lung consolidation was assessed via as a semi quantitative measurement based on visual inspection. The left lung was fixed with 10% neutral buffered formalin injected at a constant pressure of 30 cm of water. Histopathologic (H&E stained) examination was performed on the fixed lung samples.

2.3.e. Calves treatment and dosages

Ibuprofen (children Advil suspension, Pfizer inc.) was administered at 10 mg/kg three times daily and First Street Snow Cone Syrup (Amerifoods Inc, Los Angeles, CA) was administered as a placebo, as it had identical compound to the vehicle used in the ibuprofen suspension as well as smell and taste as the ibuprofen. FPI (GS-561937) was administered at 600mg (regardless of weight) as a single dose of 30 ml orally using a 50-ml catheter tipped syringe daily in the morning mixed with the syrup, as it has a bitter taste. FPI was prepared in propylene glycol and the placebo for this drug was simply the propylene glycol without the FPI also mixed with syrup to make it palatable.

Tables 3-14 show the calves treatment strategies over the three replicate studies. It is important to note that we had to redo the second replicate study as we had some difficulties with

the virus and the calves were not infected, explaining the discontinuous numbering of the replicates.

2.3.f Expected Results and Impact

This project will be the first to show how combination therapy using viral and immune modulation might affect NETs formation and ILCs in the bovine calf. The study will also give insights into treatment options in the management of Bovine RSV and Human RSV. This will also open an avenue to do more research that evaluate the effects of combined treatment on other immune components, including T and B lymphocytes and thus may inform on the immunological treatment efficacies of these treatment regimen.

Table 2.1. A table illustrating the distribution of calves in the different treatment groups

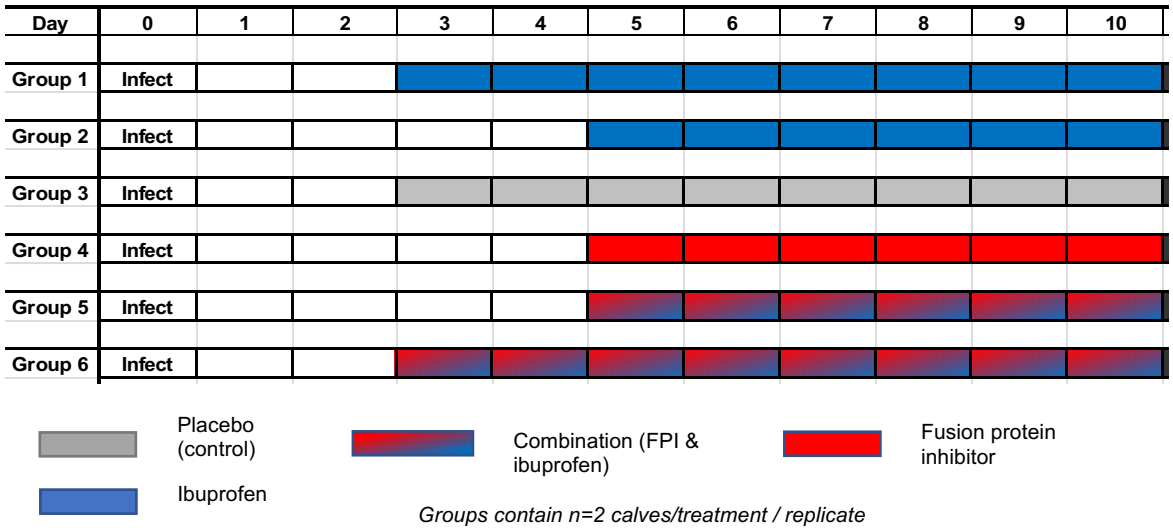

Table 2.2. Bovine respiratory syncytial virus inoculum titers for each cohort and group.

	Rep. 1A	Rep. 1B	Rep. 3A	Rep. 3B	Rep. 4A	Rep. 4B
PFU/ml	1.21 x $10^{\wedge 5}$	1.36 x $10^{\wedge 5}$	7.8 x $10^{\wedge 4}$	1.2 X$10^{\wedge 5}$	1.29 x $10^{\wedge 5}$	1.94 x $10^{\wedge 5}$
Total Dose (5 ml)	6.05 x $10^{\wedge 5}$	6.8 x $10^{\wedge 5}$	3.9 x $10^{\wedge 5}$	6.0 x $10^{\wedge 5}$	6.45 x $10^{\wedge 5}$	9.7 x $10^{\wedge 5}$

Rep – Replicate

PFU – plague forming units

A- Group infected on day 1

B – Group infected on day 2

Key for treatment tables

- Tx Grp – Treatment groups
- Wt – Weight
- PI - post infection
- FPI – Fusion Protein Inhibitor
- A- Group infected on day 1
- B – Group infected on day 2

Replicate 1

Table 2.3: Treatments and Calf Body Weight- 10/23/17

PI Day	Tx Grp	Calf #	Wt (kg)	Syrup (ml)	Ibuprofen (ml)	Ibuprofen & FPI (ml)	FPI (ml)
3	1	12 – A	63.3	X	3x34.7	1x30	X
2		16– B	68.6	X	X	X	X
3	2	11 – A	67.4	3x30	X	1x30	X
2		8 – B	68.8	X	X	X	X
3	3	6 – A	58.6	3x30	X	1x30	X
2		14 – B	69.1	X	X	X	X
3	4	9 – A	66.5	3X30	X	1x30	X
2		15 – B	66.3	X	X	X	X
3	5	10 – A	58.7	3x30	X	1x30	X
2		13 – B	60.9	X	X	X	X
3	6	7 – A	68	X	3x37	X	1x30
2		5 – B	64	X	X	X	X

Table 2.4: Treatments and Calf Body Weight - 10/24/17

PI Day	Tx Grp	Calf #	Wt (kg)	Syrup (ml)	Ibuprofen (ml)	Ibuprofen & FPI (ml)	FPI (ml)
4	1	12 – A	63.3	X	3x34.7	1x30	X
3		16– B	68.6	X	3x37.3	1x30	X
4	2	11 – A	67.4	3x30	X	1x30	X
3		8 – B	68.8	3x30	X	1x30	X
4	3	6 – A	58.6	3x30	X	1x30	X
3		14 – B	69.1	3x30	X	1x30	X
4	4	9 – A	66.5	3X30	X	1x30	X
3		15 – B	66.3	3x30	X	1x30	X
4	5	10 – A	58.7	3x30	X	1x30	X
3		13 – B	60.9	3x30	X	1x30	X
4	6	7 – A	68	X	3x37	X	1x30
3		5 – B	64	X	3x35	X	1x30

Table 2.5: Treatments and Calf Body Weight - 10/25/17

PI Day	Tx Grp	Calf #	Wt (kg)	Syrup (ml)	Ibuprofen (ml)	Ibuprofen & FPI (ml)	FPI (ml)
5-10	1	12 – A	63.3	X	3x34.7	1x30	X
4		16– B	68.6	X	3x37.3	1x30	X
5-10	2	11 – A	67.4	3x30	3x36.7	1x30	X
4		8 – B	68.8	3x30	X	1x30	X
5-10	3	6 – A	58.6	3x30	X	1x30	X
4		14 – B	69.1	3x30	X	1x30	X
5-10	4	9 – A	66.5	3x30	X	X	1x30
4		15 – B	66.3	3x30	X	X	1x30
5-10	5	10 – A	58.7	X	3x32.4	X	1x30
4		13 – B	60.9	X	X	X	1x30
5-10	6	7 – A	68	X	3x37	X	1x30
4		5 – B	64	X	3x35	X	1x30

Table 2.6: Treatments and Calf Body Weight - 10/26/2017- 10/31/17

PI Day	Tx Grp	Calf #	Wt (kg)	Syrup (ml)	Ibuprofen (ml)	Ibuprofen & FPI (ml)	FPI (ml)
6	1	12 – A	63.3	X	3x34.7	1x30	X
5-10		16– B	68.6	X	3x37.3	1x30	X
6	2	11 – A	67.4	3x30	3x36.7	1x30	X
5-10		8 – B	68.8	3x30	3x37.4	1x30	X
6	3	6 – A	58.6	3x30	X	1x30	X
5-10		14 – B	69.1	3x30	X	1x30	X
6	4	9 – A	66.5	3x30	X	X	1x30
5-10		15 – B	66.3	3x30	X	X	1x30
6	5	10 – A	58.7	X	3x32.4	X	1x30
5-10		13 – B	60.9	X	3x33.5	X	1x30
6	6	7 – A	68	X	3x37	X	1x30
5-10		5 – B	64	X	3x35	X	1x30

Replicate 3

Table 2.7: Treatments and Calf Body Weight -– 6/25/2018

PI Day	Tx Grp	Calf #	Wt (kg)	Syrup (ml)	Ibuprofen (ml)	Ibuprofen & FPI (ml)	FPI (ml)
3	1	1 – A	77.1	X	3x39	1x30	X
2		2 – B	73.5	X	X	X	X
3	2	4 – A	78.7	3x30	X	1x30	X
2		13 – B	71	X	X	X	X
3	3	6 – A	70.5	3x30	X	1x30	X
2		5 – B	74	X	X	X	X
3	4	14 – A	71.7	3X30	X	1x30	X
2		12 – B	69.1	X	X	X	X
3	5	15 – A	67.5	3x30	X	1x30	X
2		11 – B	68.9	X	X	X	X
3	6	16 – A	63.9	X	3x36	X	1x35
2		9 – B	63.8	3x30	X	X	X

Table 2.8: Treatments and Calf Body Weight t- 6/26/2018

PI Day	Tx Grp	Calf #	Wt (kg)	Syrup (ml)	Ibuprofen (ml)	Ibuprofen & FPI (ml)	FPI (ml)
4	1	1 – A	77.1	X	3x39	1x30	X
3		2 – B	73.5	X	3x37	1x30	X
4	2	4 – A	78.7	3x30	X	1x30	X
3		13 – B	71	3x30	X	1x30	X
4	3	6 – A	70.5	3x30	X	1x30	X
3		5 – B	74	3x30	X	1x30	X
4	4	14 – A	71.7	3X30	X	1x30	X
3		12 – B	69.1	3x30	X	1x30	X
4	5	15 – A	67.5	3x30	X	1x30	X
3		11 – B	68.9	3x30	X	1x30	X
4	6	16 – A	63.9	X	3x36	X	1x35
3		9 – B	63.8	X	3x36	X	1x35

Table 2.9: Treatments and Calf Body Weight - 6/27/2018

PI Day	Tx Grp	Calf #	Wt (kg)	Syrup (ml)	Ibuprofen (ml)	Ibuprofen & FPI (ml)	FPI (ml)
5-10	1	1 – A	77.1	X	3x39	1X30	X
4		2 – B	73.5	X	3x37	1x30	X
5-10	2	4 – A	78.7	X	3x40	1x30	X
4		13 – B	71	3x30	X	1x30	X
5-10	3	6 – A	70.5	3x30	X	1x30	X
4		5 – B	74	3x30	X	1x30	X
5-10	4	14 – A	71.7	3x30	X	X	1x35
4		12 – B	69.1	3x30	X	1x30	X
5-10	5	15 – A	67.5	X	3x34	X	1x35
4		11 – B	68.9	3x30	X	1x30	X
5-10	6	16 – A	63.9	X	3x36	X	1x35
4		9 – B	63.8	X	3x36	X	1x35

Table 2.10: Treatments and Calf Body Weight - 6/28/2018- 7/3/2018

PI Day	Tx Grp	Calf #	Wt (kg)	Syrup (ml)	Ibuprofen (ml)	Ibuprofen & FPI (ml)	FPI (ml)
6	1	1 – A	77.1	X	3x39	1x30	X
5 - 10		2 – B	73.5	X	3x37	1x30	X
6	2	4 – A	78.7	X	3x40	1x30	X
5-10		13 – B	71	X	3x30	1x30	X
6	3	6 – A	70.5	3x30	X	1x30	X
5-10		5 – B	74	3x30	X	1x30	X
6	4	14 – A	71.7	3x30	X	X	1x35
5-10		12 – B	69.1	3x30	X	X	1x35
6	5	15 – A	67.5	X	3x34	X	1x35
5-10		11 – B	68.9	X	3x30	X	1x35
6	6	16 – A	63.9	X	3x36	X	1x35
5-10		9 – B	63.8	X	3x36	X	1x35

Replicate 4

Table 2.11: Treatments and Calf Body Weight - 10/31/2018

PI Day	Tx Grp	Calf #	Wt (kg)	Syrup (ml)	Ibuprofen (ml)	Ibuprofen & FPI (ml)	FPI (ml)
3	1	10– A	66.9	X	3x37	1x30	X
2		8 – B	66.4	X	X	X	X
3	2	11 – A	67	3x30	X	1x30	X
2		20 – B	60.8	X	X	X	X
3	3	1 – A	73.5	3x30	X	1x30	X
2		12 – B	56.3	X	X	X	X
3	4	4 – A	75.6	3x30	X	1x30	X
2		5 – B	64.6	X	X	X	X
3	5	7 – A	64.2	3x30	X	1x30	X
2		9 – B	76.7	X	X	X	X
3	6	2 – A	71.9	X	3x39	X	1x30
2		6 – B	68.9	X	X	X	X

Table 2.12: Treatments and Calf Body Weight - 11/1/2018

PI Day	Tx Grp	Calf #	Wt (kg)	Syrup (ml)	Ibuprofen (ml)	Ibuprofen & FPI (ml)	FPI (ml)
4	1	10– A	66.9	X	3x37	1x30	X
3		8 – B	66.4	X	3x36	1x30	X
4	2	11 – A	67	3x30	X	1x30	X
3		20 – B	60.8	3x30	X	1x30	X
4	3	1 – A	73.5	3x30	X	1x30	X
3		12 – B	56.3	3x30	X	1x30	X
4	4	4 – A	75.6	3X30	X	1x30	X
3		5 – B	64.6	3x30	X	1x30	X
4	5	7 – A	64.2	3x30	X	1x30	X
3		9 – B	76.7	3x30	X	1x30	X
4	6	2 – A	71.9	X	3x39	X	1x30
3		6 – B	68.9	X	3x37	X	1x30

Table 2.13: Treatments and Calf Body Weight - 11/2/2018

PI Day	Tx Grp	Calf #	Wt (kg)	Syrup (ml)	Ibuprofen (ml)	Ibuprofen & FPI (ml)	FPI (ml)
5	1	10– A	66.9	X	3x37	1x30	X
4		8 – B	66.4	X	3x36	1x30	X
5	2	11 – A	67	X	3x36	1x30	X
4		20 – B	60.8	3x30	X	1x30	X
5	3	1 – A	73.5	3x30	X	1x30	X
4		12 – B	56.3	3x30	X	1x30	X
5	4	4 – A	75.6	3x30	X	X	1x30
4		5 – B	64.6	3x30	X	1x30	X
5	5	7 – A	64.2	X	3x35	X	1x30
4		9 – B	76.7	3x30	X	1x30	X
5	6	2 – A	71.9	X	3x39	X	1x30
4		6 – B	68.9	X	3x37	X	1x30

Table 2.14: Treatments and Calf Body Weight - 11/3/2018- 11/8 /2018

PI Day	Tx Grp	Calf #	Wt (kg)	Syrup (ml)	Ibuprofen (ml)	Ibuprofen & FPI (ml)	FPI (ml)
6 - 10	1	10– A	66.9	X	3x37	1x30	X
5 - 10		8 – B	66.4	X	3x36	1x30	X
6	2	11 – A	67	X	3x36	1x30	X
5		20 – B	60.8	X	3x33	1x30	X
6	3	1 – A	73.5	3x30	X	1x30	X
5		12 – B	56.3	3x30	X	1x30	X
6	4	4 – A	75.6	3x30	X	X	1x30
5		5 – B	64.6	3x30	X	X	1x30
6	5	7 – A	64.2	X	3x35	X	1x30
5		9 – B	76.7	X	3x41	X	1x30
6	6	2 – A	71.9	X	3x39	X	1x30
5		6 – B	68.9	X	3x37	X	1x30

REFERENCES

1. Sacco RE, McGill JL, Pillatzki AE, et al (2014) Respiratory Syncytial Virus Infection in Cattle. Vet Pathol 51:427–436. https://doi.org/10.1177/0300985813501341
2. Jordan R, Shao M, Mackman RL, et al (2015) Antiviral efficacy of a respiratory syncytial virus (RSV) fusion inhibitor in a bovine model of RSV infection. Antimicrob Agents Chemother 59:4889–4900. https://doi.org/10.1128/AAC.00487-15
3. Gilead's Investigational GS-5806 Reduces Viral Load and Clinical Symptoms in Phase 2 Respiratory Syncytial Virus (RSV) Challenge Study in Adults. https://www.gilead.com/news-and-press/press-room/press-releases/2014/5/gileads-investigational-gs5806-reduces-viral-load-and-clinical-symptoms-in-phase-2-respiratory-syncytial-virus-rsv-challenge-study-in-adults. Accessed 18 Dec 2020
4. DeVincenzo JP, Whitley RJ, Mackman RL, et al (2014) Oral GS-5806 Activity in a Respiratory Syncytial Virus Challenge Study. N Engl J Med. https://doi.org/10.1056/nejmoa1401184
5. Borchers AT, Chang C, Gershwin ME, Gershwin LJ (2013) Respiratory syncytial virus - A comprehensive review. Clin. Rev. Allergy Immunol. 45:331–379
6. Walsh P, Behrens N, Chaigneau FRC, et al (2016) A Randomized Placebo Controlled Trial of Ibuprofen for Respiratory Syncytial Virus Infection in a Bovine Model. PLoS One 11:e0152913. https://doi.org/10.1371/journal.pone.0152913
7. Cortjens B, de Jong R, Bonsing JG, et al (2019) Human respiratory syncytial virus infection in the pre-clinical calf model. Comp Immunol Microbiol Infect Dis 65:213–218. https://doi.org/10.1016/j.cimid.2019.04.006
8. Valarcher JF, Taylor G (2007) Bovine respiratory syncytial virus infection. Vet. Res.

38:153–180

9. Russell CD, Unger SA, Walton M, Schwarze J (2017) The human immune response to respiratory syncytial virus infection. Clin. Microbiol. Rev.

10. Walsh P, Lebedev M, McEligot H, et al (2020) A randomized controlled trial of a combination of antiviral and nonsteroidal anti-inflammatory treatment in a bovine model of respiratory syncytial virus infection. PLoS One 15:. https://doi.org/10.1371/journal.pone.0230245

11. Gershwin LJ, Gunther RA, Anderson ML, et al (2000) Bovine respiratory syncytial virus-specific IgE is associated with interleukin-2 and -4, and interferon-γ expression in pulmonary lymph of experimentally infected calves. Am J Vet Res 61:291–298. https://doi.org/10.2460/ajvr.2000.61.291

12. Valarcher J-F, Schelcher F, Bourhy H (2000) Evolution of Bovine Respiratory Syncytial Virus. J Virol 74:10714–10728. https://doi.org/10.1128/jvi.74.22.10714-10728.2000

13. Gershwin LJ, Berghaus LJ, Arnold K, et al (2005) Immune mechanisms of pathogenetic synergy in concurrent bovine pulmonary infection with Haemophilus somnus and bovine respiratory syncytial virus. Vet Immunol Immunopathol 107:119–130. https://doi.org/10.1016/j.vetimm.2005.04.004

14. Mcinnes E, Sopp P, Howard CJ, Taylor G (1999) Phenotypic analysis of local cellular responses in calves infected with bovine respiratory syncytial virus. Immunology 96:396–403. https://doi.org/10.1046/j.1365-2567.1999.00714.x

15. Petersen BC, Dolgachev V, Rasky A, Lukacs NW (2014) IL-17E (IL-25) and IL-17RB promote respiratory syncytial virus-induced pulmonary disease. J Leukoc Biol. https://doi.org/10.1189/jlb.0913482

16. J. S, D. Y, B. S, et al (2015) Respiratory Syncytial Virus Disease Is Mediated by Age-Variable IL-33. PLoS Pathog. https://doi.org/10.1371/journal.ppat.1005217

17. Liu T, Zaman W, Kaphalia BS, et al (2005) RSV-induced prostaglandin E2 production occurs via cPLA2 activation: Role in viral replication. Virology 343:12–24. https://doi.org/10.1016/j.virol.2005.08.012

18. Fabricius D, Neubauer M, Mandel B, et al (2010) Prostaglandin E 2 Inhibits IFN-α Secretion and Th1 Costimulation by Human Plasmacytoid Dendritic Cells via E-Prostanoid 2 and E-Prostanoid 4 Receptor Engagement . J Immunol. https://doi.org/10.4049/jimmunol.0902028

19. Shirey KA, Lai W, Pletneva LM, et al (2014) Role of the lipoxygenase pathway in RSV-induced alternatively activated macrophages leading to resolution of lung pathology. Mucosal Immunol. https://doi.org/10.1038/mi.2013.71

20. Shishikura K, Horiuchi T, Sakata N, et al (2016) Prostaglandin E2 inhibits neutrophil extracellular trap formation through production of cyclic AMP. Br J Pharmacol 173:319–331. https://doi.org/10.1111/bph.13373

21. Murawski MR, Bowen GN, Cerny AM, et al (2009) Respiratory Syncytial Virus Activates Innate Immunity through Toll-Like Receptor 2. J Virol. https://doi.org/10.1128/jvi.00671-08

22. Carvajal JJ, Avellaneda AM, Salazar-Ardiles C, et al (2019) Host Components Contributing to Respiratory Syncytial Virus Pathogenesis. Front Immunol 10:1–19. https://doi.org/10.3389/fimmu.2019.02152

23. Funchal GA, Jaeger N, Czepielewski RS, et al (2015) Respiratory syncytial virus fusion protein promotes TLR-4-dependent neutrophil extracellular trap formation by human

neutrophils. PLoS One 10:1–14. https://doi.org/10.1371/journal.pone.0124082

24. Muraro SP, De Souza GF, Gallo SW, et al (2018) Respiratory Syncytial Virus induces the classical ROS-dependent NETosis through PAD-4 and necroptosis pathways activation. Sci Rep 8:1–12. https://doi.org/10.1038/s41598-018-32576-y

25. Cortjens B, De Boer OJ, Antonis AFG, et al (2015) Neutrophil Extracellular Trap Formation In Severe Respiratory Syncytial Virus Lung Infection. Am J Respir Crit Care Med 191:no pagination

26. Ebbert JO, Limper AH (2005) Respiratory syncytial virus pneumonitis in immunocompromised adults: Clinical features and outcome. Respiration. https://doi.org/10.1159/000085367

27. Gudmundsson G, Monick MM, Hunninghake GW, et al (1999) Viral infection modulates expression of hypersensitivity pneumonitis. J Immunol

28. Filipowicz E, Sanak M, E. F, M. S (2003) Exacerbation of aspirin-induced asthma associated with RSV infection. Przegląd Lek

29. Rose JJ, Voora D, Cyr DD, et al (2015) Gene expression profiles link respiratory viral infection, platelet response to aspirin, and acute myocardial infarction. PLoS One. https://doi.org/10.1371/journal.pone.0132259

30. Gershwin LJ, Schelegle ES, Gunther RA, et al (1998) A bovine model of vaccine enhanced respiratory syncytial virus pathophysiology. Vaccine 16:1225–1236. https://doi.org/10.1016/S0264-410X(98)80123-0

CHAPTER 3

3. Effects of Fusion Protein Inhibitor and Ibuprofen on Neutrophil Extracellular Traps (NETs) in Calves Infected with Bovine Respiratory Syncytial Virus

3.1 Abstract

The function of neutrophils in viral infections has long been established and studies have been done to examine the role of neutrophil extracellular traps (NETs). Further study and analysis of NETs in viral infections may reveal a new therapeutic target. Administration of ibuprofen and GS-561937, a fusion protein inhibitor (FPI), was experimentally shown to decrease the severity of bovine respiratory syncytial virus (BRSV) infection. Our aims were to determine the effect of ibuprofen and FPI on NETs after BRSV infection as a monotherapy or combined therapy.

We conducted a randomized placebo-controlled trial of ibuprofen, FPI, or as a dual therapy initiated at 3 or 5 days after experimental infection with BRSV in 36 five to six-week-old Holstein calves (Bos Taurus). Lung tissue samples were collected and stained with antibodies conjugated with fluorescence dyes to visualize and quantify the NETs in situ. We estimated the average NETs in the sample lung tissue slides and compared the areas occupied by NETs within and between the treatment groups. There were significantly fewer NETs in the lung tissue from calves that were given ibuprofen and both ibuprofen and fusion protein inhibitor from day 3 post infection compared to the placebo group. Calves administered with ibuprofen, fusion protein inhibitor or both from day five had visually fewer NETs than the placebo but the difference was not significant.

This shows that BRSV can induce NET formation in vitro and in vivo and a combination of both drugs (Ibuprofen and FPI) resulted in less NETs observed in lung tissue of BRSV infected calves compared to the placebo or monotherapy groups.

3.2 Introduction

Neutrophils are important cells in the first line of defense against invading pathogens. Neutrophils were shown to form NETs, a distinct mode of neutrophil cell death targeting extracellular pathogens[1]. Nets are composed of a complex of processed chromatin bound to granular and cytoplasmic proteins expelled from the cell onto pathogens where they bind, disarm and kill pathogens extracellularly[2, 3]. They are assembled from granular and nuclear constituents which provide the network with antimicrobial activity[2, 4] a process termed NETosis. The mechanisms underlying NET formation requires reactive oxygen species (ROS) production.

Viruses including RSV stimulate NETosis through TLR 4, 7 and/or 8 with the release of ROS species [5–7].The pathways that promote NETosis upstream of ROS involve ROS-inducing receptors (BOX 1) and kinases, such as MEK (MAPK/ERK kinase), extracellular-signal-regulated kinase (ERK), IL-1 receptor-associated kinase (IRAK), PKC, phosphoinositide 3-kinase (PI3K) and AKT[5, 8]. NETs interact with a variety of different pathogens and have been shown to capture both Gram-positive and Gram-negative bacteria and fungi as well as viruses[9–11]. NETs provide a high local concentration of antimicrobial proteins, including proteases such as neutrophil elastase, myeloperoxidases, and α-defensins which degrade virulence factors and histones[6, 12, 13].This process may be crucial in clearing some pathogens; unfortunately, excessive formation of NETs, or the inability to clear them from the tissue may contribute to an increased inflammatory response or pathogenesis of autoimmune diseases [14, 15].

The role of NETs in viral infections vary greatly between viruses. NETs can be beneficial in trapping virions as in HIV infection and inhibiting viral dissemination as in murine pox virus [10, 16, 19] However, excessive NET formation was reported to result in airway obstruction during respiratory syncytial virus (RSV) infection in infants and it also exacerbated allergic airway inflammation during rhinovirus infection [17–20]. These factors dictate the role of NETs during viral infections; however, the effects of therapeutics on NETs in the management of the viral infections, is largely unknown.

BRSV infection in cattle continues to be a problematic disease causing serious respiratory disease that predisposes cattle to secondary infection, resulting in significant economic losses due to mortality, decreased productivity and increased costs of treatment [21–23].Human RSV (HRSV) and BRSV are closely related viruses with similarities in histopathologic lesions and mechanisms of immune modulation[24]. Immune response to RSV is dependent on the recognition of the virus by several TLRs. RSV has been shown to stimulate airway epithelial cells signaling through TLR3 while the F protein binds to TLR4 in conjunction with MD2 and CD14 leading to induction of type I IFN [25]. The virus has also evolved strategies to inhibit the IFN-induced cellular response with NS1 and NS2 proteins cooperatively mediating their resistance by targeting multiple proteins including RIG-I and MAVs interfering with induction of IFN gene expression by several transcription factors. [26, 27].

In RSV infection, patients exhibit sustained neutropenia with increased levels of pro-inflammatory mediators such as IL-8 and TNFα which activate neutrophils [28]. Studies have also indicated that RSV could induce formation of NETs in vitro [8, 19]. However, due to short half-lives of neutrophils and the short duration of RSV infection, the study of neutrophil functions, NETs, and their association with disease severity in vivo is challenging.

The majority of treatment strategies for HRSV and BRSV are supportive, focusing on fluid and respiratory maintenance and at times administering antibiotics to prevent secondary bacterial infections[29, 30]. Widely available and cost-effective preventative options are lacking for HRSV; and although numerous vaccines are available for BRSV, their efficacy is variable. Even as progress is being made in understanding the immune responses to RSV additional mechanistic insight is needed to better identify prophylactic and therapeutic targets.

Our group has demonstrated the efficacy of FPI, an antiviral drug produced by Gilead Inc., in treatment of BRSV in calves[31]. A drug similar to this is currently in clinical trials for human patients [32–34].This drug has been shown to inhibit the proliferation of the virus in respiratory epithelial cells thus reducing the virus load; however, its effect on the inflammatory response needs further evaluation. We also performed a trial with Ibuprofen, an over-the-counter anti-inflammatory drug that works by inhibiting the cyclooxygenase (COX) pathway reducing the production of PGE2, in calves as an immune modulator which minimized the inflammatory effect but failed to decrease viral replication [35].

This led to our current study in which we evaluated NETs in the lungs of calves experimentally infected with BRSV. We sought to determine if treating with ibuprofen, for its immunomodulatory effects, and FPI, to decrease viral replication, would influence NETosis in the lungs of these calves. The treatment included ibuprofen and FPI as a monotherapy or a combination of the two initiated at different time points. The results indicate a reduction of NETs in lung tissue of calves treated with ibuprofen or a combination of ibuprofen and FPI compared to the placebo group. Our study highlights possible roles of ibuprofen and other anti-inflammatory drugs against NETs formation. The findings provide a new understanding of host immune responses during RSV

infections and possible therapeutic options that can be used for treatment of RSV, BRSV and possibly other viral respiratory diseases.

3.3 Materials and Methods

3.3.1. Samples

(The animal experimental design and treatments have been described in chapter two)

The project used 36, five to six-week-old calves obtained from a dairy farm and transported to the University of California, Davis, where they were housed in an enclosed barn. An approved IACUC protocol was followed. .

For the in vitro analysis of NETs, we collected blood from the jugular vein (12–16 ml) of healthy calves into Acid Citrate Dextrose (ACD) tubes. Neutrophil isolation was carried out under sterile conditions using a modified protocol so as to collect both the mononuclear cell layer and the polymorphonuclear cell layer.

During necropsy, areas of atelectasis and consolidation were estimated semi-quantitatively as a percentage of the total lung by an experienced board-certified veterinary pathologist. The left lung was removed intact from the left mainstem bronchus. It was infused with 10% neutral buffered formalin via an intrabronchial catheter until fully expanded. Tissue samples were taken for subsequent fixation and sectioning for histologic examination; samples were taken from the trachea, right mainstem bronchus and lung. These samples were then placed in cassettes and fixed in 10% neutral buffered formalin.

Separate lung tissue samples were collected in triplicates from right lung cranial, middle and caudal lobes for NETs analysis (Figure 3.1). These samples were processed and saved until further analysis. A modified double immunolabeling protocol was utilized as explained by Li et al

[36], because the primary antibodies used to detect NE and citH3 were produced in the same species.

3.3.2. In vitro protocols

(Reagents and equipment used for experiment in chapter 3 will be found listed on appendix 1)

3.3.2.a. Separation and subsequent red blood cells lysis

Blood was collected into tubes containing anticoagulant, ACD tubes, and diluted in conical tubes at 1:1.5 dilution with sterile PBS. 10ml Lymphoprep was dispensed to the bottom of the Lymphoprep tubes and 30ml of diluted blood slowly layered on top of the Lymphoprep. The tubes were centrifuged for 20 min at 800xg at a temperature of 18-25ºC with brakes. After centrifugation, the mononuclear cells form a distinct band at the sample/medium interface as Peripheral Blood Mononuclear cells (PBMCs). The PBMCs layer was collected from the interface and saved for later use. We then pipetted the portion below the medium with the erythrocytes and polymorphonuclear cells (PMNs) into a conical tube. Red blood cells were lysed using cold distilled water for 30-60s and the pH readjusted using 10X PBS. The sample was centrifuged for 20 min at 250xg at 4 °C to pellet the cells. The red blood cell lysis was repeated until the water ran clear. We resuspended the cells in cell culture media and stored at 2-8ºC until needed. PMNs are short lived and were therefore processed within 24 hours for better results. We determined the neutrophil count using automatic cell analyzer (Guava® Muse® Cell Analyzer) following the manufacturer's instructions and viability was 98 to 100%.

3.3.2.b. Neutrophil stimulation and staining

(done under sterile conditions in a biohazard cabinet)

Neutrophils were plated on circular coverslips in 4-well glass-bottom plates and prepared in triplicates as indicated in Table 3.1. The cells were plated onto the center of the coverslips at a density of 2.5×10^3 cells/ml, by gently pipetting 200 µL of PMNs cell suspension into the wells. The cells were incubated in humified incubator (37 °C, 5 % CO 2) for 1hr for the neutrophils to adhere to the cover slips. PBS was gently added to wash away cells that had not adhered and supernatant discarded. To induce NETs with PMA, 100 µL of PMA working stock and100 µL BRSV antigen working stock solution were added into the labeled wells (Table 3.1) and incubated for 3hrs at 37 °C (5 % CO 2). After 3 hrs., the remaining liquid was discarded, and the wells washed 3 times with PBS. The cover slips were air dried for 20 min and placed in a well containing 400 µL of 4% Paraformaldehyde. The cells were fixed for 10 min at room temperature. The paraformaldehyde was gently aspirated, and the cover slips washed three times with PBS. The coverslips with adherent PMBs were transferred into wells of a new cell culture plate with PBS and stored at 4 °C until ready to perform immunofluorescence labeling.

3.3.2.c. Immunofluorescence labeling and visualization of NETs

For immunofluorescence labeling of NETs, the PBS was discarded from the wells and the adherent cells permeabilized using 1% NP-40 diluted in PBS. They were incubated for 10 min at RT and the coverslips gently washed with PBS 3 times for 5 min. Blocking buffer was added to block nonspecific binding sites and incubated for 1 hr. at RT. The first primary antibody (Rabbit anti neutrophil elastase - NE) was diluted in blocking buffer at 1µg/ml. The primary antibody was added at 200µL per well after discarding blocking buffer without an additional wash step. The

coverslips were incubated overnight at 2-8^{o}C and then washed 3 times with PBS for 5 min each. The secondary antibody (goat anti rabbit - Alexa fluor 594) was diluted to a working solution of 10µg/ml in blocking buffer (Table 3.2) and added to the coverslips at 200µL per well. The cells were incubated for 2 hrs. at RT in a dark cool place and then washed 3 times for 5 min with PBS. A final wash was done for 5 min using deionized water.

To saturate open binding sites on the first secondary antibody with IgG so that they cannot capture the second primary antibody, the coverslips were incubated 10% rabbit normal serum for 2hrs. They were then washed 3 times for 5 min with PBS, and once for 5 min with deionized water. Unconjugated Fab Goat Anti-Rabbit IgG (H+L) fragments at 50 µg/mL in PBS (Table 3.2)was added to the wells, 400µL each, to cover the rabbit IgG so that the second secondary antibody will not bind to it. They were incubated for 2hrs at RT and wash 3 times for 5 min each with PBS, then once for 5 min with deionized water. They were then incubated with 200µL of the second primary antibody (Rabbit Anti-citrullinated histones - citH3) at 2.5 µg/mL diluted in blocking buffer (Table 3.2) for 2hrs at RT. The cover slips were washed 3 times for 5 min each with TBS, then once for 5 min with deionized water. The second secondary antibody (goat anti rabbit - Alexa fluor 488) diluted in blocking buffer to10 µg/mL was added at 200µL per well and incubated for 1hr at RT. The coverslips were washed 3 times for 5 min each with PBS, then once for 5 min with deionized water.

To visualize the cell free DNA (cfDNA) and nucleus, 300 µL of 1:10000 diluted DAPI solution was added to each well and incubated for 10 minutes at RT in the dark. The coverslips were rinsed once in PBS before adding 200 µL working solution (following manufacturers' instructions) of Vector® TrueView autofluorescence quenching media which specifically binds, and quenches auto fluorescent elements enhancing signal to noise and then rinse once with PBS.

The coverslips were gently removed from the wells and mounted onto super frost microscope slides using a small drop of fluorescent mounting medium. The mounted coverslips were dried overnight by storing the slides in a slide holder at room temperature, protected from light.
Once the mounting medium solidified (approximately 24-48hrs), the slides were stored at 2-8^{o}C until needed or analyzed using an epi - fluorescence microscope.

NETs were visualized as a combination of cell free DNA (cfDNA), citrullinated histones (citH3), and neutrophil elastase(NE) staining on an epi-fluorescence microscope(EVOS microscope®), equipped with filters suitable for DAPI (excitation/emission: 345/455 nm), Alexa Fluor 594 (excitation/emission: 590/617 nm), and Alexa Fluor 488((excitation/emission: 494/519 nm). Images were captured at ×200 magnification and the NETs quantified as the average area in μm of NE and CitH3 in the 10 fields using MIPAR®, an image processing program that provides prescribed recipes to help identify stained cells and area.

Negative controls using the cell culture media with no primary antibody were included to identify non-specific staining of the secondary reagents. Other controls included were a cover slip with the primary antibody and no secondary to check for autofluorescence and an isotype control to check that the observed staining is not caused by non- specific interactions of the primary antibody.

3.3.3. Lung tissue protocol

3.3.3.a. Fixation, embedding, Freezing, sectioning and mounting of sections

(*Reagents are listed in appendix I*)

The collected fresh lung tissues were placed onto a glass petri dish with PBS and dissect into pieces of approximately 20 mm x 30 mm x 3 mm in size using a pair of scissors or scalpel. The specimens were immersed into 4% paraformaldehyde solution with the volume of fixative at least 20x that of the tissue and fixed at 4ºC for 8−20 h. The samples were rinsed with PBS, dried on a paper towel and mounted onto embedding molds using optimal cutting temperature compound (Tissue-Tek® O.C.T) compound. The mounted samples were placed on a rack in a container with liquid nitrogen so as just the vapor gets to the tissue, to ensure they freeze evenly with minimal crystal formation. Cryosectioning was done using a cryostat at -22ºC to prepare 3 µm tissue sections, affixed them on super plus slides and incubated overnight at 37 °C to bond the tissue to the glass. The slides were then stored in -20ºC.

3.3.3.b. Rehydration, heat-induced epitope retrieval, staining, mounting, microscopic analysis

The slides were thawed at room temperature for 10-20 minutes and the tissue sections surrounded with a hydrophobic barrier using a barrier pen. The tissue was rehydrated using PBS for 15 minutes and permeabilized with 0.3% Triton® X-100 diluted in PBS. To retrieve epitopes, the slides were placed in a jar filled with heat-induced epitope retrieval buffer (HIER) pH 9 and the jar placed in a water bath heated to 95ºC in a steamer and steamed for 20 minutes with the temperature maintained at 98 °C in the steam cooker. After steaming the jar was let it cool to RT,

approximately 30 min to 1hr. The sectioned were rinsed 3 times with deionized water and once with PBS (pH 7.4). Excess liquid was removed from slides between sections with rolled filter paper, leaving sections hydrated. The tissue sections were permeabilized using 1% NP-40 diluted in PBS, incubated for 10 min at RT and then washed with PBS 3 times for 5 min. Blocking was done using a blocking buffer incubated for 1 hr. at RT to prevent unspecific binding. The first primary antibody (Rabbit anti neutrophil elastase - NE) was diluted in blocking buffer at 1µg/ml (Table 3.2) and added to the slides after discarding blocking buffer without an additional wash step. The sections were incubated overnight at 2-8ºC and then washed 3 times with PBS for 5 min. The secondary antibody (goat anti rabbit - Alexa fluor 594) was diluted to a working solution of 10µg/ml in blocking buffer (Table 3.2) and added to the slides. The slides were incubated for 2 hrs. at RT in a dark cool place and then washed 3 times for 5 min with PBS. To saturate open binding sites on the first secondary antibody with IgG so that they cannot capture the second primary antibody, the slides were incubated with 10% rabbit normal serum for 2hrs. They were then washed 3 times for 5 min with PBS, and unconjugated Fab Goat Anti-Rabbit IgG (H+L) fragments at 50 µg/mL in PBS (Table 3.2) was added to cover the rabbit IgG so that the second secondary antibody will not bind to it. They were incubated for 2hrs at RT and washed 3 times with PBS for 5 min. The second primary antibody (Rabbit Anti-citrullinated histones - citH3) at 2.5 µg/mL diluted in blocking buffer (Table 3.2) was added and incubated for 2hrs at RT. After the 2 hrs. the slides were washed 3 times for 5 min with PBS and the second secondary antibody (goat anti rabbit - Alexa fluor 488) diluted in blocking buffer to10 µg/mL (Table 3.2) was added. The slides were then incubated for 1hr at RT and later washed 3 times for 5 min with PBS.

To visualize the cell free DNA (cfDNA) and nucleus, 300 µL of 1:10000 diluted DAPI solution was added to the slides and incubated for 10 minutes at RT in the dark. The slides were

rinsed once in PBS before adding 200 µL TrueView autofluorescence quenching media which specifically binds, and quenches auto fluorescent elements enhancing signal to noise. After this the slides were rinses once with PBS and cover slips mounted using a small drop of fluorescent mounting medium. The slides were dried overnight by storing the slides in a slide holder at room temperature, protected from light. Once the mounting medium solidified (approximately 24-48hrs), the slides were stored at 2-8^{o}C until needed or analyzed using an epi - fluorescence microscope.

NETs were visualized as a combination of cell free DNA (cfDNA), citrullinated histones (citH3), and neutrophil elastase(NE) staining on an epi-fluorescence microscope(EVOS microscope®), equipped with filters suitable for DAPI (excitation/emission: 345/455 nm), Alexa Fluor 594 (excitation/emission: 590/617 nm), and Alexa Fluor 488((excitation/emission: 494/519 nm). Images were captured at ×200 magnification and the NETs quantified as the average area in µm of NE and CitH3 in the 10 fields using MIPAR®, an image processing program that provides prescribed recipes to help identify stained cells and area.

Negative controls using the cell culture media with no primary antibody were included to identify non-specific staining of the secondary reagents. A control with just the primary antibody and no secondary was included to correct for autofluorescence and an isotype control to check that the observed staining is not caused by non- specific interactions of the primary antibody.

3.3.4. Cellular morphology, intracellular citH3 expression and NET quantification

An EVOS FL Cell Imaging System (ThermoFisher Scientific, Rockford, IL) was used to acquire the immunofluorescent images. Prior to image capture and analysis, the investigators were blinded to the conditions by randomly assigning a number to each slide. At 20× magnification, 10

random fields were captured for each sample and the images analyzed using available software (MIPAR®). Exposure times of each channel (blue, green or red) were kept constant throughout the analysis.

Neutrophils were identified based on nuclear morphology, cell diameter of less than 15 μm (Figure 3.2) and presence of NE within the cytoplasm. NETs were identified based on cfDNA, extracellular NE, and citH3. The quantity of NETs in each slide was expressed as an average area of staining in 10 random fields.

3.4. Statistics

Differences between groups were analyzed with ANOVA. For data that were not normally distributed, differences between groups were examined using the Kruskal Wallis test. Correlations were tested by Pearson's correlation coefficient in normally distributed data and Spearman's correlation coefficient in skewed data. All statistical tests with a p value equal to or less than 0.05 were reported as statistically significant. Statistical calculations were performed using JMP (SPSS Inc., Chicago, IL). We compared each of the treatment groups with each other and the placebo group as referent.

3.5. Results

3.5.1. Clinical and pathological scores

All calves developed clinical illness and viral shedding with the details of the clinical outcomes described in detail elsewhere [31]. Briefly, daily physical exams were performed, and the clinical scores tabulated by a vet blinded to the treatment groups. All calves had higher clinical scores from day 3 post infection compared to their baseline clinical scores. Animals in Group 3,

the placebo group that were infected with BRSV but received the vehicle instead of the drugs, had high clinical scores indicating more severe disease compared to other groups. Group 6 (combined therapy of the FPI and ibuprofen starting day 3) had the lowest clinical score. Ibuprofen increased viral shedding as described previously [35] and FPI decreased viral shedding, but the combination therapy of both drugs led to viral loads similar to those in calves given FPI alone [31].

The details of histopathological scores and the viral loads measured using nasal swabs has been published [37]. In brief, the results indicated that histopathological scores were highest in calves receiving placebo throughout and those administered ibuprofen from day 5, as indicated by lung consolidation and atelectasis using semiquantitative scoring (Table 3.3). Histopathology scores were markedly reduced when combination therapy with ibuprofen and FPI was started on day 3 post inoculation. Differences between the treatment groups receiving dual therapy with ibuprofen and FPI three days after inoculation when compared with placebo reached statistical significance with respect to overall histopathological score [37].

3.5.2. Pathology and NETs induced by BRSV in bovine neutrophils *in vivo*

The lungs of the BRSV infected calves had gross lesions with a cranioventral distribution with areas of consolidation distributed multifocally across the cranial, middle, and caudal lobes. Microscopic evaluation performed by a qualified veterinary pathologist indicated that lesions in cranioventral lobes are those of a broncho-interstitial pneumonia, necrotizing bronchiolitis, syncytia formation, type II pneumocyte hyperplasia, and exudative or proliferative alveolitis, as explained by Carvallo et al[37]. The severity of lesions may not often correlate with viral load or viral distribution, suggesting that the tissue damage is more a result of host response rather than primary viral infection [27, 38, 39]. Since we know that NETs can exacerbate disease pathology

[40], evaluating the extend of NETs in these calves' lung tissue could provide a possible clue to the damage caused by the host immune response and possible ways to minimize it.

3.5.3. In vitro NETs analysis

Studies have shown that neutrophils release NETs upon exposure to RSV in vitro [19, 28, 41]. To confirm that neutrophils respond to BRSV, we examined isolated bovine neutrophils exposed to PMA, BRSV or both in vitro (Figure 3.2). In line with results from other studies, we observed web-like networks of extracellular DNA around denaturing bovine neutrophils challenged with BRSV, and PMA (as the positive control) with more abundant NETs in PMA-stimulated than BRSV-challenged neutrophils (Figure 3.2). At 3hrs, PMA-stimulated neutrophils had significantly more NE and citH3 area and loss of plasma membrane integrity compared to BRSV-stimulated neutrophils. PMA-stimulated neutrophils were also surrounded by vast strands of extracellular DNA. These extracellular DNA structures were coated with neutrophil elastase and citH3, indicating the formation of NETs similar to other studies[16]. Some intact neutrophils stained positive for citH3, which may represent an early stage of NETosis

3.5.4. NETs analysis in frozen tissue

The lungs of the BRSV infected calves revealed widespread NETosis and deposition of NETs, as indicated by positive CitH3 and NE staining (Figure 3.3). NETs were visualized in the lungs of BRSV infected calves on samples collected from the cranial, middle, and caudal lobes, on the left hemisphere of the lung, as shown in Figure 3.2. 3-5mm lung sections were stained with immunofluorescent dyes for visualization. NETs were assessed as the area covered by citH3 and

NE in mm^2, normalized for total area of cells (nucleus staining). We found NETs deposition in both intraluminal and interstitial areas.

There was a significance difference in NETs staining between the treatment groups ($p=0.0123$) for citH3 and ($p=0.0085$) for NE. Samples from the placebo group contained significantly more staining of citH3 compared to the treatment group receiving a combination of FPI and ibuprofen ($p=0.034$) and the treatment group receiving ibuprofen alone ($p=0.012$), when treatment was started on day 3 (Figure 3.4A). The placebo group also showed a significantly higher staining for NE compared to three of the six treatment groups: FPI and ibuprofen starting day 3 ($p=0.0163$), ibuprofen alone starting day 3 ($p=0.0116$) and FPI and ibuprofen starting day 5 ($p=0.0224$) (Figure 3.4B). NETs staining evaluated between the cranial, middle, and caudal lung lobes showed a significant difference ($p<0.0001$) for citH3 and ($p=0.0078$) for NE with more NETs in the cranial lobes (Figure 3.5A). The cranial lobe showed highly significant difference from the middle lobe ($p<0.0001$) and the caudal lobe ($p=0.0003$) for citH3 and no significant differences between the middle and caudal lobes ($p>0.05$). Additionally, the cranial lobe was significantly different from the middle lobe ($p=0.0108$) and caudal lobe ($p=0.0322$) for NE with no significant difference between the middle and the caudal lobes (Figure 3.5B). Since the experiment was done in batches, we also examined possible differences between replicates analyzed as different batches. The analysis showed a slight difference between the batches but no significant batch effect ($p = 0.4207$) (Figure 3.6).

The lungs samples were assessed semi quantitatively, in collaboration with a veterinary pathologist, for neutrophilic exudates present within bronchi, bronchioles and alveoli. Lower percentage of these exudates were observed in calves treated with ibuprofen and FPI from day 3 (Table 3.3) compared to the other four treatment groups. The correlation between the sum of the

area stained from citH3 and NE, lung consolidation percentages and the neutrophil exudates (Table 3.3) was analyzed. The NE staining showed a significant correlation with lung consolidation percentages ($p=0.0188$,) bronchiole ($p=0.0416$) and alveolus ($p=0.0416$) neutrophils exudates, while there was no significant correlation between citH3 and the lung consolidation percentages or neutrophil exudates (Figure 3.7).

3.6. Discussion

NETS have been shown to worsen disease conditions, including disease due to RSV, by forming plugs that block the respiratory airways [19, 29, 43]. Safe and effective management of NETosis in various diseases is an ongoing research topic with very few compounds being approved for human treatment. For example, DNase I, which was found to denature NETs in vivo [44], is to our knowledge the only compound approved by the United States Food and Drug Administration (FDA) for the treatment of NETs in cystic fibrosis [45]. More studies are still required to ascertain the safety and efficacy of DNase I in the management of other conditions and to identify other compounds that reduce NETs. Non-steroidal anti-inflammatory drugs (NSAIDS) have been widely used to reduce pain, fever, and inflammation associated with acute infections and have been shown to minimize clinical signs and pathology in various diseases, including RSV[35].

Our rationale for including ibuprofen, an over the counter NSAID, in this study was because of its known function as an immunomodulator. It acts by inhibiting the cyclooxygenase enzymes (COX-1 and COX-2), preventing the conversion of arachidonic acid into its biologically active derivatives and thereby altering prostaglandin homeostasis. Although ibuprofen is not a drug commonly prescribed in cattle, it is a readily available NSAID approved for use in management of clinical symptoms in children with RSV infection [46]. The results of our studies

are therefore beneficial to both, human and veterinary medicine, as any observed effects of ibuprofen could inform about potential effects of other NSAIDS. Cox inhibitors inhibit migration of neutrophils by suppressing IL-17 production [47]. IL-17 is a key cytokine that links T cell activation to neutrophil mobilization and activation. An experiment by Walsh and our lab has previously shown that ibuprofen, started one day after infection with BRSV, decreases interleukin-17 (IL-17) [35, 49]. Ibuprofen also suppresses IL-6 and IL-8 mRNA levels, inactivating NF-κB and STAT3 pathway alterations [50]. It also induces shedding of adhesion molecules, decreasing the expression of L-selectin on neutrophils and thereby inhibiting their activation, locomotion, aggregation, and degranulation [51]. Studies also indicated that NSAIDS application can increase serum levels of anti-inflammatory cytokines interleukin-13 (IL-13) and interleukin-4 (IL-4) [47, 52] that exert an inhibitory effect on neutrophils, affecting neutrophil migration and tissue infiltration as well as neutrophil effector functions [53]. Taken together these immunomodulatory effects on neutrophils should potentially influence neutrophil functions including netosis.

The experiments outlined here show that ibuprofen alone administered on days 3 after BRSV infection, did not make much of a difference in the percentage of neutrophil exudates in the airways (Table 3.3) but it had a significant negative effect on NET formation (Figure 3.4A). There was also a significant difference with less NETs in the combination therapy of ibuprofen and FPI starting day 3 on NETs and on the neutrophil exudates compared to placebo. Initiating ibuprofen treatment early, as done here on day 3 after BRSV infection, seems to more strongly reduce netosis, possibly by early interference of the neutrophil recruiting cytokines(IL-17, IL-13, IL-4) function. In the combination therapy, there could be a double positive effect; the FPI inhibits viral replication thus minimizing neutrophil activation, while the ibuprofen further decreases neutrophil function. However, when treatment was initiated later in the infection, day 5, the lack of an effect maybe

due to the fact that pro-inflammatory cytokines were already secreted. However, we could see an effect on the NE during combined therapy (Figure 3.4B). This could be due to reduced activation of neutrophils due to the FPI-mediated reduction in viral loads.

We also considered differences in NET depositions in the three major lung lobes. The cranial lobe had significantly higher deposition of NETs compared to the middle and caudal lobes (Figure 3.5A and 3.5B), but there was no significant difference between the middle and caudal lobes. These results are consistent with the fact that BRSV infection has a cranioventral presentation with consolidated lesions present throughout the cranial, middle, and accessory lobes, while the caudal lobes are often distended with edematous lesions [39, 54]. NE staining showed a significant positive correlation with lung consolidation percentages, bronchiole, and alveolus neutrophils exudates, while there was no significant correlation between citH3 and the lung consolidation percentages or neutrophil exudates (Figure 3.7). A study done by Obermayer et.al also indicated that NE occurred in high densities in NETosis while citH3 was much less abundant. They concluded that release of DNA studded with non-citrullinated histones was a common feature of in vivo NETosis [55]. This potentially explains the difference observed in the levels of citH3 and NE in the different lung lobes (Figure 3.5A and 3.5B) with NE being higher than citH3 in the middle and caudal lobes compared to the citH3.

We also assessed the difference between NETs in three replicates to rule out batch effects. Although it appeared that the third replicate had more NETs than the other two, this difference did not reach statistical significance (Figure 3.6). The increase in NETs in the third replicate might have been due to ambient temperature during processing, as this replicate experiment was conducted during higher temperature than the other two batches that were analyzed.

3.7. Conclusion

In conclusion, BRSV induces NET formation *in vitro* and *in vivo.* NET formation was observed in the lungs, suggesting that they contribute to immunopathology in RSV disease. Both, Ibuprofen and FPI single therapy decreased clinical severity of illness and NET formation in a bovine model of RSV but were most successful in doing so when used as a combination therapy. The combination of both drugs was effective when given at days 3 and 5 after infection, with earlier initiation leading to better outcomes. Our work underscores the need for more studies into compounds that influence NET formation. Early diagnosis of diseases exacerbated by NET might be critical for this therapy to be effective, however, as it functions best before a strong onset of inflammatory responses.

3.8. Limitations

Limitation encountered in this study include microscopic evaluation, which is subject to observer bias. To minimize this, we utilized a standardized protocol to acquire and analyze images in a randomized and blinded manner. Unfortunately, this technique is labor intensive, requiring multiple incubation steps and advanced training in microscopy. Another limitation was accurate identification of NETs. When neutrophils undergo NETosis they have chromatin decondensation, leading to non-lobulated and rounded nuclei, which may affect our ability to accurately identify neutrophils and hence incorrectly estimate the quantity of NETs produced. Having a specific marker for NETs could allow for more accurate cell enumeration. Direct visualization and quantification of NETs in samples can also be challenging, due to the lack of standardized cell counts and variable cell types. Because the number of NETs is dependent on the number of neutrophils in each sample, we measured NE and citH3 positive neutrophils relative to the number

of neutrophils. We also employed robust criteria to classify and quantify neutrophils due to the presence of other various cell types. Further studies are needed to validate this technique in a larger population of cattle and to determine its diagnostic and prognostic value in calves with BRSV.

Table 3.1: Neutrophil stimulation with PMA and BRSV

	PMA(120nM)	**BRSV(30µg/ml)**	**PMN ($2.5x10^3$ cells/ml)**
PMN	-	-	200µL
PMN+PMA	100µL	-	200µL
PMN+BRSV	-	100µL	200µL
PMA (control)	100µL	-	-
BRSV (control)	-	100µL	-

BRSV – Bovine Respiratory Syncytial Virus PMA – phorbol 12-myristate 13-acetate

PMN – Polymorphonuclear cells

Table 3.2. Antibodies used in staining for NETS and their dilutions

Antibodies	**use**	**Dilution**	**Lot number**	**Company**
Rabbit polyclonal anti-neutrophil elastase (NE) antibody	Primary	1:200 (1 µg/ml)	ab68672	Abcam, Cambridge, MA
Rabbit polyclonal anti-citrullinated histones(citH3) antibody	Primary	1:400 (2.5µg/ml)	ab5103	Abcam, Cambridge, MA
Alexa Fluor® 488-Goat Anti-Rabbit IgG (H+L	Secondary	1:400 (10 µg/ml))		ThermoFisher Scientific, Rockford, IL
Alexa Fluor® 594-Goat Anti-Rabbit IgG (H+L)	Secondary	1:400 (10 µg/ml)		ThermoFisher Scientific, Rockford, IL
Unconjugated goat anti-rabbit Fab fragments		50 µg/mL		Jackson Immuno-Research Laboratories, West Grove, PA

Table 3.3: Lung consolidation as a percentage of the total consolidation score and comparison of neutrophil exudates in the three major airways (Bronchi, Bronchiole and Alveoli) between the treatment groups.

Lung Pathology				
Treatment groups	Lung consolidation (%)	Neutrophil exudates in Bronchi (%)	Neutrophil exudates in Bronchiole (%)	Neutrophil exudates in Alveoli (%)
Day 3 Ibuprofen	22.5	22	18	16
Day 5 Ibuprofen	33.1	13	19	19
Placebo	31.5	21	21	23
Day 5 FPI	24.2	17	16	15
Day 5 FPI+ Ibuprofen	25	16	16	17
Day 3 FPI+ Ibuprofen	9.3	9.8	10	9.6
FPI – fusion protein inhibitor Percentages are semi quantitatively scored				

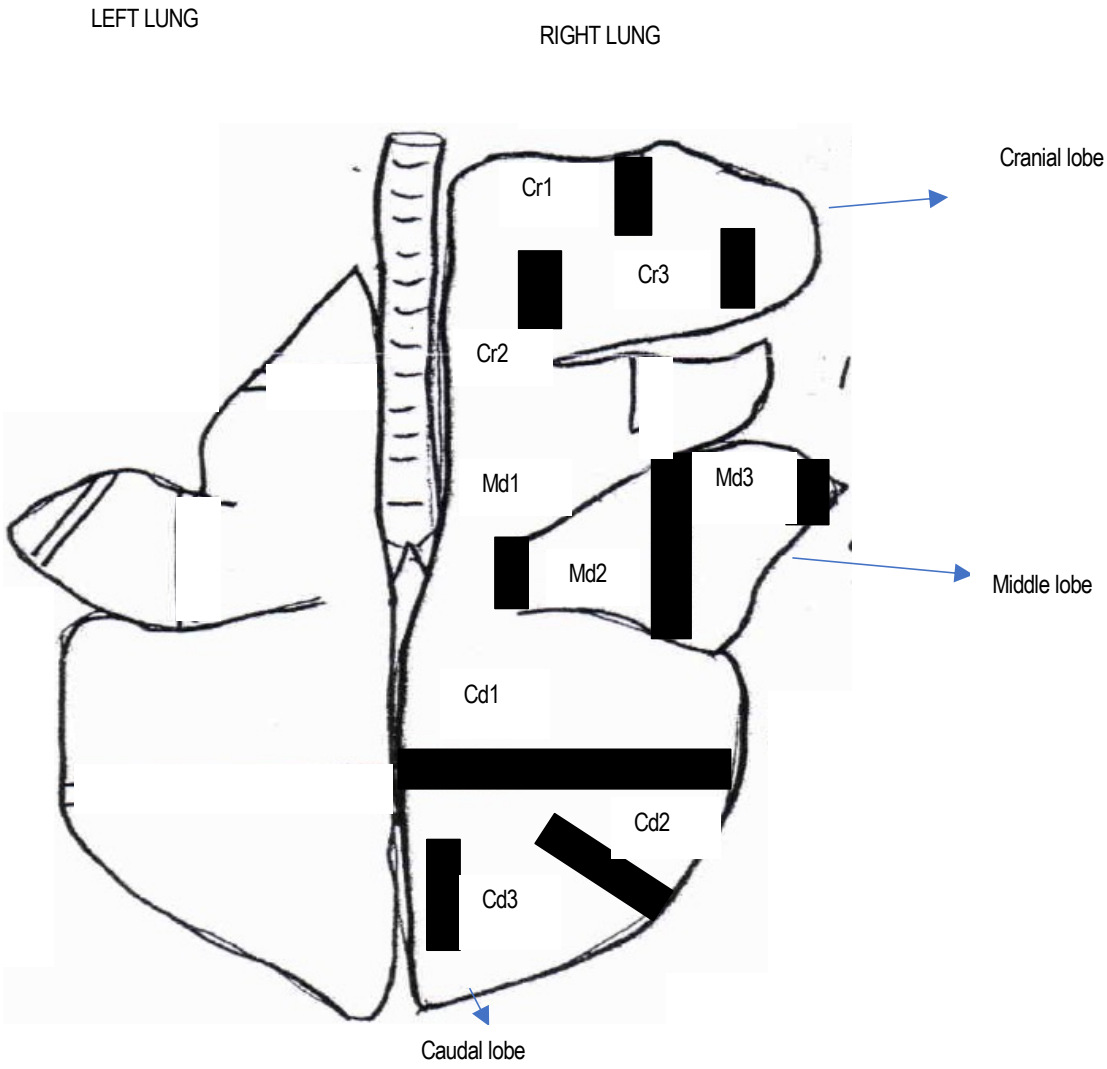

Figure 3.1: A drawing of bovine lung indicating areas where tissue samples were collected and cryopreserved using liquid nitrogen. We collected at least three samples from each lobe.

(Cranial lobe - Cr1, Cr2, Cr3 Middle lobe – Md, Md2, Md3 Caudal lobe – Cd1, Cd2, Cd3)

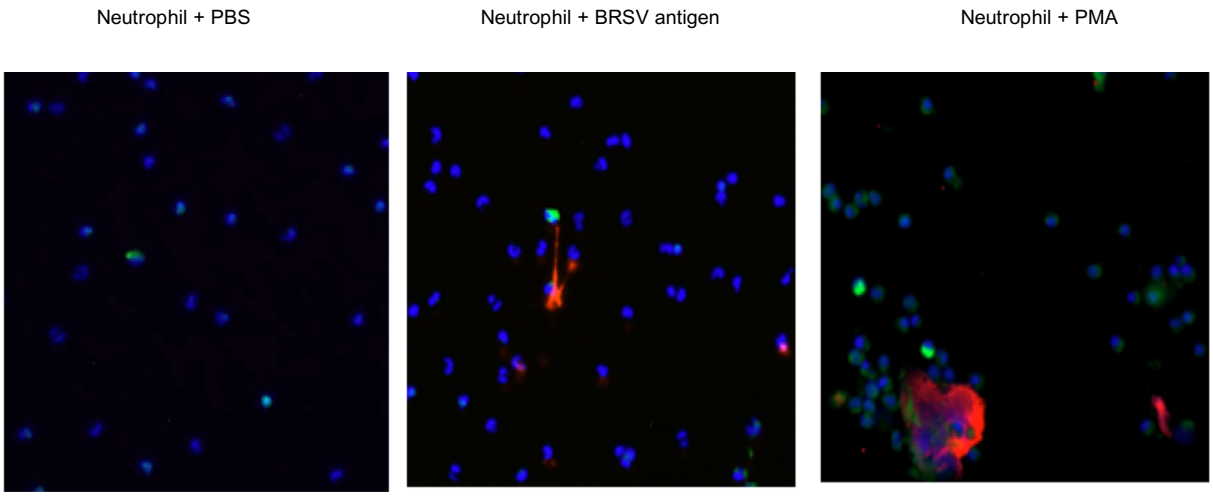

Figure 3.2: Representative immunofluorescent images of cytology samples from healthy calves. Cells were fixed, permeabilized and stained for citrullinated histone H3 (citH3, red), Neutrophil elastase (NE, green) and DNA (blue). NETs were identified by co-localization of citH3, and NE. Cells were identified to be neutrophils based on lobulated nuclei. Original image X200 magnification.

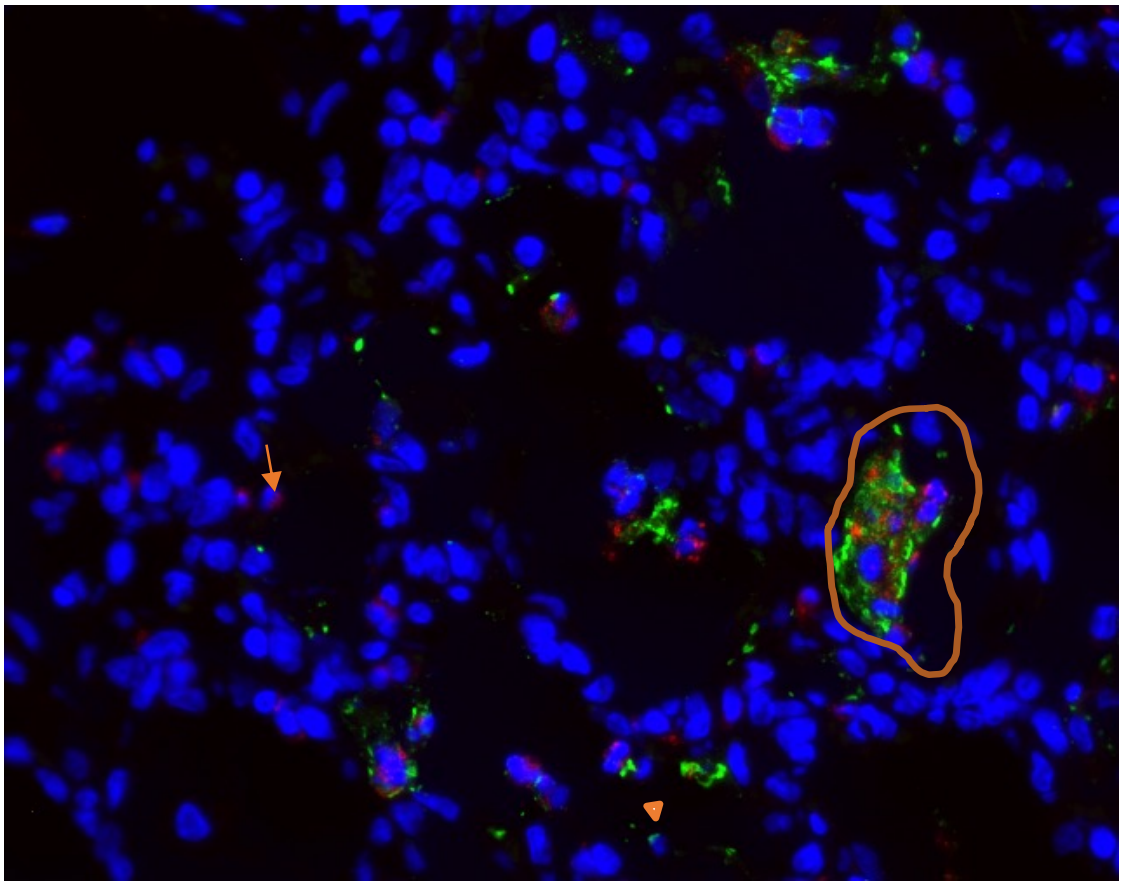

Figure 3.3: A representative immunofluorescent image of frozen bovine lung tissue. Tissues were fixed, permeabilized and stained for citrullinated histone H3 (citH3, green) and neutrophil elastase (NE, red). DNA was stained with DAPI-blue.

Note the intracellular expression of citH3 (arrow heads) and NE (arrows) in neutrophils, and release of NETs decorated with NE and citH3 (circled). Original 400x magnification

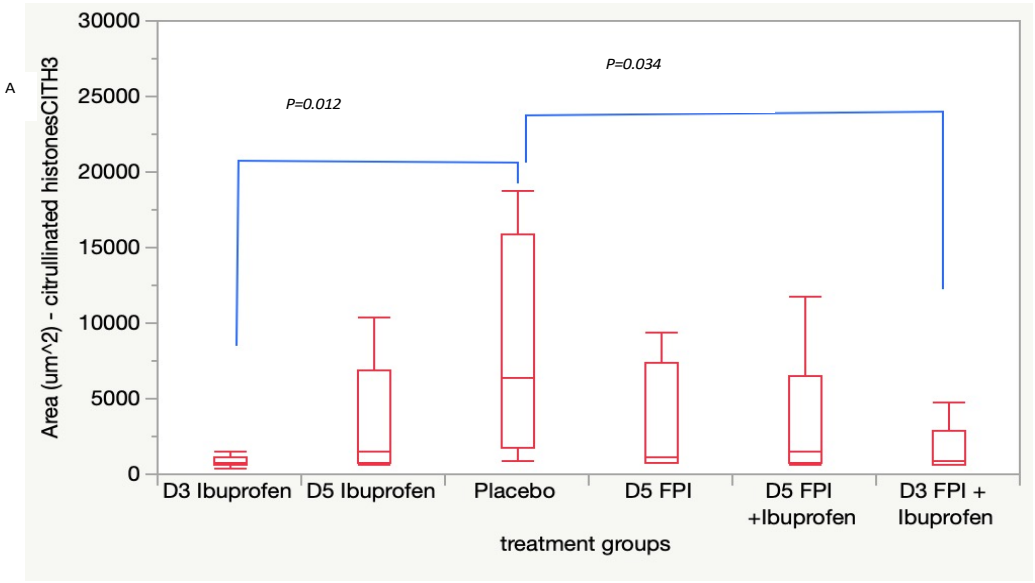

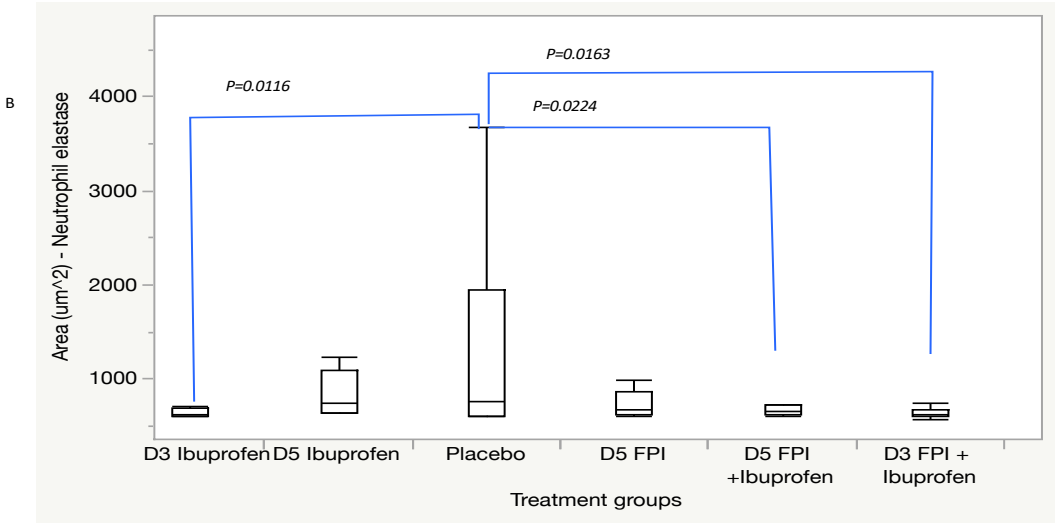

Figure 3.4: Distribution of NETs in the frozen lung tissue between the treatment groups.

NETs were visualized as presence of citrullinated histones (citH3), and neutrophil elastase(NE) staining using an epi-fluorescence microscope. Images were captured at ×200 magnification and the NETs quantified as the average area in µm of NE and CitH3 in 10 microscopic fields. The graphs show the different treatment groups for FPI, ibuprofen or both initiated on day 3 and 5 of BRSV infected calves.

A) CitH3 B) NE staining in frozen lungs tissue (n=6 per treatment group). Values are means + SE

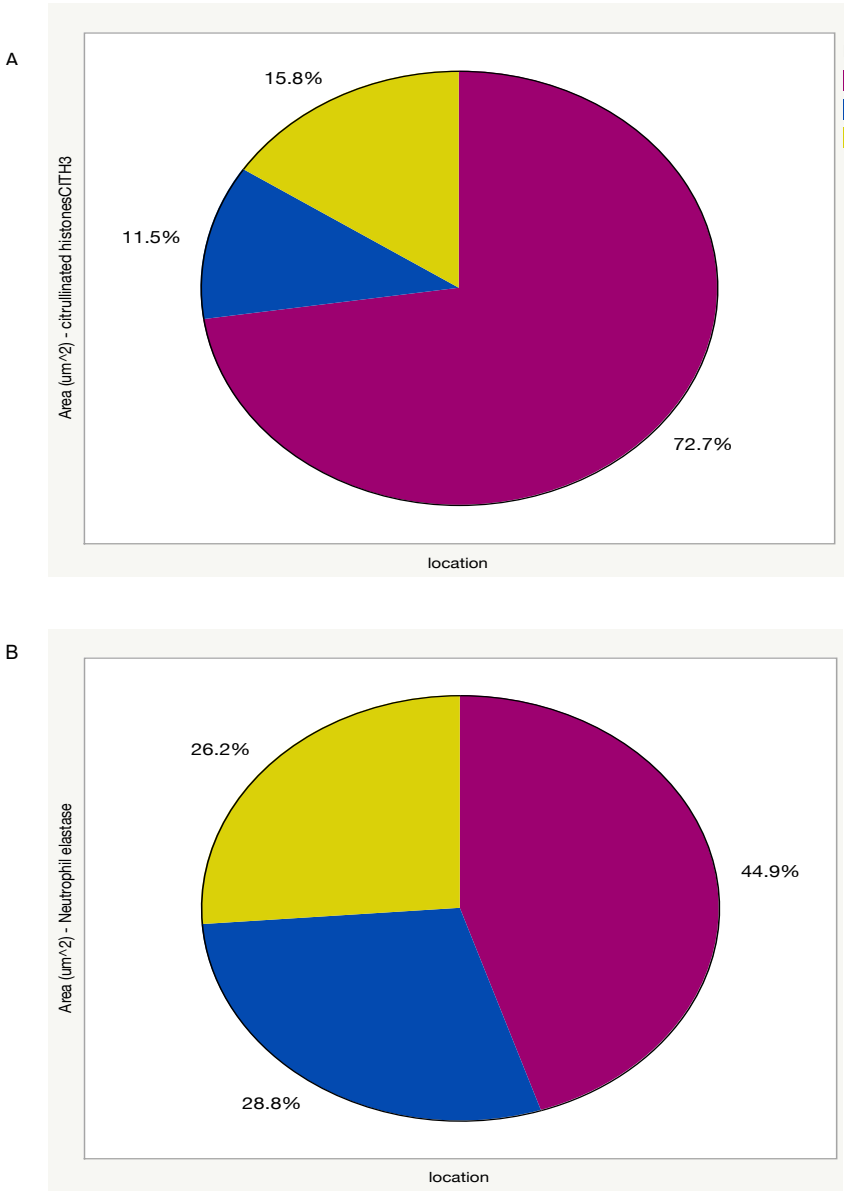

Figure 3.5: Distribution of NETs in the lobes of frozen lung tissue of calves infected with BRSV and treated with FPI, ibuprofen or both.

NETs were analyzed as presence of citrullinated histones (citH3), and neutrophil elastase(NE) staining in the lung tissues using an epi-fluorescence microscope. Images were captured at ×200 magnification and the NETs quantified as the average area in µm of NE and CitH3 in 10 microscopic, A) citH3 and B) NE staining represented as a percentage of the total of three replicates(n=36).

Red – Cranial lobe, Yellow – middle lobe, Blue – caudal lobe

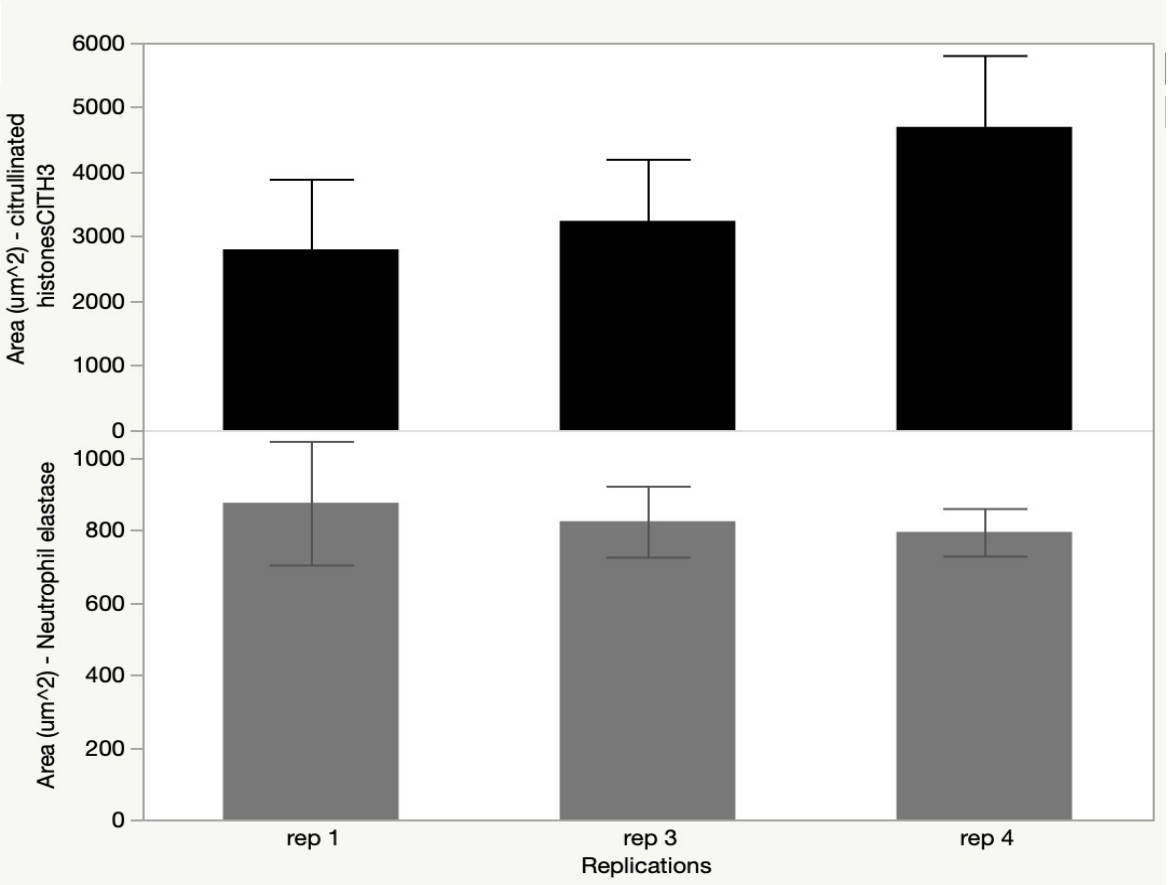

Figure 3.6: Batch analysis of NETs between the three replicates.

The bars show presence of CitH3 and NE in the lung tissues analyzed as different batches representing the replicates n=36.

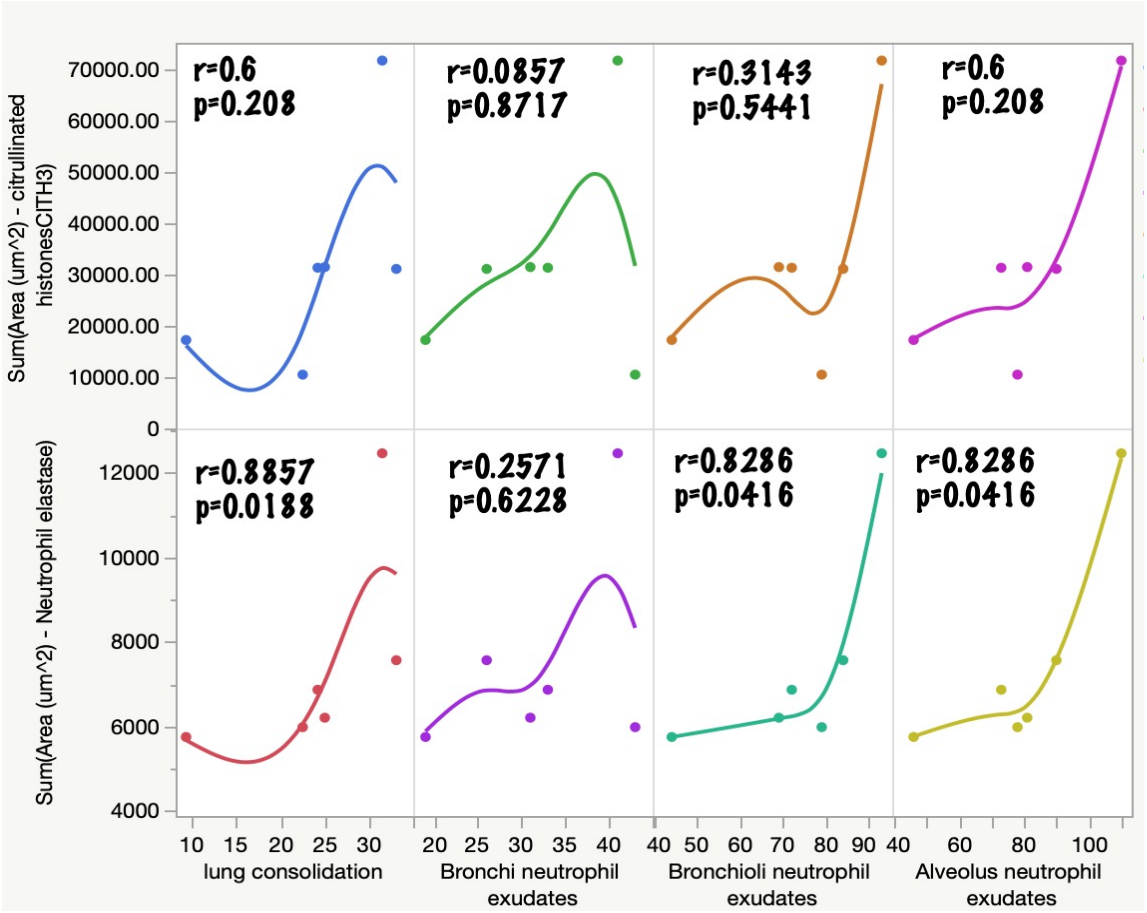

Figure 3.7: Correlation between the lung consolidation, neutrophil exudates and NETs in the lungs of calves infected with BRSV and treated using FPI, ibuprofen or both.

Scatter plot showing correlation between the levels of NE and CitH3 with the percentages of lung consolidation and neutrophil exudates in the bronchi, bronchiole, and alveoli airways.

REFERENCES

1. Remijsen Q, Berghe T Vanden, Wirawan E, et al (2011) Neutrophil extracellular trap cell death requires both autophagy and superoxide generation. Cell Res 21:290–304. https://doi.org/10.1038/cr.2010.150
2. Papayannopoulos V, Metzler KD, Hakkim A, Zychlinsky A (2010) Neutrophil elastase and myeloperoxidase regulate the formation of neutrophil extracellular traps. J Cell Biol 191:677–691. https://doi.org/10.1083/jcb.201006052
3. Chen R, Kang R, Fan XG, Tang D (2014) Release and activity of histone in diseases. Cell Death Dis.
4. Mitiku F, Hartley CA, Sansom FM, et al (2018) The major membrane nuclease MnuA degrades neutrophil extracellular traps induced by Mycoplasma bovis. Vet Microbiol 218:13–19. https://doi.org/10.1016/j.vetmic.2018.03.002
5. Muraro SP, De Souza GF, Gallo SW, et al (2018) Respiratory Syncytial Virus induces the classical ROS-dependent NETosis through PAD-4 and necroptosis pathways activation. Sci Rep 8:1–12. https://doi.org/10.1038/s41598-018-32576-y
6. Saitoh T, Komano J, Saitoh Y, et al (2012) Neutrophil extracellular traps mediate a host defense response to human immunodeficiency virus-1. Cell Host Microbe 12:109–116. https://doi.org/10.1016/j.chom.2012.05.015
7. Narasaraju T, Yang E, Samy RP, et al (2011) Excessive neutrophils and neutrophil extracellular traps contribute to acute lung injury of influenza pneumonitis. Am J Pathol 179:199–210. https://doi.org/10.1016/j.ajpath.2011.03.013
8. Huang H, Tohme S, Al-Khafaji AB, et al (2015) Damage-associated molecular pattern-activated neutrophil extracellular trap exacerbates sterile inflammatory liver injury.

Hepatology 62:600–614. https://doi.org/10.1002/hep.27841

9. Brinkmann V, Reichard U, Goosmann C, et al (2004) Neutrophil Extracellular Traps Kill Bacteria. Science (80-) 303:1532–1535. https://doi.org/10.1126/science.1092385

10. Schönrich G, Raftery MJ (2016) Neutrophil extracellular traps go viral. Front Immunol 7:11–14. https://doi.org/10.3389/fimmu.2016.00366

11. Díaz-Godínez C, Carrero JC (2019) The state of art of neutrophil extracellular traps in protozoan and helminthic infections. Biosci. Rep. 39

12. Narayana Moorthy A, Narasaraju T, Rai P, et al (2013) In vivo and in vitro studies on the roles of neutrophil extracellular traps during secondary pneumococcal pneumonia after primary pulmonary influenza infection. Front Immunol 4:56. https://doi.org/10.3389/fimmu.2013.00056

13. Metzler KD, Goosmann C, Lubojemska A, et al (2014) Myeloperoxidase-containing complex regulates neutrophil elastase release and actin dynamics during NETosis. Cell Rep 8:883–896. https://doi.org/10.1016/j.celrep.2014.06.044

14. Goel RR, Kaplan MJ (2020) Deadliest catch: Neutrophil extracellular traps in autoimmunity. Curr. Opin. Rheumatol. 32:64–70

15. Jorch SK, Kubes P (2017) An emerging role for neutrophil extracellular traps in noninfectious disease. Nat. Med. 23:279–287

16. Cortjens B, Lutter R, Boon L, et al (2016) Pneumovirus-induced lung disease in mice is independent of neutrophil-driven inflammation. PLoS One. https://doi.org/10.1371/journal.pone.0168779

17. Shao S, Fang H, Dang E, et al (2019) Neutrophil extracellular traps promote inflammatory responses in psoriasis via activating epidermal TLR4/IL-36R crosstalk. Front Immunol 10:.

https://doi.org/10.3389/fimmu.2019.00746

18. Funchal GA, Jaeger N, Czepielewski RS, et al (2015) Respiratory syncytial virus fusion protein promotes TLR-4-dependent neutrophil extracellular trap formation by human neutrophils. PLoS One 10:1–14. https://doi.org/10.1371/journal.pone.0124082

19. Cortjens B, De Boer OJ, De Jong R, et al (2016) Neutrophil extracellular traps cause airway obstruction during respiratory syncytial virus disease. J Pathol. https://doi.org/10.1002/path.4660

20. Toussaint M, Jackson DJ, Swieboda D, et al (2017) Host DNA released by NETosis promotes rhinovirus-induced type-2 allergic asthma exacerbation. Nat Med 23:681–691. https://doi.org/10.1038/nm.4332

21. Baker JC, Ellis JA, Clark EG (1997) Bovine respiratory syncytial virus. Vet Clin North Am Food Anim Pract 13:425–454. https://doi.org/10.1016/S0749-0720(15)30307-8

22. Gershwin LJ (1996) Bovine respiratory syncytial virus infection: Immunopathogenic mechanisms. Anim. Heal. Res. Rev. 8:207–213

23. Berghaus LJ, Corbeil LB, Berghaus RD, et al (2006) Effects of dual vaccination for bovine respiratory syncytial virus and Haemophilus somnus on immune responses. Vaccine 24:6018–6027. https://doi.org/10.1016/j.vaccine.2006.03.077

24. Taylor G, Thom M, Capone S, et al (2015) Efficacy of a virus-vectored vaccine against human and bovine respiratory syncytial virus infections. Sci Transl Med. https://doi.org/10.1126/scitranslmed.aac5757

25. Shirey KA, Pletneva LM, Puche AC, et al (2010) Control of RSV-induced lung injury by alternatively activated macrophages is IL-4Rα-, TLR4-, and IFN-B-dependent. Mucosal Immunol. https://doi.org/10.1038/mi.2010.6

26. Collins PL, Melero JA (2011) Progress in understanding and controlling respiratory syncytial virus: Still crazy after all these years. Virus Res.

27. Van Drunen Littel-Van Den Hurk S, Watkiss ER (2012) Pathogenesis of respiratory syncytial virus. Curr. Opin. Virol. 2:300–305

28. Carvajal JJ, Avellaneda AM, Salazar-Ardiles C, et al (2019) Host Components Contributing to Respiratory Syncytial Virus Pathogenesis. Front Immunol 10:1–19. https://doi.org/10.3389/fimmu.2019.02152

29. Cortjens B, Yasuda E, Yu X, et al (2017) Broadly Reactive Anti-Respiratory Syncytial Virus G Antibodies from Exposed Individuals Effectively Inhibit Infection of Primary Airway Epithelial Cells. J Virol. https://doi.org/10.1128/jvi.02357-16

30. Jha A, Jarvis H, Fraser C, Openshaw PJM (2016) Respiratory syncytial virus. ERS Monogr. https://doi.org/10.1183/2312508X.10010315

31. Walsh P, Lebedev M, McEligot H, et al (2020) A randomized controlled trial of a combination of antiviral and nonsteroidal anti-inflammatory treatment in a bovine model of respiratory syncytial virus infection. PLoS One 15:. https://doi.org/10.1371/journal.pone.0230245

32. Gilead's Investigational GS-5806 Reduces Viral Load and Clinical Symptoms in Phase 2 Respiratory Syncytial Virus (RSV) Challenge Study in Adults. https://www.gilead.com/news-and-press/press-room/press-releases/2014/5/gileads-investigational-gs5806-reduces-viral-load-and-clinical-symptoms-in-phase-2-respiratory-syncytial-virus-rsv-challenge-study-in-adults. Accessed 18 Dec 2020

33. DeVincenzo JP, Whitley RJ, Mackman RL, et al (2014) Oral GS-5806 Activity in a Respiratory Syncytial Virus Challenge Study. N Engl J Med.

https://doi.org/10.1056/nejmoa1401184

34. Jordan R, Shao M, Mackman RL, et al (2015) Antiviral efficacy of a respiratory syncytial virus (RSV) fusion inhibitor in a bovine model of RSV infection. Antimicrob Agents Chemother 59:4889–4900. https://doi.org/10.1128/AAC.00487-15

35. Walsh P, Behrens N, Chaigneau FRC, et al (2016) A Randomized Placebo Controlled Trial of Ibuprofen for Respiratory Syncytial Virus Infection in a Bovine Model. PLoS One 11:e0152913. https://doi.org/10.1371/journal.pone.0152913

36. Li RHL, Johnson LR, Kohen C, Tablin F (2018) A novel approach to identifying and quantifying neutrophil extracellular trap formation in septic dogs using immunofluorescence microscopy. BMC Vet Res 14:1–7. https://doi.org/10.1186/s12917-018-1523-z

37. Carvallo Chaigneau FR, Walsh P, Lebedev M, et al (2021) A randomized controlled trial comparing non-steroidal anti-inflammatory and fusion protein inhibitors singly and in combination on the histopathology of bovine respiratory syncytial virus infection. PLoS One 16:e0252455. https://doi.org/10.1371/journal.pone.0252455

38. Ellis J, Waldner C, Gow S, Jackson M (2013) Relationship of the extent of pulmonary lesions to the partial pressure of oxygen and the lactate concentration in arterial blood in calves experimentally infected with bovine respiratory syncytial virus. Can J Vet Res 77:205–210

39. Valarcher JF, Taylor G (2007) Bovine respiratory syncytial virus infection. Vet. Res. 38:153–180

40. Kumar S V, Desai J, Anders H-J (2016) Neutrophil extracellular traps in tissue pathology. Artic Histol Histopathol. https://doi.org/10.14670/HH-11-816

41. Tayyari F, Marchant D, Moraes TJ, et al (2011) Identification of nucleolin as a cellular receptor for human respiratory syncytial virus. Nat Med. https://doi.org/10.1038/nm.2444

42. Cortjens B, De Jong R, Bonsing JG, et al (2018) Local dornase alfa treatment reduces NETs-induced airway obstruction during severe RSV infection. Thorax 73:578–580. https://doi.org/10.1136/thoraxjnl-2017-210289

43. Cortjens B, De Boer OJ, Antonis AFG, et al (2015) Neutrophil Extracellular Trap Formation In Severe Respiratory Syncytial Virus Lung Infection. Am J Respir Crit Care Med 191:no pagination

44. Leal AC, Mizurini DM, Gomes T, et al (2017) Tumor-Derived Exosomes Induce the Formation of Neutrophil Extracellular Traps: Implications For The Establishment of Cancer-Associated Thrombosis. Sci Rep 7:. https://doi.org/10.1038/s41598-017-06893-7

45. Shak S, Capon DJ, Hellmiss R, et al (1990) Recombinant human DNase I reduces the viscosity of cystic fibrosis sputum. Proc Natl Acad Sci U S A 87:9188–9192. https://doi.org/10.1073/pnas.87.23.9188

46. Symptoms and Care of RSV (Respiratory Syncytial Virus) | CDC. https://www.cdc.gov/rsv/about/symptoms.html. Accessed 11 Jun 2021

47. Lemos HP, Grespan R, Vieira SM, et al (2009) Prostaglandin mediates IL-23/IL-17-induced neutrophil migration in inflammation by inhibiting IL-12 and IFNγ production. Proc Natl Acad Sci U S A 106:5954–5959. https://doi.org/10.1073/pnas.0812782106

48. Erik Lubberts Davelaar and, Asmawidjaja PS, W Hazes Sandra M J Paulissen JM, Piet van Hamburg J (2021) Independent of IL-23 Pathway, 2 Cyclooxygenase/Prostaglandin E Pathogenicity via the Synovial Fibroblasts Directly Induce Th17 Downloaded from. J Immunol J Immunol by guest. https://doi.org/10.4049/jimmunol.1300274

49. Cupedo T (2011) Human lymph node development: An inflammatory interaction. Immunol. Lett.

50. Sun F, Zhang Y, Li Q (2017) Therapeutic mechanisms of ibuprofen, prednisone and betamethasone in osteoarthritis. Mol Med Rep 15:981–987. https://doi.org/10.3892/mmr.2016.6068

51. Díaz-González F, González-Alvaro I, Campanero MR, et al (1995) Prevention of in vitro neutrophil-endothelial attachment through shedding of L-selectin by nonsteroidal antiinflammatory drugs. J Clin Invest 95:1756–1765. https://doi.org/10.1172/JCI117853

52. Al-Waeli H, Nicolau B, Stone L, et al (2020) Chronotherapy of Non-Steroidal Anti-Inflammatory Drugs May Enhance Postoperative Recovery. Sci Rep 10:1–14. https://doi.org/10.1038/s41598-019-57215-y

53. Heeb LEM, Egholm C, Impellizzieri D, et al (2018) Regulation of neutrophils in type 2 immune responses. Curr. Opin. Immunol. 54:115–122

54. Antonis AFG, Schrijver RS, Daus F, et al (2003) Vaccine-Induced Immunopathology during Bovine Respiratory Syncytial Virus Infection: Exploring the Parameters of Pathogenesis. J Virol 77:12067–12073. https://doi.org/10.1128/jvi.77.22.12067-12073.2003

55. Obermayer A, Stoiber W, Krautgartner WD, et al (2014) New aspects on the structure of neutrophil extracellular traps from chronic obstructive pulmonary disease and in vitro generation. PLoS One 9:97784. https://doi.org/10.1371/journal.pone.0097784

CHAPTER 4

4. Preliminary Isolation and Identification of Innate Lymphoid Cells in Calves Lungs

4.1 Abstract

Innate lymphoid cells (ILCs) comprise of a family of relatively rare lymphoid cells that direct mucosal immune responses including initiating, sustaining, and even curbing immune responses. ILCs lack classical cell-surface markers and can be divided into five main types (NKs, ILC1s, ILC2s, ILC3s, and Lti cells) based on differences in cytokine production, phenotype, and developmental pathway. Since their discovery ILCs have gained greater relevance in the field of immunology due to their multiple functions in the innate immune response. ILCs are mostly tissue-resident cells tightly bound to the tissue structure and can be found in mucosal and barrier organs like skin, gut, and lungs. Due to ILCs locations and low numbers, they require long and complex protocols that do not always provide sufficient yield for analysis. ILCs can only be identified by combinations of cell surface markers and cytokine production thus multicolor flow cytometry is the most reliable method to purify, characterize, and assess their functionality. Currently very little is known about the isolation and identification of ILCs in bovine lung tissue. Here, we describe a method for sample collection, cell preparation and flow cytometric analysis of bovine lung immune cells isolated from the lungs of calves to identify bovine ILCs. The cell marker panel and flow cytometry gating strategies were done on cells that fit the description as ILCs. This can constitute a useful tool for future investigations of bovine ILCs.

4.2. Introduction

The immune system is tasked with surveying its surroundings and discriminating between harmless and potentially harmful materials. Regulation of innate immunity at mucosal surfaces is important for preventing pathogen invasion, and also for preventing inappropriate immune activation and pathology. In the last 10 years, innate lymphoid cells (ILCs) have been identified as a family of hematopoietic cells bearing a resemblance to the CD4 T helper (Th) Th1, Th2, and Th17 cell subsets in their effector and regulatory functions, while lacking specific antigen receptors (e.g. TCR)[1]. ILCs are predominantly found at mucosal sites(Table 4.1), although they have been isolated from nearly every tissue. They are mainly tissue resident cells that have the potential to expand locally during acute inflammation [2, 3].

ILCs institute their function by producing an array of soluble mediators, including cytokines and eicosanoids that direct the reactions of local hematopoietic and epithelial cells as illustrated in Table 4.1. They also take part in the recruitment of immune cells, tissue and metabolic homeostasis, pathogen resistance and anti-cancer immunity. Improper development of ILCs can also lead to immune dysregulation [1, 4, 5].

The relatively recent identification and isolation of ILCs in mice has led to an explosion of studies, yet many questions remain surrounding their development, regulation, and function in homeostasis and disease, and their presence in species other than the mouse. In this chapter, we focus on the basic methods for identifying and isolating ILCs from the calf lung. This chapter does not show definite characterization of bovine ILCs but represents an attempt towards this goal.

4.2. Materials and Methods

4.2.1. Samples

Blood was drawn from 6 healthy cattle at the University of California Davis Department of Animal Science, meat lab and processed on the same day. Peripheral Blood Mononuclear Cells (PBMCs) were isolated using Lymphoprep density gradient centrifugation. The PBMCs used for panel development and troubleshooting the protocol.

Lung samples were collected from 36, five to six-week-old calves obtained from a dairy for use in the treatment study described in chapter 2. Briefly the calves were infected with Bovine Respiratory Syncytial virus and treated with a fusion protein inhibitor, ibuprofen or a combination of the two. The calves were euthanized on day 10 post infection and lung samples collected into sterile containers with Hanks Buffered Salt Solution (HBSS) supplemented with gentamicin to minimize contamination and maintain cellular integrity. As a control, fresh lung samples were obtained from 2 healthy cows and one 6 week old calf from the University of California Davis Department of Animal Science, meat lab.

4.2.2. Methods

(Reagents, tools and equipment used in this chapter are listed on appendix II)

4.2.2.a. Isolation of calf lung and preparation of single cell suspension

Lung samples in a container with cell media buffer were transferred into a petri dish on ice and mechanically tissue dissociated with sterilized razor blades or dissection scissors into fragments of tissue ~1mm in size. The tissues pieces were places into a 50ml conical tubes containing 30ml of lung digestion medium. They were incubated at 37°C for 30 minutes with

gently agitation every 10 minutes and cell media buffer added at the end to stop enzymatic activity. The digested tissue and media were passed through a 70µm cell strainer using the plunger end of a 1mL syringe to make a single cell suspension and the cell strainer washed with 5–10mL of cell media to ensure collection of all cells. The media was centrifuged to pellet the cells at xg 400 4°C for 10 minutes with brakes. The supernatant was discarded, and the cells re-suspended in 10mL cell media buffer. To separate the lymphoid cells from the cells collected, 10ml of Lymphoprep was dispensed into Lymphoprep tubes and the resuspended cells slowly layered on it. The mixture was centrifuged at xg 500 for 30 minutes at 4°C with no brakes and minimal acceleration. The cells at the interface were carefully collect, transferred to a 15mL conical tube and washed with 5–10mL of complete RPMI-1640 medium by centrifugation at xg 400 for 10 minutes at 4°C.

The supernatant was discarded, cells re-suspend in cell media with 10% DMSO and stored in liquid nitrogen for further analysis.

4.2.2.b. Magnetic enrichment of live cells

The enrichment of live cells from a single cell suspension of digested lung tissue can be beneficial in removing debris, dead and dying cells especially from samples that have been preserved in liquid nitrogen for long. This step was mainly performed on the lung cells collected from the replicates and stored in liquid nitrogen as they contained a high number of dead cells due to long the storage. The cells were quickly thawed from liquid nitrogen and placed in 15ml conical tubes. The DMSO was washed off by adding10ml cell media buffer and centrifuged at xg 400 for 10 minutes at 4°C. Total cell number and viability were determined automatically using a MUSE counter.

The cell pellet was resuspended in 100 µL of dead cell removal micro beads per 10^7 total cells as per manufacturer's instructions mixed well and incubated for 15 minutes at room temperature (20−25 °C). After incubation 500ul of binding buffer (provided with the Dead cell removal kit) was added to the sample the cell suspension passed through a 40µm sterile filter to remove cell clumps which may clog the column. The suspension was applied onto the column and magnetic separation performed using the MS column. The live cell fraction is collected as the flow through containing unlabeled cells while the labeled dead cells remain trapped in the column. The column was removed from the magnetic separator and placed on a 15ml conical tube. The magnetic labeled cells were flushed out from the column by adding 5ml biding buffer to the column and plunging the cells out with a syringe plunger (provided with the MS column). To increase purity and yield of live cells, the eluted live and dead cell fractions were passed over a fresh magnetic column for each fraction and after washed with binding buffer by centrifugation at xg 400 for 10min at 4°C.

The cells were resuspended using FACs media, the cell number and viability determined using a MUSE counter. Cell viability in the thawed sample was 30-40% and after removing dead cells with the dead cell removal kit, the viability rate was increased to 78-84%.

4.2.2.c. Separation of lymphocytes from blood and subsequent red blood cells lysis

Blood was collected into tubes containing anticoagulant, ACD tubes, and diluted in conical tubes at 1:1.5 dilution with sterile PBS. 10ml Lymphoprep was dispensed to the bottom of the Lymphoprep tubes and 30ml of diluted blood slowly layered on top of the Lymphoprep. The tubes were centrifuged for 20 min at 800xg at a temperature of 18-25^{o}C with brakes. After centrifugation, the mononuclear cells form a distinct band at the sample/medium interface as peripheral blood

mononuclear cells (PBMCs). The PBMCs layer was collected from the interface into a conical tube. Red blood cells were lysed using cold distilled water for 30-60s and the pH readjusted using 10X PBS. The sample was centrifuged for 20 min at 250xg at 4 °C to pellet the cells. The red blood cell lysis was repeated until the water run clear after which cells were resuspended in FACs media, and the cell number and viability determined using a MUSE counter. Cell viability was 94-97%. The PBMCs were used fresh or stored in liquid nitrogen with 10% DMSO until needed.

4.2.2.d. Antibody staining panel and Flow cytometry analysis to identify ILCs.

The ILCs were identified using a 4 laser, 18 color BD LSRII cytometer. An appropriate live dead discriminator DAPI or Aqua viability fixable dye (when analyzing fixed cells) was used for all samples to exclude non-viable cells. Lineage antibodies (Abs) included CD3ε, CD4, CD8, CD21, MHCII and ILCs gating antibodies CD45, CD90 and CD127 (Table 4.2).

The cells collected from blood (PBMCs) and lung cells were stained for analysis either as fresh cells after isolation, from liquid nitrogen storage or after live cell enrichment step. The cells (3 to 5×10^6 cells) in FACs buffer were centrifuged at xg 400 for 10 minutes at 4°C and the supernatant discarded. The cells were then wash by adding 1mL of PBS per 10^6 cells at the same speed and re-suspend cells in 1mL of PBS (azide and protein-free) per 10^6 cells. 1mL of previously optimized Aqua viability fixable live dead fixable dye was added if the cells were to be fixed to be analyzed at a later date Incubate cells at 4°C for 15 minutes in the dark. Cells were washed by adding 1mL of FACS buffer per 10^6 cells and centrifuged at xg 400 for 10 minutes at 4°C. The supernatant was discarded, and the pellet washed again. The cells were re-suspended in 1mL blocking buffer per 10^6 total cells and add FcR block. After incubating for 30 minutes on ice the sample was

centrifuged at xg 400 for 10 minutes at 4°C for 10 minutes and supernatant discarded. Controls included were unstained, single stained and fluorescence minus one (FMO) control.

Antibody master mix was prepared using optimally titrated directly conjugated antibodies diluted in FACS buffer. The cells were re-suspended in 50uL master mix and incubated at 4°C for 30 minutes in the dark. Cells were washed by adding 1mL of FACs buffer and centrifuged at xg 400 for 10 minutes at 4°C . The supernatant was discarded, and the wash step repeated. After washing, cells were re-suspended in 500uL of FACS buffer and filtered through a 20µm filter into 5mL round bottom test tube prior to flow cytometric analysis. The cells were kept on ice in the dark during the staining process and before analysis. For samples that were analyzed on the same day DAPI, was added just before analysis and the aqua viability dying step skipped. DAPI was preferred as it had a better signal to noise fluorescence difference compared to aqua.

After staining the cells ~1million events were acquired using the BD LSR II flow cytometer. Compensation was performed using adsorbed microspheres treated with the same antibodies used for staining. All antibodies were titrated to define an optimal concentration for specific staining. Cell gating was determined using the isotype control values or the fluorochrome minus 1 (FMO) setting to all parameters. Cell debris and dead cells were excluded from the analysis based on side scatter and fixable live dead discriminator fluorescence (DAPI or Aqua viability dye).

4.3. Data analysis

Data collected from flow cytometry was analyzed using Flow Jo 10 software (Flow Jo LLC) and evaluated for cells percentages of the ILCs.

4.4. Results

Due to time constrains and limitation on acquiring antibodies specific to bovine cells, only a few samples including PBMCs, cells from the 6 week old calf (healthy control) and a sample from replicate three of the treatment study (chapter 2) infected with BRSV and not treated with FPI or ibuprofen, were analyzed and a preliminary gating strategy developed. ILCs were identified based upon a combination of markers denoting live, $CD45^{+}$, lineage negative cells (lacking CD3, CD4, CD8, CD21, and MHCII), which also expressed CD90 and CD127 [6, 7]). Based on this indication, we first determined a gating strategy to identify ILC population on bovine peripheral cells (PBMCs), as illustrated in Figure 1A. This was first used to troubleshoot the antibodies and set a rudimentary gating strategy.

Compensation beads (single stained control) were used to calculate the compensation matrix which was applied to the samples before analysis. The samples were first gated on the forward (FSC) vs side scatter (SCC) excluding debris with this population labeled cells of interest (Figure 4.1.A). This was done to encompass all possible populations since identification of these ILCs in bovine is novel and we do not know how they are distributed. Doublets were excluded by gating on singlets using a gating window of side scatter area vs. side scatter height. Subsequently, live cells were gated on aqua viability/DAPI vs CD90 (Figure 4.1.B). The selected population was then gated on $lineage^{-}$ (CD3ε, CD4, CD8, CD21, MHCII) and $CD45^{+}$ to ensure that the cells selected are lymphocytes lacking these specific receptors(Figure 4.1.C). The expression of CD90(Figure 4.1.D) and CD127 (Figure 4.1.E)was analyzed and bovine ILCs identified as Lineage- $CD45^{+}CD90^{+}$ and CD 127^{+} (Figure 4.1.E). This gating strategy was applied to the other samples with an unstained sample as a control (Figure 4.2), sample from the 6 week old calf(Figure 4.3) and a sample from replicate 3 after live cell enrichment step (Figure 4.4). On further analysis

of the sample from the calf in replicate three (infected with BRSV but received no treatment) the cells staining for Lineage- $CD45^{+}CD90^{+}$ and CD 127^{+} were located higher on the side scatter compared to normal lymphocytes (Figure 4.5) and will need further analysis to concretely characterize these cells.

4.5. Discussion

This chapter presents a preliminary method for isolation and identification of ILCs in bovine lung tissue. A consistent method will need to be developed for obtaining a high yield, which is of particular importance due to the expected low percentage of ILCs represented in most tissues [8, 9]. Isolation of ILCs in bovine lung tissue consists of 5 essential steps: clean sample collection, enzymatic digestion, Lymphoprep gradient centrifugation and staining with appropriate antibodies. This protocol requires the addition of DNAase in the digestion medium in order to prevent cell clumping but despite including these modifications in the protocol, it is not certain that there will be high yield of ILCs[10].

Characterization of lung ILCs calls for a complex multiparametric flow cytometry analysis due to the lack of a unique differential cell marker[11, 12]. Many ILC markers are also expressed in other immune cells, and the use of several T cell markers, such as CD3, CD4, CD8 help in identifying the lineage- population. Although research on ILCs and their related cytokines is still in its infancy, significant progress has been made toward elucidating their functions as regulators of immunity, inflammation, and tissue homeostasis[2, 13, 14]. ILCs are present in nearly all tissues examined (albeit in very small numbers), yet substantially enriched in mucosal tissues [3, 6, 13, 15]. It is now clear that these cells play important roles in diverse physiological responses:

resistance to pathogens, regulation of chronic inflammation, tissue remodeling, cancer, and promoting metabolic homeostasis [14]

The challenge in working with ILCs lies in the fact that research has not (yet) discovered a unique cell surface molecule that can be used to distinguish these cells by either flow cytometry or immunohistochemistry. Therefore, the best method remains a detailed multi-color analysis of lineage negative cells that express the lymphoid associated markers CD90 and CD127. Intracellular staining for transcription factors may help to further distinguish the three different groups ILC1, ILC2 and ILC3. Similarly, intracellular staining for cytokines may then link ILC subsets with functional capabilities [5, 13, 16]

In this study we were able to tentatively identify a population of cells in the bovine that express a set of markers found to identify ILCs in mice[17–19]. The biggest challenge was finding commercially-available antibodies for various cell surface markers of bovine for use in flow cytometry. Unfortunately, we were not able to find specific bovine antibodies for some important ILC markers, mainly CD 127 and CD 90 ns instead opted to use antibodies raised against human epitopes, which have roughly 80% homology to bovine.

Given the limitations of this study, future work will be required clearly identify the bovine ILC population. This would include sorting purified ILC subsets followed by *in vitro* manipulation to interrogate their function.

4.6 . Conclusions and future plans

In the last 10 years discovery of ILCs has added to our understanding of innate immunity. However, an understanding of ILC phenotypes and function in the bovine species is lacking. ILC classification and categorization in bovines will improve understanding of the mechanisms

underlying the development and function of ILCs. Focusing on ILCs may provide new strategic therapeutic approaches for different conditions.

Future efforts to elucidate the tissue distribution and molecular mechanisms underlying the functions of ILCs in triggering immunity, inflammation and tissue repair will result in a more comprehensive view of how ILCs regulate immunological and physiological processes.

Table 4.1: Overview of ILCs and their function

ILC subset	**ILC lineage**	**Major stimulating cytokine**	**Signature cytokine produced**	**Transcription Factors**	**Localization**
ILC1	ILC1 NK cell	IL-12 IL-15 IL-18	IFN-γ TNFα, perforin, granzymes	T-bet Eomes	Skin, intestine, lymphoid tissues, thymus, liver
ILC2	iILC2 nILC2	IL-25 IL-33 TSLP	IL-5, IL-9, IL-13, amphiregulin	RORα, Bcl-11b	Spleen, liver, lung, intestine, skin, bone, adipose tissue, brain
ILC3	LTi ILC17 ILC22	IL-1β IL-23 IL-7	LTα/β, IL-17, IL-22 IL-17, IFNγ IL-22	RORγt, AhR, Notch, RUNX1, TCF-1, GATA-3	Lymphoid tissues, intestine, lung, skin, liver, tonsils

Table 4.2: Antibodies conjugated to different fluorophores used in identification of ILCs

Gate	Antibody	clone	Conjugation	Company
Lineage negative	CD3ε	MM1A	FITC	Bio-Rad laboratories
	CD4	CC8	FITC	Bio-Rad laboratories
	CD8	CC63	FITC	Bio-Rad laboratories
	CD21	CC21	FITC	Bio-Rad laboratories
	MHCII	CC108	FITC	Abcam
ILCs	CD45	CC1	APC-Cy7	Abcam
	CD90	DG3	APC	Abcam
	CD127	MB15-18C9	PE	Miltenyi Biotec

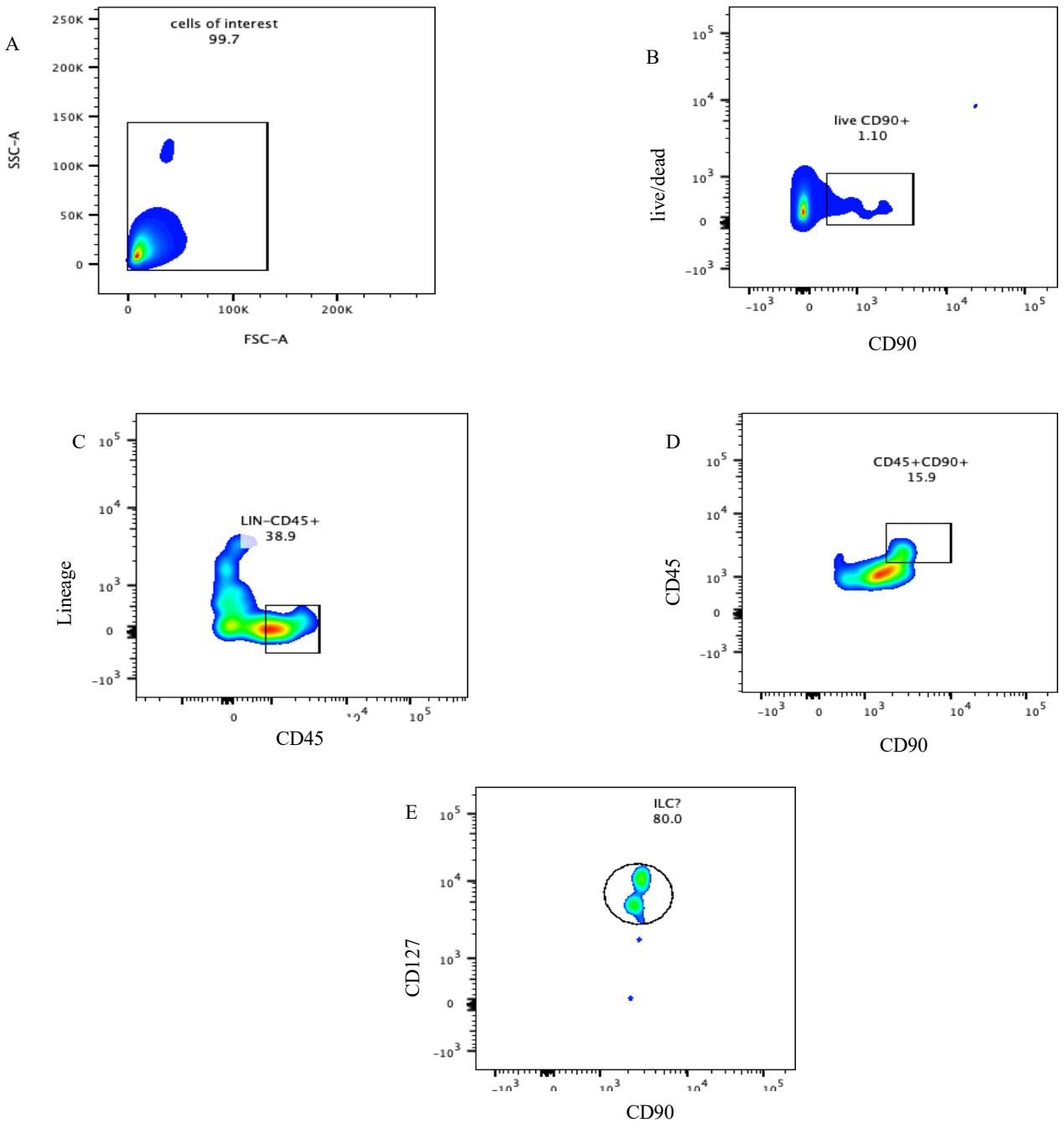

Figure 4.1 Gating strategy for analysis of innate lymphoid cells from bovine lung tissue.

(A) leukocytes were gated with the forward scatter/side scatter (FSC/SSC) method. (B) Single and CD90+ live cells were considered for the analysis. (C) Negative lineage and CD45+cells were gated to analyze innate lymphocyte cells. (D) Expression of CD45+ and CD90+ served to distinguish cells with a lymphoid origin. (E) Staining of CD127+ was used to identify a possible ILC population**.**

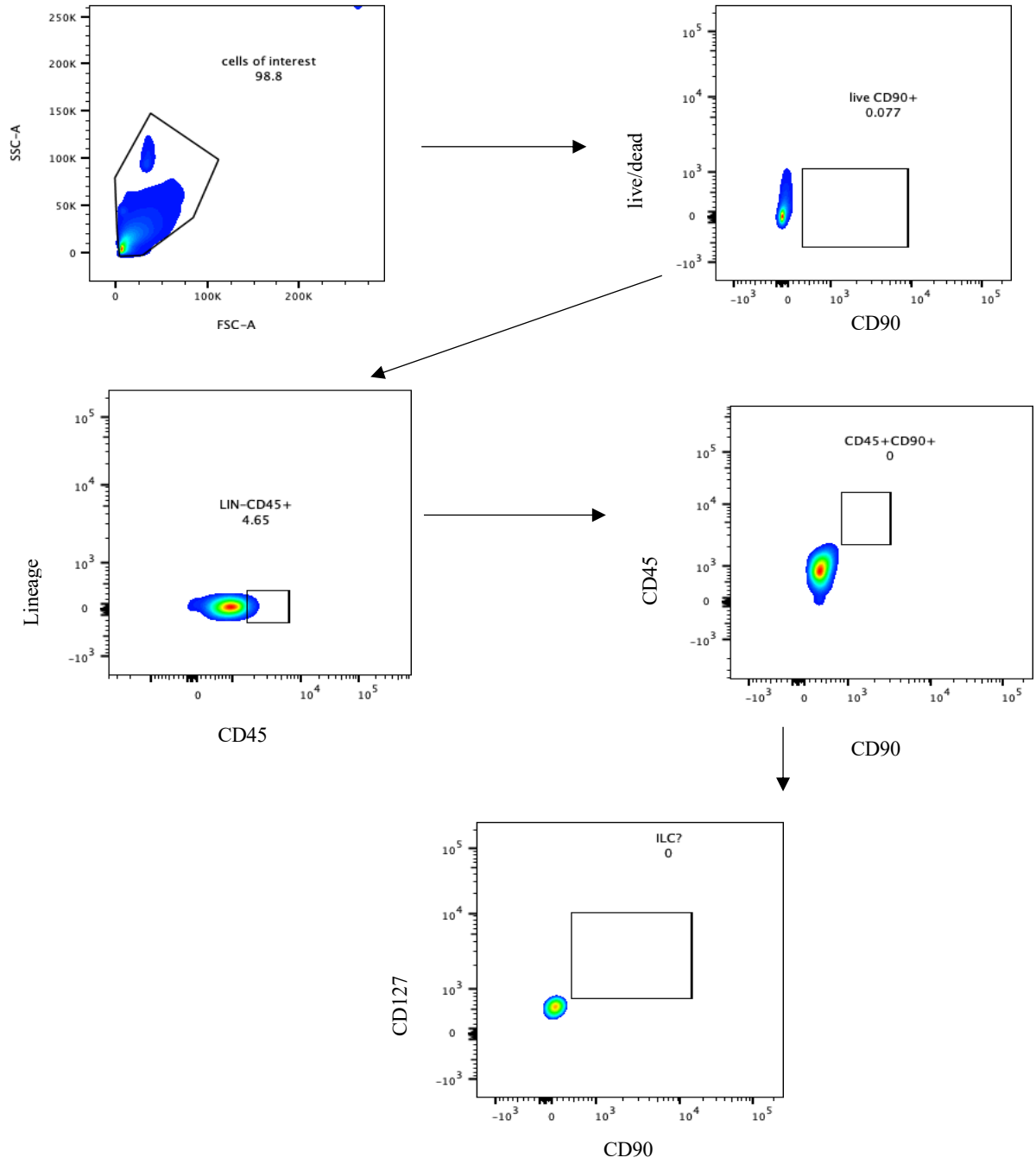

Figure 4.2 Gating strategy for analysis of innate lymphoid cells from bovine lung tissue.

Unstained sample used as a negative control. Cells gated for live, lineage- and $CD90^{+}$ $CD127^{+}$ showing a negative ILC population.

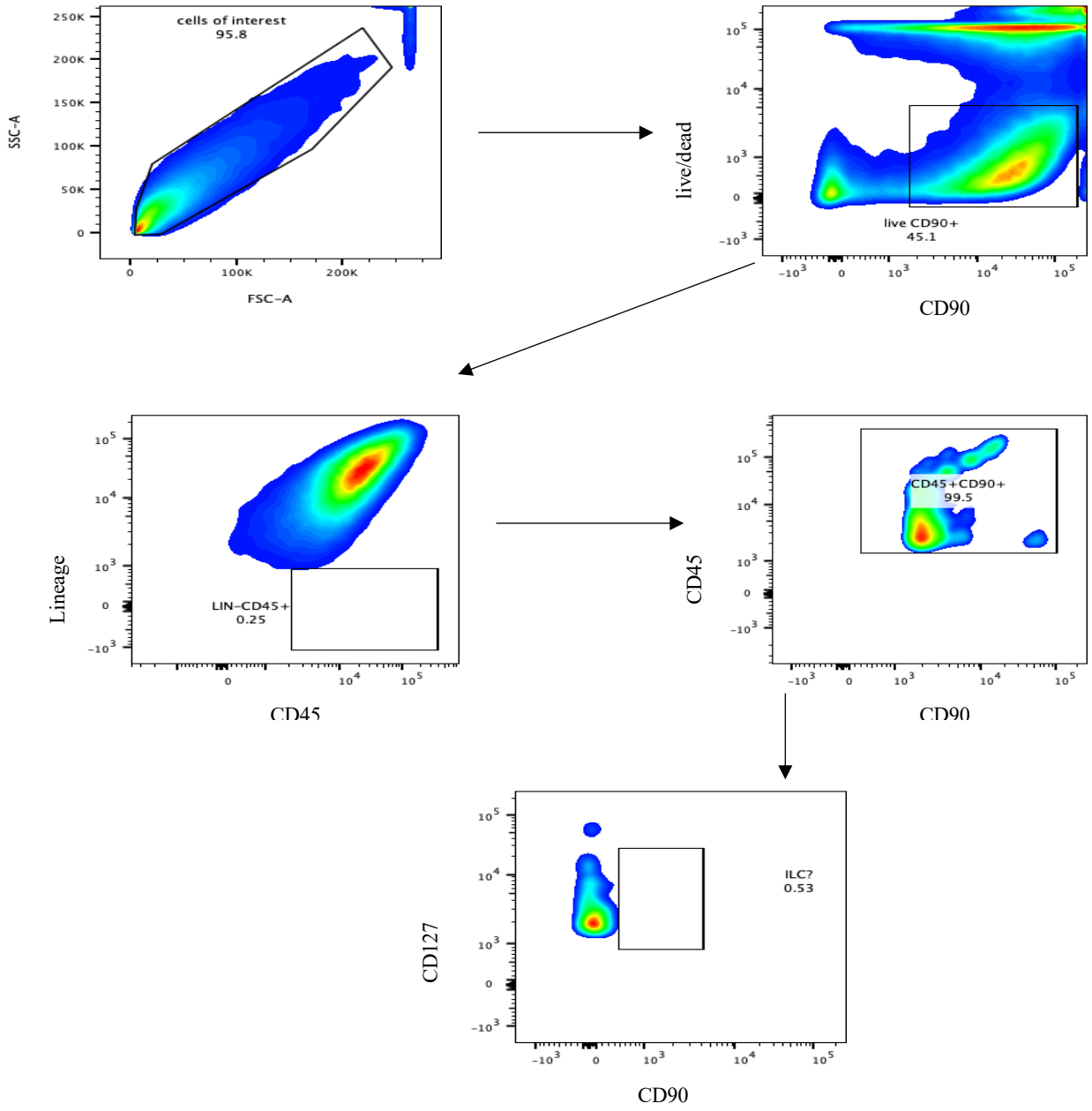

Figure 4.3. Gating strategy for analysis of innate lymphoid cells from bovine lung tissue.

Fluorescence staining of samples collected from a 6 week old calf. Cells gated for live, lineage- and $CD90^{+}$ $CD127^{+}$ showing a negative ILC population.

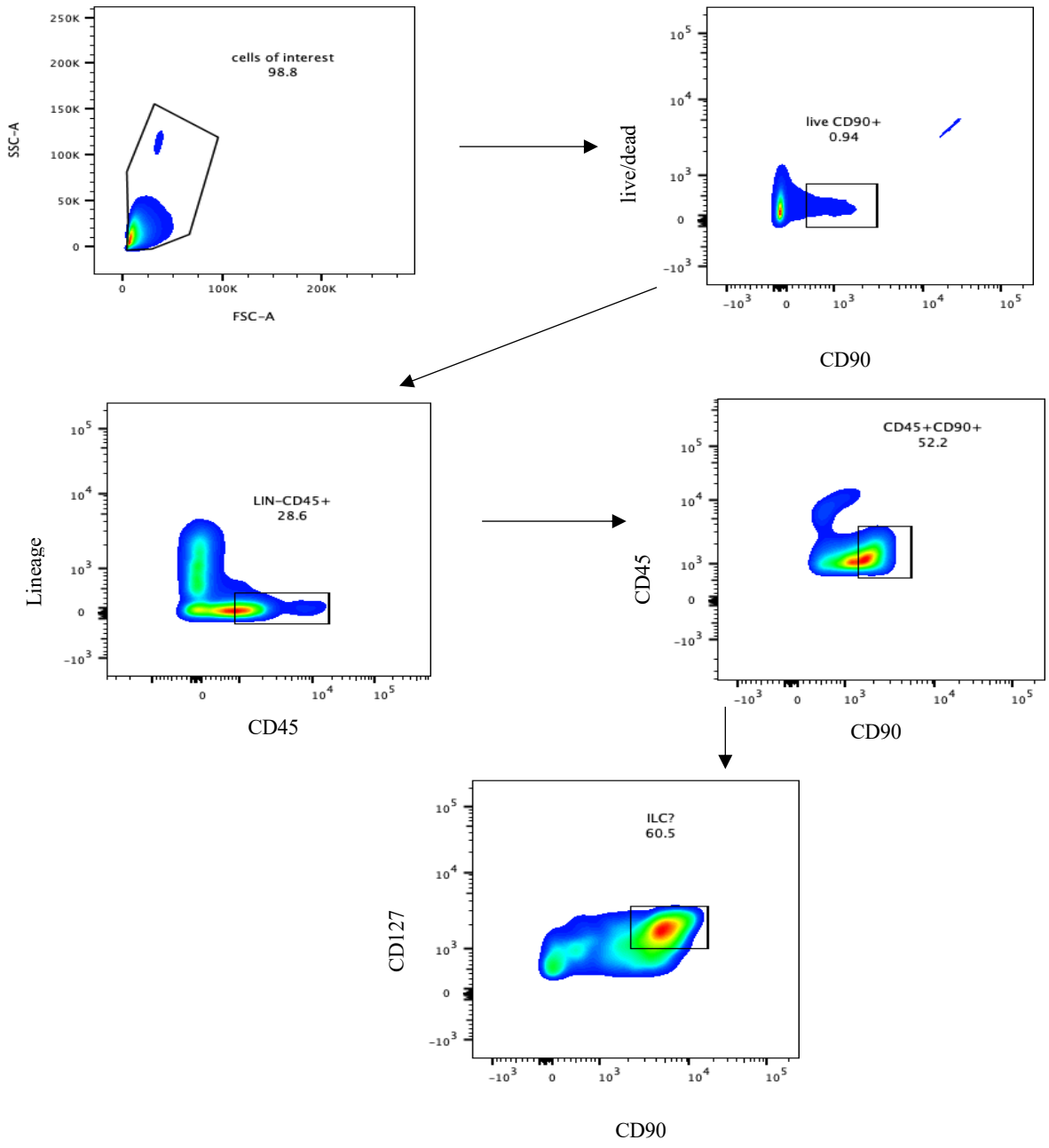

Figure 4.4. Gating strategy for analysis of innate lymphoid cells from bovine lung tissue

Sample from a calf in replicate 3 (chapter 2) part of the placebo group infected with BRSV with no treatment and the population of cells gated for Lineage− $CD45^{+}$ $CD90^{+}$ $CD127^{+}$.
The sample was enriched for live cells using a dead cell removal kit.

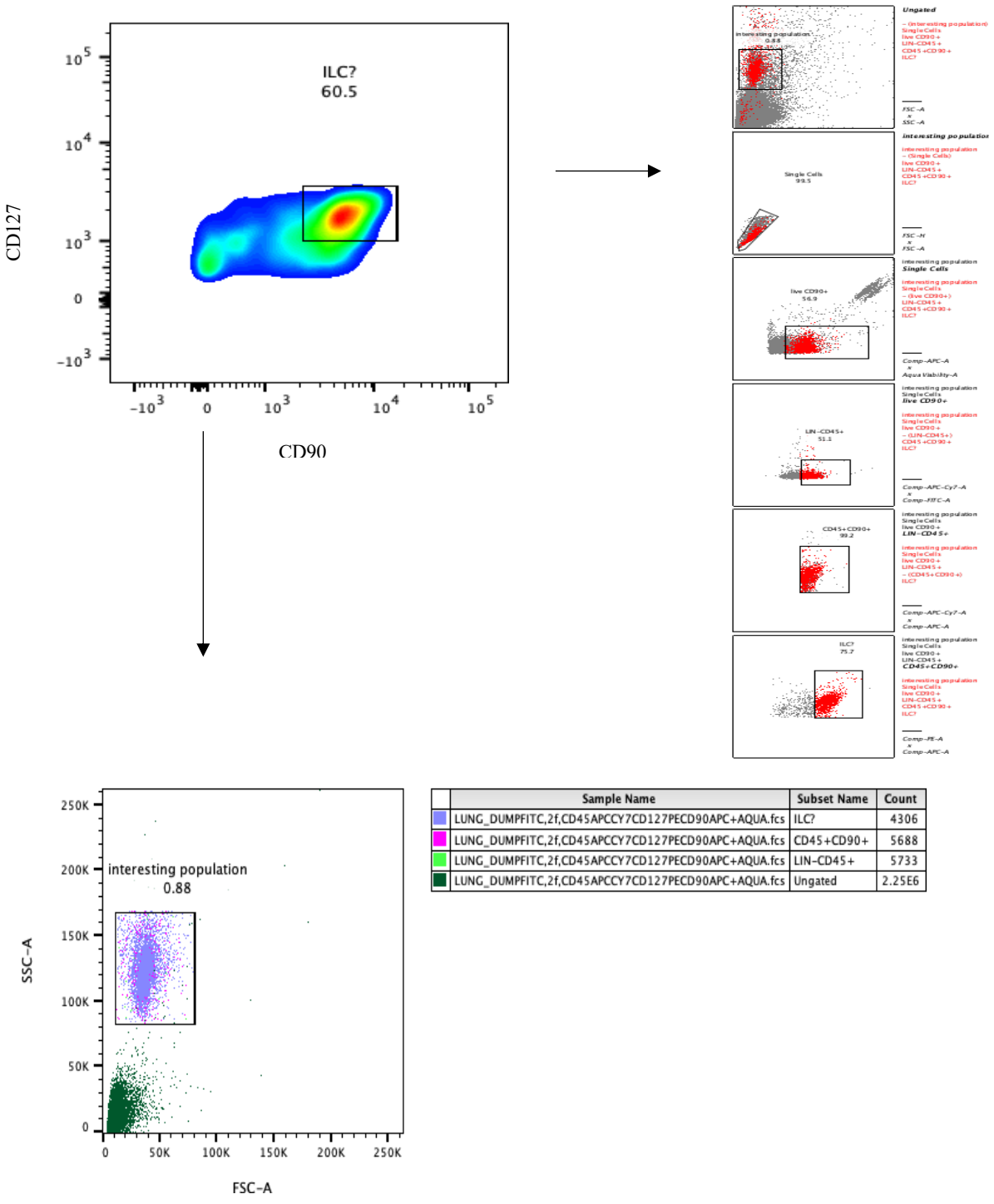

	Sample Name	Subset Name	Count
	LUNG_DUMPFITC,2f,CD45APCCY7CD127PECD90APC+AQUA.fcs	ILC?	4306
	LUNG_DUMPFITC,2f,CD45APCCY7CD127PECD90APC+AQUA.fcs	CD45+CD90+	5688
	LUNG_DUMPFITC,2f,CD45APCCY7CD127PECD90APC+AQUA.fcs	LIN-CD45+	5733
	LUNG_DUMPFITC,2f,CD45APCCY7CD127PECD90APC+AQUA.fcs	Ungated	2.25E6

Figure 4.5. Back gating and analysis of lung cell sample from a calf in replicate 3(chapter 2).

Sample from a calf (part of the placebo group) infected with BRSV with no treatment and the population of cells gated for Lineage− CD45+ CD90 + CD127+ (Figure4.4). The sample was enriched for live cells using the dead cell removal kit. This shows a population positive for ILC markers but has a higher side scatter than is normal for lymphocytes.

REFERENCES

1. Vivier E, Van De Pavert SA, Cooper MD, Belz GT (2016) The evolution of innate lymphoid cells. Nat Immunol. https://doi.org/10.1038/ni.3459

2. Sonnenberg GF, Artis D (2015) Innate lymphoid cells in the initiation, regulation and resolution of inflammation. Nat. Med.

3. Bernink JH, Peters CP, Munneke M, et al (2013) Human type 1 innate lymphoid cells accumulate in inflamed mucosal tissues. Nat Immunol. https://doi.org/10.1038/ni.2534

4. Vosshenrich CAJ, Di Santo JP (2013) Developmental programming of natural killer and innate lymphoid cells. Curr. Opin. Immunol.

5. Allan DSJ, Kirkham CL, Aguilar OA, et al (2015) An in vitro model of innate lymphoid cell function and differentiation. Mucosal Immunol. https://doi.org/10.1038/mi.2014.71

6. Yudanin NA, Schmitz F, Flamar AL, et al (2019) Spatial and Temporal Mapping of Human Innate Lymphoid Cells Reveals Elements of Tissue Specificity. Immunity. https://doi.org/10.1016/j.immuni.2019.01.012

7. Fan X, Rudensky AY (2016) Hallmarks of Tissue-Resident Lymphocytes. Cell

8. Barlow JL, McKenzie ANJ (2019) Innate Lymphoid Cells of the Lung. Annu. Rev. Physiol.

9. Crome SQ, Nguyen LT, Lopez-Verges S, et al (2017) A distinct innate lymphoid cell population regulates tumor-associated T cells. Nat Med. https://doi.org/10.1038/nm.4278

10. Valle-Noguera A, Gómez-Sánchez MJ, Girard-Madoux MJH, Cruz-Adalia A (2020) Optimized Protocol for Characterization of Mouse Gut Innate Lymphoid Cells. Front

Immunol 11:2934. https://doi.org/10.3389/FIMMU.2020.563414/BIBTEX

11. Yazdani R, Sharifi M, Shirvan A, et al Characteristics of innate lymphoid cells (ILCs) and their role in immunological disorders (an update). Elsevier

12. Walker JA, Barlow JL, McKenzie ANJ (2013) Innate lymphoid cells-how did we miss them? Nat. Rev. Immunol.

13. Mortha A, Burrows K (2018) Cytokine networks between innate lymphoid cells and myeloid cells. Front. Immunol.

14. Akama Y, Satoh-Takayama N, Kawamoto E, et al (2020) The role of innate lymphoid cells in the regulation of immune homeostasis in sepsis-mediated lung inflammation. Diagnostics

15. Goto Y, Kurashima Y, Kiyono H (2015) Roles of the gut mucosal immune system in symbiosis and immunity. Rinsho Ketsueki. https://doi.org/10.11406/rinketsu.56.2205

16. Spits H, Cupedo T (2012) Innate lymphoid cells: Emerging insights in development, lineage relationships, and function. Annu. Rev. Immunol.

17. Gronke K, Kofoed-Nielsen M, Diefenbach A (2016) Innate lymphoid cells, precursors and plasticity. Immunol Lett. https://doi.org/10.1016/j.imlet.2016.07.004

18. Saravia J, You D, DeVincenzo J, et al (2014) Group 2 innate lymphoid cells and IL-33 in infant respiratory syncytial virus infection. J Immunol

19. Doherty TA, Khorram N, Lund S, et al (2013) Lung type 2 innate lymphoid cells express cysteinyl leukotriene receptor 1, which regulates TH2 cytokine production. J Allergy Clin Immunol. https://doi.org/10.1016/j.jaci.2013.03.048

APPENDIX I

1 Rabbit normal serum – 10% for blocking

2 Wash Buffer: 1X PBS (0.145 M NaCl, 0.0027 M KCl, 0.0081 M Na_2HPO_4, 0.0015 M KH_2PO_4, pH 7.4)

3 4% Paraformaldehyde (Thermofisher)

4 Permeabilization media -10 % Triton X-100 (stock) with a working solution of 0.3% Triton® X-100 in PBS

5 1% NP-40 (Surfact-AMPs™ NP-40, Pierce, Rockford, IL)

6 Blocking buffer: 10% normal goat serum in PBS

7 Cell culture media - RPMI 1640 (Gibco, Grand Island, NY, USA) with 2% fetal calf serum (FCS) and 0.01% Gentamycin.

8 4',6-diamidino-2-phenylindole diacetate (DAPI) - Invitrogen. Working solution: Add 1 µL of 14.3 mM stock for every 5 mL of PBS. Store any unused DAPI at 2-8 °C, wrapped in aluminum foil.

9 Mounting Medium (Fluromount-G by Southernbiotech)

10 Cell buffer - RPMI 1640 (Gibco, Grand Island, NY, USA) with 2% fetal calf serum (FCS) and 0.01% Gentamycin

11 PMA working solution (120 nM P1585, Sigma Aldrich)

12 Bovine respiratory syncytial virus (BRSV) antigen working solution (30 µg/ml)

13 Lymphoprep™ has a density of 1.077 g/mL (Sodium diatrizoate 9.1% w/v, Polysaccharide 5.7% w/v) (StemCell technologies)

14 Lymphoprep™ Tubes (StemCell technologies)

15 Dimethyl sulfoxide (DMSO)

16 Small dissection scissors.

17 Forceps.

18 Lint-free wipes.

19 Sterile polyethylene disposable transfer pipettes.

20 60 × 15 mm sterile polystyrene petri dishes.

21 50 mL conical tubes.

22 15 mL conical tubes.

23 Ice-cold distilled water.

24 Hank's Balanced Saline Solution (HBSS) with calcium chloride (corning)

25 Humidified CO_2 incubator.

26 Microplate-sealing tape.

27 12 mm round poly- L-lysine-coated glass coverslips.

28 75 × 25 × 1 mm Superfrost® Plus slides (Thermo Scientific)

29 2 mL microcentrifuge tubes.

30 Nalgene® Mr. frosty and 100% Isopropyl alcohol

31 PAP-pen

32 Fc receptor blocker (Innovex biosciences NB309),

33 Acid Citrate Dextrose (ACD) tubes

34 TrueView autofluorescence quenching solution (Vector)

APPENDIX II

1. Alcohol wipes (VWR)
2. dissecting pins and board,
3. 2 pairs of fine serrated forceps,
4. fine scissors (sharp-blunt tips),
5. 2 pairs of fine curved hemostats
6. Single edge razor blades (VWR)
7. 100mm sterile petri dishes (Thermofisher)
8. 15 and 50mL conical tubes (BD Falcon)
9. Collagenase D (Worthington)
10. DNAse I (Sigma-Aldrich)
11. RPMI 1640 medium (Gibco, Grand Island, NY, USA)
12. Sodium pyruvate (Atlanta Biologicals)
13. Fetal bovine serum (FBS, Atlanta Biologicals)
14. Bovine serum albumin (BSA, Atlanta Biologicals)
15. HEPES (Atlanta Biologicals)
16. Gentamicin 50mg/mL(Thermofisher)
17. EDTA (Sigma Aldrich)
18. 4 % Paraformaldehyde (PFA, Invitrogen)
19. Sodium Azide (NaN3), (Invitrogen)
20. Eppendorf desk top Centrifuge (Fisher scientific)
21. Cell media: RPMI-1640: with L-glutamine, 10% FBS, 25mM HEPES, 10mM sodium pyruvate, 50 µg/ml gentamicin.

22. lung digestion medium: cell media with 2mg/mL collagenase D + 0.02mg/mL DNase I
23. 70µm sterile cell filters (corning)
24. 40µm sterile cell filters (corning)
25. 1mL syringes (BD)
26. Lymphoprep™ has a density of 1.077 g/mL. (Sodium diatrizoate 9.1% w/v, Polysaccharide 5.7% w/v) (StemCell technologies))
27. Lymphoprep™ Tubes (StemCell technologies)
28. Dead cell elimination microbeads (Miltenyi Biotec)
29. MACS columns & magnets (Miltneyi Biotec)
30. 40µm sterile cell filters (BD and Corning)
31. MACS Buffer: PBS (pH 7.2) containing 0.5% bovine serum albumin (BSA) and 2 mM EDTA
32. 5mL round-bottom polystyrene test tubes (BD Falcon)
33. Multicolor flow cytometer (BD™ LSR II Flow Cytometer-BD Biosciences, USA))
34. FACS buffer: PBS (pH 7.2) containing 0.5% bovine serum albumin (BSA), 2 mM EDTA, 2 mM NaN3
35. Blocking buffer: PBS (pH 7.2) containing 10% fetal bovine serum
36. FcR blocking buffer (Innovexbio)
37. Compensation beads (Thermo Fischer Scientific)
38. Aqua viability fixable live-dead discriminator (Invitrogen or Thermo Fischer Scientific)-working solution 1 µL stock solution for 2mL PBS, prepared fresh.
39. DAPI - 4',6-diamidino-2-phenylindole di acetate (DAPI; Invitrogen). Working solution: 1 µL of 14.3 mM stock for every 5 mL of PBS store at 2-8 °C, wrapped in aluminum foil.